LEVEL II

DOCUMENT 315-79

RSG

AD A068714

DDC FILE COPY

RISK ANALYSIS TECHNIQUES

RANGE SAFETY GROUP
RANGE COMMANDERS COUNCIL

DISTRIBUTION STATEMENT A
Approved for public release;
Distribution Unlimited

KWAJALEIN MISSILE RANGE
WHITE SANDS MISSILE RANGE
YUMA PROVING GROUND

NAVAL WEAPONS CENTER
PACIFIC MISSILE TEST CENTER
ATLANTIC FLEET WEAPONS TRAINING FACILITY
NAVAL AIR TEST CENTER

AIR FORCE FLIGHT TEST CENTER
AIR FORCE SATELLITE CONTROL FACILITY
SPACE AND MISSILE TEST CENTER
EASTERN TEST RANGE
WESTERN TEST RANGE
ARMAMENT DEVELOPMENT AND TEST CENTER
AIR FORCE TACTICAL FIGHTER WEAPONS CENTER

DDC
RECEIVED
MAY 30
D

79 05 17 009

UNCLASSIFIED

SECURITY CLASSIFICATION OF THIS PAGE (When Data Entered)

REPORT DOCUMENTATION PAGE		READ INSTRUCTIONS BEFORE COMPLETING FORM
1. REPORT NUMBER 315-79	2. GOVT ACCESSION NO.	3. RECIPIENT'S CATALOG NUMBER
4. TITLE (and Subtitle) Risk Analysis Techniques		5. TYPE OF REPORT & PERIOD COVERED Technical Report
		6. PERFORMING ORG. REPORT NUMBER
7. AUTHOR(s) Range Safety Group Range Commanders Council White Sands Missile Range, NM 88002		8. CONTRACT OR GRANT NUMBER(s)
9. PERFORMING ORGANIZATION NAME AND ADDRESS Same as Block 7		10. PROGRAM ELEMENT, PROJECT, TASK AREA & WORK UNIT NUMBERS
11. CONTROLLING OFFICE NAME AND ADDRESS Secretariat, Range Commanders Council ATTN: STEWS-SA-R White Sands Missile Range, NM 88002		12. REPORT DATE March 1979
		13. NUMBER OF PAGES 147
14. MONITORING AGENCY NAME & ADDRESS(if different from Controlling Office) Same as Block 11		15. SECURITY CLASS. (of this report) UNCLASSIFIED
		15a. DECLASSIFICATION/DOWNGRADING SCHEDULE

16. DISTRIBUTION STATEMENT (of this Report)
Approved for Public Release; Distribution Unlimited.

17. DISTRIBUTION STATEMENT (of the abstract entered in Block 20, if different from Report)

18. SUPPLEMENTARY NOTES

19. KEY WORDS (Continue on reverse side if necessary and identify by block number)
Risk analysis, casualty expectation, impact probabilities, debris lethality, TOMAHAWK, SHAZAM, launch risk, malfunction turn, impacting fragments, failure mode, population center, and population/structures data.

20. ABSTRACT (Continue on reverse side if necessary and identify by block number) Foreword

The goal of Range Safety is to prevent injury of personnel or damage to property by taking all reasonable precautions consistent with operational requirements. Achievement of this goal begins early in the evaluation of a proposed test program, in fact, in many instances prior to the definition and design of the range safety system that will be used during real-time operation. To ascertain the degree of protection required, the system to be tested must be evaluated to determine the geographic boundaries and makeup of the test area. If the area contains no facilities or personnel, no precautions are necessary other than surveillance of the

DD FORM 1 JAN 73 1473 EDITION OF 1 NOV 65 IS OBSOLETE UNCLASSIFIED over/

SECURITY CLASSIFICATION OF THIS PAGE (When Data Entered)

area to ensure that it remains clear during the test. But, if the test area is large and contains facilities and personnel, it is necessary to determine, either by qualitative or quanitative analysis, those hazards produced by the test. The results of this analysis will define the level of risk and, therefore, the restrictions that must be placed on the test program or the risk that must be accepted in order for the tests to be conducted.

A survey of five of the test ranges represented in the Range Safety Group (RSG), Range Commanders Council (RCC), was made to determine the types of risk analyses conducted and the uses to which risk data are put in developing test restrictions. This information is presented in this document to provide all ranges with the various techniques employed which may have merit for their application. A general section introducing the subject of risk analysis has been prepared; however, there is no intent to establish a standard model for performing risk analysis applicable for all ranges.

ACCESSION for
NTIS White Section ☒
DDC Buff Section ☐
UNANNOUNCED ☐
JUSTIFICATION
BY
DISTRIBUTION/AVAILABILITY CODES
SPECIAL
A

(14) RSG-210-71

DOCUMENT 315-79

(6) RISK ANALYSIS TECHNIQUES

(1) Technical rept.

Prepared by

Range Safety Group
Range Commanders Council

(12) 150p

(11) Mar[redacted]79

Published by

Secretariat
Range Commanders Council
White Sands Missile Range,
New Mexico 88002

DDC
RECEIVED
MAY 18 1979
D

APPROVED FOR PUBLIC RELEASE: DISTRIBUTION UNLIMITED

79 05 17 003

408 173

Table of Contents

	Page
List of Figures	v
List of Tables	vii
Foreword	ix
1.0 Introduction	1-1
1-1 Background	1-1
1-2 Scope and Objective	1-1
2.0 Discussion	2-1
2.1 General	2-1
2.2 Utilization of Results	2-1
3.0 The Essentials of Casualty Expectation	3-1
3.1 Calculations Associated with Testing	3-1
3.1.1 System	3-2
3.1.2 Impact Probabilities	3-3
3.1.3 Debris Lethality	3-3
3.1.4 Population/Structures Data	3-3
3.1.5 Test Planning	3-4
4.0 Individual Range Risk Analysis Techniques	4-1-1
4.1 Armament Development Test Center (ADTC) Risk Assessment Methodology, A Detailed Overview	4-1-1
4.1.1 Introduction	4-1-1
4.1.2 The Mathematics of Risk Assessment	4-1-5
4.1.3 Program PTRAJ Overview	4-1-12
4.1.4 Program DENGEN Overview	4-1-16
4.1.5 Program RISK Overview	4-1-22
4.1.6 Risk Assessment Program Capabilities and Limitations	4-1-41
References	4-1-44
4.2 Kwajalein Missile Range (KMR) Risk Analysis Techniques	4-2-1
4.2.1 General	4-2-1
4.2.2 Risk Analysis Models	4-2-2
4.3 Pacific Missile Test Center (PMTC) Risk Analysis Models	4-3-1
4.3.1 Hazard Analysis for TOMAHAWK Cruise Missile Inland Tests	4-3-1
4.3.2 Safety Hazard Analysis Program (SHAZAM)	4-3-21

		Page
4.4	Space and Missile Test Center (SAMTEC)	4-4-1
	4.4.1 Launch Area Risk Analysis	4-4-1
	4.4.2 Target Planning Optimization/Coutour Plot	4-4-15
	References	4-4-47
4.5	White Sands Missile Range (WSMR) Risk Analysis Techniques.	4-5-1
	4.5.1 Range Safety Authority	4-5-1
	4.5.2 Minimizing Risk.	4-5-1
	4.5.3 Risk Analysis.	4-5-1
	4.5.4 General Risk Programs.	4-5-2

List of Figures

Figure Number	Title	Page
4-1-1	ADTC Risk Assessment Methodology Program Interaction and Data Flows	4-1-2
4-1-2	Risk Assessment Library Data Bases	4-1-3
4-1-3	PTRAJ Macro Flow Diagram	4-1-13
4-1-4	DENGEN Macro Flow Diagram	4-1-21
4-1-5	Sample DENGEN Output Showing Rate of Convergence of PDF Mean and Standard Deviation for U Coordinate	4-1-26
4-1-6	Sample DENGEN Output Showing Rate of Convergence of the PDF Mean and Standard Deviation for V Coordinate	4-1-27
4-1-7	Sample DENGEN Output Showing Shape of Computed PDF for Impacts of the Intact Vehicle	4-1-28
4-1-8	RISK Macro Flow Diagram	4-1-30
4-1-9	E_c Map for Sample Test Case 2	4-1-40
4-2-1	Circular Dispersion Model	4-2-3
4-2-2	HP-65 Program Form	4-2-4
4-2-3	Elliptical Dispersion Model	4-2-7
4-2-4	Results of Analysis Using Risk Contour Model	4-2-8
4-3-1	Impact Hazards Model	4-3-2
4-3-2	Impact Hazards Model Functional Flow Diagram	4-3-4
4-3-3	Impact Probability Computation for Roads	4-3-5
4-3-4	Air Collision Model Geometry	4-3-7
4-3-5	Altitude Collision Model	4-3-9
4-4-1	Risk Computation	4-4-1
4-4-2	Launch Risk Analysis Procedure	4-4-3
4-4-3	Centerline Transformation	4-4-4
4-4-4	Development of the Malfunction Turn Impact Distribution	4-4-8
4-4-5	Malfunction Turn Vacuum IIP Distribution	4-4-9
4-4-6	Procedure for TARGOP Usage	4-4-6
4-4-7	TARGOP Flowchart	4-4-18
4-4-8	CONTUR Flowchart	4-4-21
4-4-9	Relevant Coordinate Systems	4-4-22
4-4-10	3σ Uncertainty Ellipse for jth Fragment	4-4-26
4-4-11	Bivariate Normal Distribution for Nominal Flight Fragment Impact Uncertainty	4-4-27

Figures (Continued) Page

4-4-12 Energy Relationships Between Impacting Fragments and Resisting Structures. 4-4-35
4-4-13 Casualty Density Function for a Population Center. 4-4-36
4-4-14 Relationship Between Original Target Point and a Typical Grid Point. 4-4-39
4-4-15 Grid Boundaries Typical Mission Run No. 2 . . 4-4-41
4-4-16 3-Sigma Impact Ellipses Typical Mission Run No. 2 4-4-42
4-4-17 P_I Typical Mission Run No. 2. 4-4-43
4-4-18 E_{cu} Typical Mission Run No. 2 4-4-44
4-4-19 E_{cs} Typical Mission Run No. 2 4-4-45
4-4-10 R_c Typical Mission Run No. 2. 4-4-46

List of Tables

Table Number	Title	Page
4-1-I	PTRAJ Namelist Data	4-1-14
4-1-II	Explanation of Printout Heading Parameters	4-1-17
4-1-III	Sample Output Data with Intermediate Print	4-1-19
4-1-IV	DENGEN Input Data Required in Addition to PTRAJ DATA	4-1-23
4-1-V	Failure Mode Data Array Structure	4-1-24
4-1-VI	RISK User Supplied Data	4-1-32
4-1-VII	Default Option Values	4-1-34
4-1-VIII	Failure Mode Data Array Structure	4-1-35
4-1-IX	Explanation of Calculated Output	4-1-37
4-1-X	Explanation of Calculated Output for Each Hazarded Population Center	4-1-38
4-1-XI	Case7, 750LB Bomb, Fragmentation, No Wind, Lod=0 Skip Lock	4-1-39
4-1-XII	Expected Casualty by Area in Descending Order of Importance	4-1-40
4-3-I	Failure Mode Impact Dispersion Data	4-3-12
4-3-II	Mean Impact Point Locus - NWC to DPG - Nominal Flight Path	4-3-14
4-3-III	Mean Impact Point Locus - VAFB to NWC - Nominal Flight Path	4-3-15
4-3-IV	Mean Impact Point Locus - VAFB to NWC - Alternate Flight Path	4-3-15
4-3-V	Hazardous Impacting Fragments	4-3-16
4-3-VI	Population Centers	4-3-18
4-3-VII	Road Locations	4-3-19
4-3-VIII	Air Traffic Data (Low Altitude)	4-3-20
4-3-IX	Vehicle Dimensions	4-3-21

FOREWORD

The goal of Range Safety is to prevent injury of personnel or damage to property by taking all reasonable precautions consistent with operational requirements. Achievement of this goal begins early in the evaluation of a proposed test program, in fact, in many instances prior to the definition and design of the range safety system that will be used during real-time operation. To ascertain the degree of protection required, the system to be tested must be evaluated to determine the geographic boundaries and makeup of the test area. If the area contains no facilities or personnel, no precautions are necessary other than surveillance of the area to ensure that it remains clear during the test. But, if the test area is large and contains facilities and personnel, it is necessary to determine, either by qualitative or quantitative analysis, those hazards produced by the test. The results of this analysis will define the level of risk and, therefore, the restrictions that must be placed on the test program or the risk that must be accepted in order for the tests to be conducted.

A survey of five of the test ranges represented in the Range Safety Group (RSG), Range Commanders Council (RCC), was made to determine the types of risk analyses conducted and the uses to which risk data are put in developing test restrictions. This information is presented in this document to provide all ranges with the various techniques employed which may have merit for their application. A general section introducing the subject of risk analysis has been prepared; however, there is no intent to establish a standard model for performing risk analysis applicable for all ranges.

1.0 INTRODUCTION

1.1 BACKGROUND

Task RS-2, Risk Analysis Techniques, was adopted by the Range Safety Group at their 40th meeting held at Fort Bliss, Texas, 31 August - 2 September 1976, and subsequently approved by the Range Commanders Council in October 1976. The ad hoc committee appointed by the RSG for task accomplishment met in March 1977 at the Tactical Fighter Weapons Center, Nellis Air Force Base, Nevada, to discuss risk analysis techniques and to formulate the method for task accomplishment.

1.2 SCOPE AND OBJECTIVE

The purpose of this document is to discuss the subject of risk analysis in the general sense, i.e., input data required, assumptions made and the uses to which such analyses are put. There is no attempt to define the "right" way to perform a risk analysis since no two ranges have the same factors that must be considered. The main objective is to provide under one cover a description of the methods used at each range so that other ranges can benefit from the methods that currently exist. Section 2.0 of this document contains a discussion of the broad aspects of risk analysis procedures and how the results can be utilized. Section 3.0 deals with the general methodology employed to quantify casualty expectation. Lastly, section 4.0 contains inputs from each participating range describing specific analytical methods for determining risk values and the use made of the results.

2.0 DISCUSSION

2.1 GENERAL

The safety evaluation effort performed for program planning or support of a specific test consists of several factors, one of which is risk analysis. An important factor in the risk assessment effort is early definition by the user of the program or test to be conducted. Knowing the program concept and objectives provides the range with immediate insight into the hazards involved. Judgments can then be made concerning the requirements for and the sophistication of any necessary risk analysis. Risk analysis techniques vary considerably from complex computer program models to simplified calculations made on a hand calculator. Regardless of the method, the function of risk analysis is to quantitatively identify the program or test risk values.

Risk values are generally categorized in two ways: (1) the probability of impact and (2) casualty estimation. The probability of impact generally used is the probability of at least one object impact in a specific area. The casualty estimation generally used is one of two types: (1) the expected number of casualties, defined as the number of persons expected to sustain an injury as a result of at least one object impact in a specific area; or (2) the probability of casualty, defined as the probability of one or more persons sustaining an injury. In many cases these two casualty parameters are approximately equal. Although there are variations from range to range, these are the basic values which can be used to quantify risk.

The result of a risk analysis is not an end in itself but rather a means to accomplish other goals. Simple identification of risk values provides insight to the overall acceptability of the program. If the risk appears unacceptably high, the analysis can provide information needed for reduction of risks since, during the identification of all input variables, one dominant factor may be identified that can be controlled. Risk analyses can provide range management with pertinent decision-making information. In addition, during test countdown, risk information can indicate the acceptability of continuing the test if unexpected events occur.

2.2 UTILIZATION OF RESULTS

Risk analyses are performed for many diversified reasons; each test range having its own motivations. The end product is valid only to the degree of the reliability of inputs and applicability to a given test or test range. Because each test range has unique applications, a valid result for one test range may be relatively meaningless for another range.

In all instances the risk analysis results must never be assumed absolutely accurate, since the results generally reflect a number of uncertain assumptions. For this reason it should be understood that risk studies are merely tools/aids used in conjunction with other factors in the decision making process (experience, precedent, known factors not included in study, national interests, etc.). Acceptable risk levels are not in general established. Risks are minimized to the extent feasible and then, based upon considerations of test objectives and national interests, the tests are performed or rejected.

The following is a list of general uses and applications of risk analysis results:

1. A tool used in the total decision-making process.

2. Excessive risk may reveal the need for a Flight Termination System (FTS) or other program restrictions.

3. Results may indicate the requirement that an existing or predesigned FTS be redesigned, if such a redesign can significantly reduce excessive risks.

4. Results can indicate the need for evacuation of personnel, roadblocks, restricted airspace, movement of critical equipment, call-up/purchase of additional real estate or justification for currently controlled land.

5. Results might show the necessity to modify the support plans of other range support elements permitted within the evacuated test area, i.e., manned optical tracking sites.

6. Results might reveal the need and advantage of providing positive protection for nonevacuated personnel (shelters, barricades, bunkers, blockhouses, etc.) and critical test equipment required in the evacuated test area.

7. Results can be used in the development of missile flight safety operational support plans to include procedures, destruct criteria, and single piece versus destruct case (many pieces) impact decisions.

8. Results can be used to alert management to excessive risks when indicated for given tests or total test programs. It is then the decision of management on which course to proceed.

9. Results might identify test scenarios and patterns that require redesign/modification or allow the selection of less hazardous scenarios when options exist.

10. Results may indicate the need to construct new facilities in cases where it is not acceptable to utilize existing facilities.

11. Results can be used in establishing and fabricating limiting criteria which may be used both quantitatively and qualitatively. Single tests or cumulative test programs can be compared in this manner.

12. Risk studies can provide documented evidence that hazards were considered in developing test operations plans.

13. "Risks to test" results identifying the reliability of the support test range can be used for the following purposes:

a. Identifing high risk from range support elements and therefore, assisting in increasing total reliability and reducing hazards involved in testing.

b. Increasing test range supportability.

c. Increasing test range attractiveness to potential users.

All the above considerations can result in significant cost savings when employed to identify and reduce risks.

3.0 THE ESSENTIALS OF CASUALTY EXPECTATION

3.1 CALCULATIONS ASSOCIATED WITH TESTING

There are two aspects to the problem of assessment of risks. The first is the quantification of the risk and the second is the interpretation of the question, "how safe is safe enough?" Many papers addressing both of these aspects are available. This report addresses only the first aspect and in particular a general methodology that can be used to calculate quantitative measures of risk associated with range activities.

The measure most frequently employed to quantify the risk associated with the testing of a system is called casualty expectation, E_c. This measure is the number of persons expected to be killed or injured if a system is tested according to a specified plan. The specific approach toward computation of casualty expectation is adapted by the national ranges to fit their specific problems and test situations. In general, E_c is obtained by considering the following quantities:

- The area A in which debris impacts can occur partitioned into A_i subsets of areas.

- The fragment impact probability density (P_I) conditioned by a given system failure on A_i.

- The hazard area A_{Hi} associated with an impact on A_i.

- N_i, the number of people in A_i subjected to the hazard encompassed by A_{Hi}.

These quantities are then used in an equation, of the form

$$E_c = P_I \frac{A_{Hi}}{A_i} N_i \qquad (1)$$

The E_c estimate of risk for a given test is often calculated by summing the risk over the hazarded area for the test with each element of the sum weighted according to the probability of the failure.

Actual risk assessment programs developed by the various ranges utilizing the above factors are described in section 4.0 of this document to provide an assortment of methods, applications and uses. A generalized methodology that satisfies all possible analytical problems does not exist. Historically the ranges have developed risk studies and analyzes, as appropriate, in response to specific tests, weapons systems or range operations problems. Although little standardization exists between the

ranges regarding methodology, computer programs and analytical tools; the major elements of a risk analysis do recur. A typical risk analysis requires five basic categories of data:

- Weapon/system failure modes and probabilities.

- Impact probabilities and distributions resulting from failures or normal tests.

- A measure of lethality of impacting debris.

- Location and nature of population and structures hazarded by the test/mission.

- Test plans.

Various elements of these categories may be considered in development of a risk analysis for a proposed system test. The following subparagraph discusses and lists typical elements that occur in risk analysis studies.

3.1.1 System

Test vehicle physical data utilized may include:

Fragmentation characteristics

Mass

Shape

Ballistic coefficients

Flight dynamics

Propellants

Flight Termination System (FTS)

Explosive/fuel/chemical properties

Guidance and control

Stage burn times and separation characteristics

Fragmentation/lethality

Flight control and termination system properties

The failure modes and associated probability of failure are required if other than a normal test is addressed. Estimates for probabilities of failure mode occurrence are typically based upon knowledge of the vehicle's critical systems and expert assessment of their reliability combined with historical data when available.

3.1.2 Impact Probabilities

The regions or test areas subjected to a hazard must be identified. The regions may be subdivided into smaller sections, critical locations of people, or buildings that are specified for subsequent risk calculations. All risk analyses require estimates of the probabilities of debris/fragments from a failed vehicle impacting within hazardous distances of personnel or structures in the test region.

The design and engineering associated with the development of a system is geared to producing a properly functioning vehicle. As a consequence, there are generally no data defining vehicle performance characteristics after a critical failure has occurred. These data are, however, required for risk assessment. To provide these data, computer models have been developed to simulate vehicle responses after a given gross failure mode has occurred. These computer models may be used as part of the computational process for generating impact probabilities and definitions for the so-called debris impact probability density functions. These models combine, statistically and dynamically, well defined vehicle data with expert engineering estimates to predict vehicle performance after a failure occurs.

3.1.3 Debris Lethality

An important aspect of the vehicle data problem that must be addressed prior to performing risk calculations is the delineation of what occurs after vehicle impact. This ultimately will define the hazard area for a given vehicle or fragment impact. The data items which are often developed for this part of the problem include: an impact energy distribution budget, explosive energies available (if any) at impact, secondary fragments which may result from impact, and ricochet probabilities and characteristics. Items such as these are used to calculate hazard areas for the various hazard mechanisms.

3.1.4 Population/Structures Data

The major purpose of risk analysis is to determine the magnitude of hazards to personnel and structures posed by a test and/or total test program. Locations of buildings and structures and the distribution of populations throughout the test areas must be known. Other elements commonly addressed are:

Sheltering capability of occupied structures; the ability to withstand debris impact and protect against overpressures from explosions or impact kinetic energy conversion.

Frequently, populated distributions may be functions of the time of day or day or week and may be significant in risk tradeoff studies.

Risk levels can be directly affected and controlled to some extent by population control, sheltering, range clearance, or physically preventing personnel from entering these test areas.

3.1.5 Test Planning

The actual employment of the system under test conditions ultimately determines actual risk levels. Integral to the analysis are the test constraints posed by the following:

Test areas/range geometry

Targeting optics

Nominal flight trajectories/profiles

Launch/release points

Destruct and impact limit lines

FTS criteria

Wind/weather restrictions

Warhead arming, fusing, detonation requirements

Instrumentation

Essential support/personnel requirements

The test scenario is investigated and possible system failure modes are superposed against the nominal test plan. Hazards and risks resulting from the hypothetical failures are summed in the overall E_c for the test.

The following section provides a compendium of specific models and applications of risk analysis methodology developed by several of the major test ranges.

4.0 INDIVIDUAL RANGE RISK ANALYSIS TECHNIQUES

4.1 ARMAMENT DEVELOPMENT AND TEST CENTER (ADTC) RISK ASSESSMENT METHODOLOGY - A DETAILED OVERVIEW

4.1.1 Introduction

The risk assessment methodology at ADTC for air-to-ground weapons consists of three integrated computer programs and their related data bases. This section provides an overview of the three programs, interprogram data flows, related data requirements and computed outputs, and a discussion of the mathematics of risk assessment. Included also is a discussion of the basic assumptions and limitations which were imposed during the development of the program.

4.1.1.2 Risk Assessment Programs and Data Bases

As previously mentioned, the ADTC risk assessment methodology is embodied in three computer programs and their associated data bases. These programs have been structured and integrated together to enable the range safety analyst to use the best data available for a given weapon system, and test to estimate the associated risks. Since engineering design, performance and reliability data of the type required for risk assessment are often unavailable at the time risk assessments must be made, a portion of the computational methodology is designed to enable the range safety analyst to estimate these required data prior to the calculation of the measures of risk. Should these data be available from other sources, the computational methodology has provisions for their usage.

The three computer programs which together comprise the computational portion of the ADTC risk assessment methodology are called PTRAJ, DENGEN and RISK. The relationship between these programs, the interprogram data flows and their associated data bases are shown in Figure 4-1-1 and Figure 4-1-2.

Program PTRAJ is a 3-degree of freedom (3-DOF) trajectory generation program. It provides a means for simulating the performance of thrusting, maneuvering and guiding air-launched vehicles. Its function in the risk assessment methodology is to provide a means for generating nominal test flight profiles and for adjusting the actual or estimated aerodynamic data, thrust profiles and guidance constants for a given vehicle to enable the 3-DOF simulation to closely match the predicted performance profiles generated by more detailed 6-DOF simulations. The primary outputs of Program PTRAJ are the adjusted vehicle specification data and nominal test trajectories. A report entitled "A Guided Vehicle Impact Predictor for Use in Statistical Models"[1] describes the computational details, the input/output (I/O) and the user instructions for Program PTRAJ. Subparagraph 4.1.3 to this section provides an overview of Program PTRAJ.

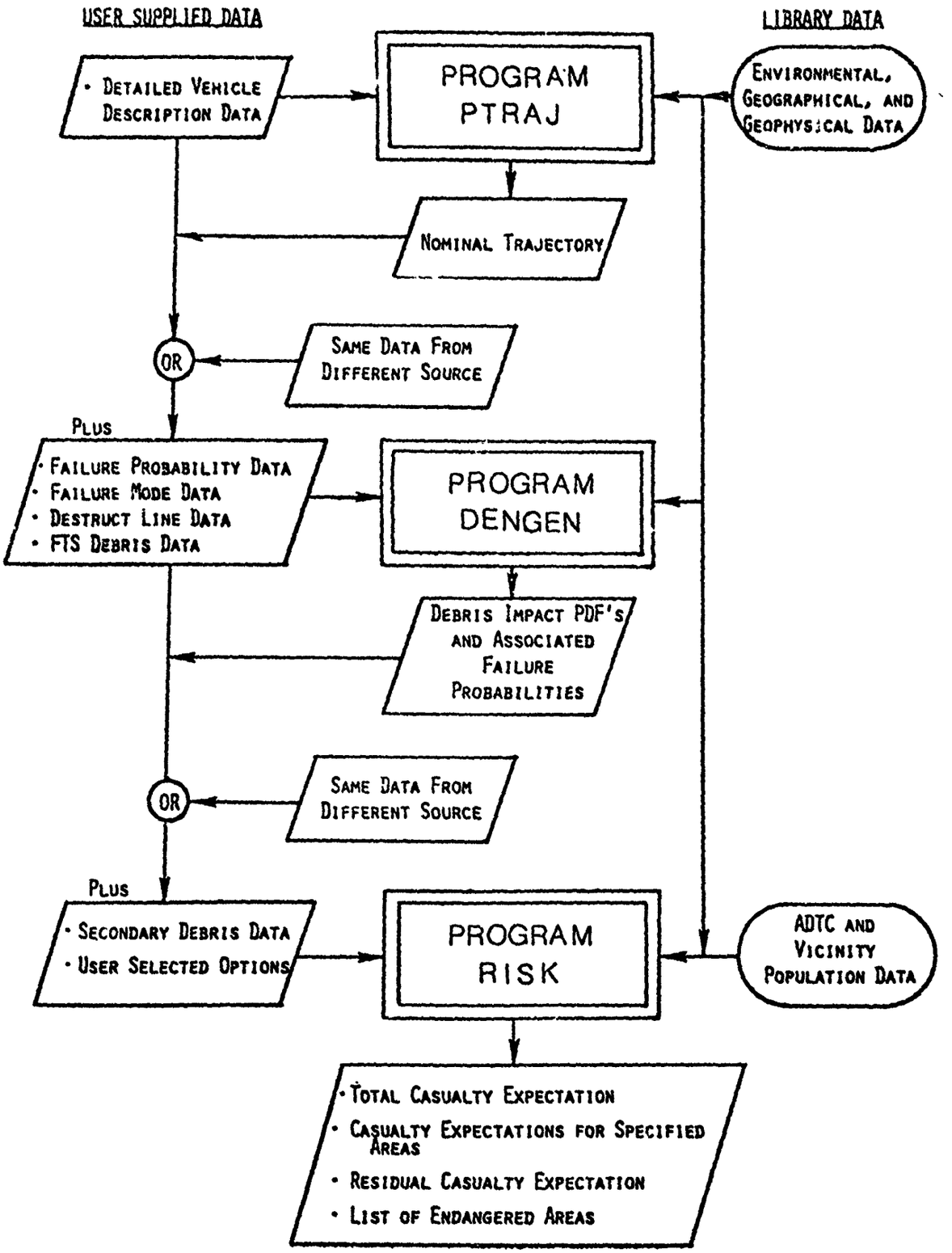

Figure 4-1-1. ADTC Risk Assessment Methodology Program Interaction and Data Flows

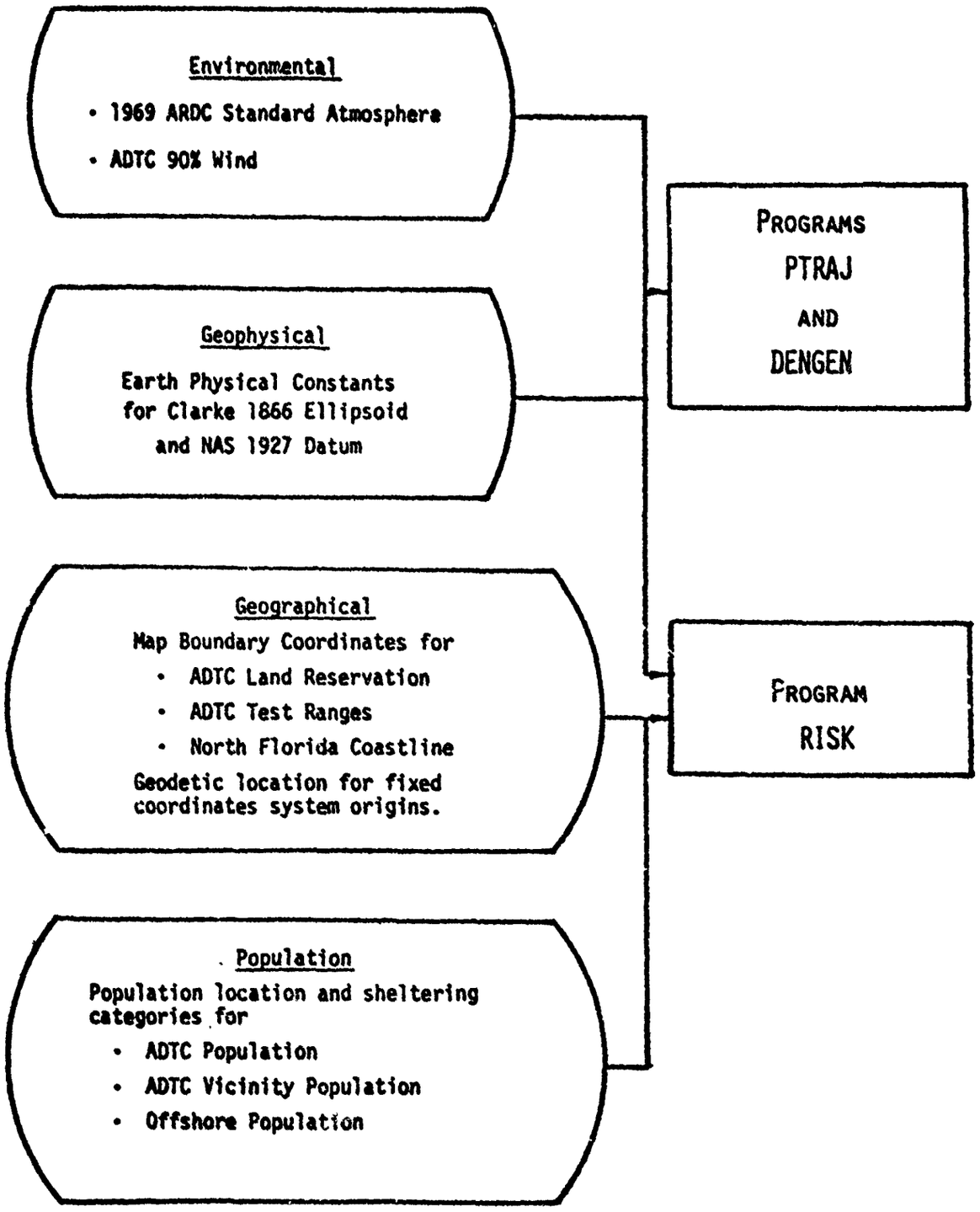

Figure 4-1-2. Risk Assessment Library Data Bases

Program DENGEN is a Monte Carlo program which calculates the debris impact probability density functions (PDFs) associated with a failed vehicle. The computational core of Program DENGEN is the impact predictor portion of Program PTRAJ. The guidance models of Program PTRAJ are supplemented by guidance failure mode effect models, and the propulsion model is supplemented with a thrust failure mode effect model. The program uses Monte Carlo sampling techniques to derive bivariate tabular descriptions and the associated statistics for the debris impact PDF. The derived PDFs include the effects, when appropriate, imposed by the use of flight termination systems (FTS) and the resulting types of debris. Program DENGEN also makes use of computational techniques to estimate the sufficiency of the Monte Carlo sample sizes and multivariate nonlinear regression techniques to improve the quality of the PDF representations.

The report entitled "Program for Generating Debris Impact Probability Density Functions (Program DENGEN)"[2] describes the computational details, the program I/O and the user instructions for Program DENGEN. The report entitled "Impact Probability Density Function Enhancement"[3] describes the computational details for determining sample size sufficiency and the multivariate regression techniques employed.

Program RISK is the program which actually calculates the measures of risk associated with a specific weapon test. This program requires the output of both Programs PTRAJ and DENGEN or comparable data from other sources. Program RISK is particularized to ADTC. The program uses both built-in and external data bases which are dependent upon geometry, coordinate systems and geographical, geophysical and statistical data which have application only to ADTC and its immediate environs. The computational algorithms contained in Program RISK are ADTC particularizations of computational algorithms which were evolved over a long period of time and which have a history of application at other national test ranges.

The report "Risk Assessment Program - Phase II"[4] describes the computational details, program I/O, available options, and user instructions for Program RISK. The report "Population Library Update II"[5] describes the data base containing population related data for ADTC and its environs. Numerous other source documents (references 6 through 9) describe other data items and data sets particular to ADTC and which are built into Program RISK.

A portion of the ADTC risk assessment methodology which is still evolving is the data bases comprised of the outputs of Program PTRAJ and DENGEN. These data which consist of vehicle descriptions, failure modes, PDFs, etc., are for specific weapon types and tests, and are valuable for estimating performances of future or hypothetical weapon types and tests for which there currently exist little or no useable data.

4.1.2 The Mathematics of Risk Assessment at ADTC

4.1.2.1 A Definition of Risk

The risk associated with the conduct of a specific weapon test is of a probabilistic nature. It is measured by calculating the statistical estimate of the number of injuries expected to occur as a result of the test. This measure is called the casualty expectation and is denoted by E_C. It is important to note that for range safety purposes, an injury is considered to be any type of bodily harm and this includes, of course, fatalities.

The primary phenomena associated with inert weapon tests which can cause bodily harm are overpressure and flying debris. Other factors are important but can be considered as contributors to one or both of the basic phenomena. The phenomena associated with live weapon tests include, additionally, fire and secondary debris. Because the region hazarded by fire is generally less than that for either overpressure or flying debris, the measure of risk, i.e., casualty expectation, can be defined as the number of injuries expected to occur as a result of exposure to overpressures greater than 2 psi[10] or of being struck by flying debris - primary or secondary - with impact energies greater than 33.3 ft-lbs.[10]

4.1.2.2 The Calculation of E_C

4.1.2.2.1 Data Bases for E_C Calculations

There are numerous data items necessary to support the E_C analysis which are not test dependent and for which values have been compiled and stored in data bases for use from test to test. Some of these data require periodic updating and some are nominal values. Whenever data other than the nominal are required, they must be explicitly provided by the user. These data and their relationship to the risk assessment programs are shown in Figure 4-1-2.

4.1.2.2.1.1 Environmental Data Base

The environmental data base consists of values selected from the 1969 Air Research Development Command (ARDC) Standard Atmosphere and supplemented with the 90 percent wind data for ADTC (see references 8 and 9). These data are required by the impact predictor portions of Programs PTRAJ, DENGEN and RISK.

4.1.2.2.1.2 Geophysical Data Base

The geophysical data base consists of the earth physical and geopotential constants for the 1866 Clarke Ellipsoid and 1927 National Academy of Science (NAS) Datum (see reference 9). These data fit ADTC and its environs very well and are required by the impact predictor portions of Programs PTRAJ, DENGEN and RISK.

4.1.2.2.1.3 Geographical Data Base

The geographical data base consists of several sets of coordinate data. These data sets correspond to points along the boundaries of the ADTC land reservation, several of the major ADTC test areas and the north Florida coastline. These data are used in Program RISK for drawing maps which show the population regions of major concern. Contained in this data set are also the geodetic locations of the earth fixed reference coordinate system origins.

4.1.2.2.1.4 Population Data Base

The population data base contains the location names and sizes, number of people present, and the amount of sheltering afforded the population for all known population areas on and within the vicinity of ADTC. The geographical region covered by this data base extends from Mexico Beach, Florida, westward to Mobile, Alabama, and from about 200 nautical miles offshore northward to the Alabama state line. This data base is updated periodically and is documented in reference 5.

4.1.2.2.2 E_c Calculation Overview

Superficially, the calculation of E_c appears to be a straightforward process. This is, however, not the case. The problems encountered by the range safety analyst are virtually the opposite of those encountered by the weapon system design and test engineers. During the RDT&E phases of weapon system development, the problems are centered around the performance optimization for a properly working weapon system. Such problems are generally well defined and bounded in scope. Further, there exists a wealth of technology and applicable historical data for addressing these problems. In contrast, the range safety analyst is concerned with the understanding and prediction of the behavior of weapon systems after they have malfunctioned in any of a variety of failure modes. These failure mode processes are inherently poorly defined, probabilistic in nature and subject to considerable uncertainty. Further, there seldom exists during the analysis performance period any substantial data of the type required to support a detailed risk analysis.

These problems are formidable. The data voids have been filled through the utilization of predictive methodologies developed by coupling specialized range safety technology with existing broadbased RDT&E technology. It is important to note that it is imperative to the E_c calculation process that the gross behavior of a failed weapon system be predictable.

The actual calculations for the total E_c for a given weapon test proceed in a stepwise manner yielding in the process numerous calculated quantities of interest to the range safety analyst. Depending upon the quantity and quality of data available to the range safety analyst at

the time the analysis is begun, the computational process shown in Figure 4-1-1 may be entered at any one of three points. Ultimately, the computational process will require consideration in turn of each of the weapon system's failure modes, their probability of occurrence, the type and hazard potential of the resulting debris, where the debris impacts, and the effect upon the population in the region influenced by the test. In the ADTC risk assessment programs, a separate casualty expectation is calculated for each of the populated areas affected by each type of debris resulting from each of the vehicle failure modes. These individual E_c's are then accumulated in accordance with the algebra for conditional probabilities to yield an estimate for the total E_c for the weapon test.

If an E_c estimate is required for an ill-defined or hypothetical weapon, the range safety analyst would first exercise Program PTRAJ to establish a useable dynamical description for the vehicle and to develop a set of nominal flight trajectories for the proposed test. If the vehicle is well defined and nominal trajectories are available, these available data may be used in lieu of exercising Program PTRAJ.

Secondly, an analysis must be performed to establish failure related data for the vehicle. The gross failure modes and their effects must be identified and their probability of occurrence established. If an FTS is deemed necessary, a vehicle breakup description should be developed. The determination of vehicle failure modes and their probability of occurrence are among the most difficult factors to establish in the E_c analysis. Currently, estimates based upon historical data for related systems and vendor supplied analysis are considered to be the most reliable sources for these types of data.

Given the failure mode and effects data along with a dynamical description of the vehicle and a nominal test trajectory, the PDFs for the debris impact points can be derived. The debris impact PDFs are essential to the E_c calculations. Along with the failure mode probabilities of occurrence, the determination of the debris impact PDFs pose the most difficult computational requirements in the entire risk assessment process, and they are the sources of considerable uncertainty in the E_c calculations. An entire block of the ADTC risk assessment methodology, i.e., Program DENGEN, is devoted to the development of the required PDFs and to the reduction of the uncertainty in this segment of the E_c calculations. Again, should these data be available from a previous analysis or from the weapon system vendor, the use of Program DENGEN can be bypassed.

When the above described data are established, the actual E_c calculations can be performed. (The computational flow for this segment of the calculations is shown in Figure 4-1-8.) These calculations are all carried out in Program RISK along with various bookkeeping and data management calculations typical of large scale computer programs.

The components of the equation for E_c are: (1) the probability of hitting a populated area, (2) the probability of subjecting the people in the populated area to a hazard from either flying debris or from hazardous overpressures, and (3) the number of people subjected to the hazard. The probability of hitting a populated area and the probability of the people in the area being subjected to a hazard are in general different. This is because in many instances a portion of the population is protected to some degree by sheltering. The extent of the hazard is evaluated through a modeling of the impact process and the resulting secondary effects. These calculations allocate portions of the debris impact kinetic energy and energy available from unspent fuel or explosive detonations to secondary processes such as structural penetration by fragments, production of hazardous overpressures, and the production of secondary debris. The occurrence of debris impact can, but may not necessarily, result in all of these hazardous processes. Further, for a given failure mode, different types and quantities of debris are generated each of which can produce different hazardous effects upon impact. Since some of the people in the populated areas are afforded varying degrees of shelter, the hazardous effects produced by debris impact must be matched against the sheltering to determine the actual number of people hazarded.

This matching process yields a probabilty of hazard which is a function of the hit probability, the hazardous effects produced upon or immediately after impact, the type of shelter available to the people in the affected area, and the ability of the available shelter to mitigate the hazardous effects.

At ADTC, the population data are divided into three classes, and for efficiency, separate algorithms have been developed to calculate the hazard probabilities and E_c for each data class. The population concentrations located in the vicinity of ADTC are tabulated relative to a fixed grid system. The finest subdivision of this grid is a rectangular area with dimensions of ½ minute by ½ minute. The population in this area is assumed to be uniformly distributed and afforded no shelter. The population located on ADTC is assumed to be concentrated in the various buildings which are in turn located at various places on the ADTC land reservation. The population concentrations in these buildings are afforded varying degrees of shelter ranging from no shelter to the equivalent of four inches of reinforced concrete. Lastly, there are certain parts of the ADTC land reservation which are open to public usage for hunting, fishing, hiking, etc. In these areas the population is assumed to be uniformly distributed, afforded no shelter, and the density dependent upon the season. This population is referred to as the residual population.

For the population located in the ½ minute by ½ minute regions, the hit probability is determined by integrating the impact PDF function for each

specific debris type over the area. Thus, for the ith area, jth failure mode and kth debris type, the hit probability is given by

$$P_{H_{ijk}} = \int_{A_i} f_{jk}(A)dA, \qquad (1)$$

where

f_{jk} (A) is the debris impact PDF for the jth failure mode and kth debris type,

A_i is the ith populated area.

The hazard probability is then calculated from

$$P^{12}_{HAZ_{ijk}} = P_{H_{ijk}} A_{H2}/A_i \qquad (2)$$

where

A_{H2} is the hazard area associated with a 2 psi overpressure and any secondary debris generated at impact.

The probability of hazard to the residual population is calculated in the same fashion except that the integration is carried out over the area containing the residual population.

For the population located within a specific building, the hazard probability is broken into four separate and mutually exclusive parts to account for the mitigation of the hazardous effects by the available shelter. In this instance both impacts on and in the near vicinity of the building are accounted for in terms of their generated overpressures and primary debris penetration capability. The four hazard probabilities are obtained by integrating the distribution of impact points over the areas within and around the buildings that are affected by each of the hazardous processes. Thus,

$$P^{N2}_{HAZ_{ijk}} = \int_{I \varepsilon A_N} f_{jk}(A)dA \quad , \qquad N= 1, 2, 3, 4 \qquad (3)$$

where

A_N refers to the area affected by the Nth (N = 1, 2, 3, 4) hazardous process,

N=1 Area A_1 is contained completely within A_1. The 2 psi overpressure applies to all populations identified by the debris penetration flags,

=2 Area A_2 contained partially within A_1. The 2 psi overpressure applies to all population identified by the debris penetration flags,

=3 impacts occur exterior to building perimeter but 2 psi overpressure applies to that fraction of population contained in A_3 which is unsheltered,

=4 impacts occur exterior to building perimeter. The 30 psi overpressure applies to that fraction of population contained in A_4 which is sheltered by less than four inches of reinforced concrete.

Once the probability of hazard from the primary debris impact has been determined, the casualty expectation can be calculated. Thus, the E_C for the ith populated area due to the kth debris type generated as a result of the occurrence of the jth failure mode can be written as

$$E_{C_{ijk}} = (P^{12}_{HAZ_{ijk}} + P^{22}_{HAZ_{ijk}}) \sum_{\ell=1}^{3} N^{i}_{pc_\ell} S^{jk}_{pc_\ell} \tag{4}$$

$$+ P^{32}_{HAZ_{ijk}} (N^{i}_{pc_2} + N^{i}_{pc_3}) + P^{42}_{HAZ_{ijk}} N^{i}_{pc_1},$$

where

$N^{i}_{pc_\ell}$ = number of people in the ith building protected by the ℓth level of sheltering,

$S^{jk}_{pc_\ell}$ = Penetration flag denoting whether or not the jkth debris type can penetrate the ℓth shelter level.

For both the residual population areas and the population areas in the vicinity of the ADTC land reservation,

$$P^{22}_{HAZ_{ijk}} = P^{32}_{HAZ_{ijk}} = P^{42}_{HAZ_{ijk}} = 0. \tag{5}$$

To calculate the total E_c for a given test, the E_c's for each debris type and failure mode must be accumulated. This process requires estimates for the probabilities of occurrence for each failure mode and FTS generated debris type. Program DENGEN calculates estimates for the probability of occurrrence for each debris type given the occurrrence of a specific failure mode. These debris types are: (1) the intact vehicle, which assumes that either the FTS was not employed or it failed; and (2) up to three categories of fragments which differ in weight and/or ballistic coefficient. The fragment occurrence probabilities as calculated in DENGEN are denoted by P_{IV} and P_F, and the E_c for a given (jth) failure mode is given by

$$E_{c_j} = \sum_{i=1}^{N_P} (P_{IV} E_{c_{ij}} + (1-P_{IV}) P_f \sum_{k=2}^{N_F} E_{c_{ijk}}). \tag{6}$$

The ADTC risk assessment program can handle the probability of failure mode occurrence in any one of several ways depending upon the type and availability of data. First, the failure probability may be modeled by a Weibull or exponential distribution, or if similar weapon type historical data are used, the failure probability can be estimated as a function of the current test number. If insufficient data are available to model the failure probability as a function with reliability, mean-time-between-failure (M-T-B-F), or current test number as the independent variable, historical data may be used to estimate the failure probability as a single number. In any case, the end result is an estimate of the probability that a given failure mode occurs, and this number is denoted by P_{Fail_j}. The conditional probability that the jth failure mode occurs and not the others is given by

$$CP_{Fail_j} = (1-CP_{Fail_{j-1}}) P_{Fail_j} \tag{7}$$

where

$$CP_{Fail_1} = P_{Fail_1}$$

The total E_c for the test due to all failure modes is given by

$$E_{c_T} = \sum_{j=1}^{N_{FM}} CP_{Fail_j} E_{c_j} \tag{8}$$

The set of casualty expectations denoted by E_{c_T}, E_{c_j} and $E_{c_{ijk}}$ are the end item outputs of Program RISK.

4.1.3 Program PTRAJ Overview

4.1.3.1 PTRAJ Background

Program PTRAJ is a modified version of the ADTC Program P2020.[9] Program P2020 in its original form possessed many of the features required of an impact predictor algorithm slated for use in a statistical model designed to produce impact PDFs. Although it did not have a guidance model or a thrust model, the program structure was such that these features could be easily added. Reference 1 documents the modifications to Program P2020 and the algorithms which were added to give it the required capabilities.

4.1.3.2 Program PTRAJ Computational Sequence

Program PTRAJ is a 3-DOF trajectory generation program. It is set up to calculate the trajectory of an air-to-ground thrusting, guiding vehicle. It assumes that the target is stationary and that the guidance system employs a proportional navigation guidance law. The equations of motion are set up relative to an earth defined by the 1966 Clarke spheroid and 1927 NAS Datum. The aerodynamic forces are evaluated based upon the 1969 ARDC Standard Atmosphere and the 90 percent wind table for ADTC. The macro flow diagram for Program PTRAJ is shown in Figure 4-1-3.

4.1.3.3 Program PTRAJ I/O

4.1.3.3.1 PTRAJ Input Data

The input data for Program PTRAJ are broken into two classes: (1) the library data and (2) the user supplied data. The mathematical, geophysical and environmental data which are peculiar to ADTC are built directly into the program. Further, the most commonly used values for the user supplied data are also built directly into the program. Having such library data built into the program greatly simplifies the data deck setup and facilitates the program usage.

The user furnished data are supplied to Program PTRAJ in NAMELIST format. Use of NAMELIST further simplifies the program usage and aids in the elimination of clerical or bookkeeping errors. The NAMELIST data are shown in Table 4-1-I.

4.1.3.3.2 PTRAJ Output Data

The output from Program PTRAJ is basically a position/velocity time history augmented by guidance and force data. The guidance and force

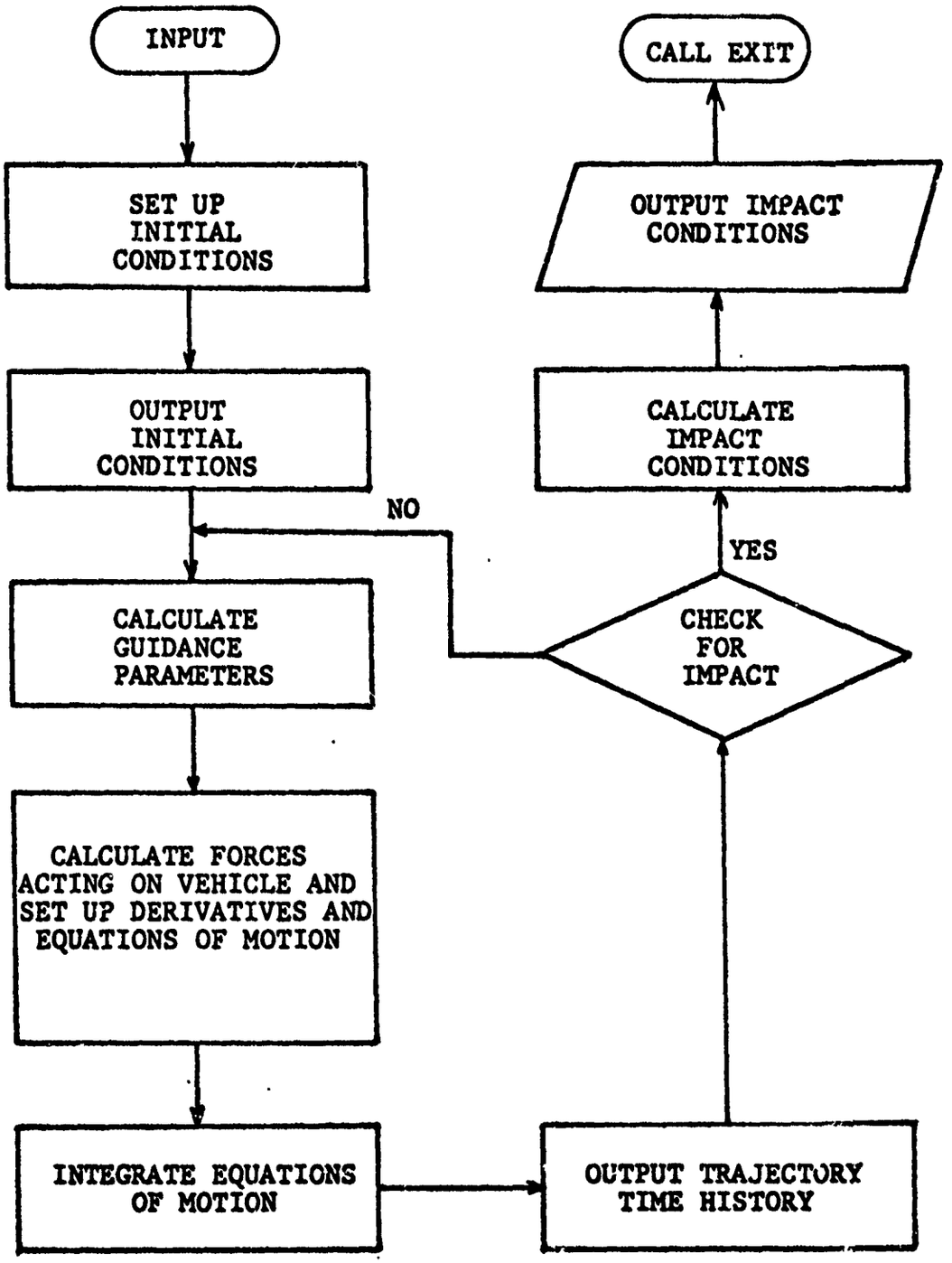

Figure 4-1-3. PTRAJ Macro Flow Diagram

Table 4-1-I

PTRAJ Namelist Data

TMACH	Vector of mach number values (up to 10 values) in the table lookup for C_A and C_N.
TALPHA	Vector of angle of attack values (up to 10 values) used in the table lookup for C_A and C_N.
TABCNA	Table of normal force coefficient values corresponding to the values in TMACH and TALPHA (up to 100 values).
TABCA	Table of axial force coefficient values corresponding to the values in TAMCH and TALPHA (up to 100 values).
TABTHR	Table of thrust vs time values (up to a total of 30 values)
NMACH	Number of values in TMACH
NALPH	Number of values in TALPHA
NP	Number of thrust values in TABTHR
NAVCON	Navigation constant used in proportional guidance routine.
ALPHAD, BETAD	Initial values for pitch angle of attack and sideslip angle
TLAT, TLON	Latitude and longitude of target
GLATLM	Lateral acceleration limit
ADLIM, BDLIM	Limits on $\dot{\alpha}$ and $\dot{\beta}$
ALPLIM, BETLIM	Limits on α and β
PVHIST	Nominal time history trajectory $(t,x,y,z,\dot{x},\dot{y},\dot{z})$
PHIORI, LAMORI, PSIORI	Latitude, longitude and azimuth of the x-axis used in PVHIST. Normally PHIORI and LAMORI will correspond to the launch point.
WEATHER	Table defining reference atmosphere and wind to be used in lieu of a standard atmosphere.

Table 4-1-I (Continued)

IWEATH	Number of data vectors in WEATHER table
NOWIND	= 0 Zero out wind values = 1 Use wind values
NOLIFT	= 0 Do not calculate C_N from table = 1 Calculate C_N from table
NODRAG	= 0 Use CAO or ABETA to calculate C_A = 1 Calculate C_A from table
NOTHRUST	= 0 Set thrust to zero = 1 Calculate thrust from table
CAO	User supplied constant value for C_A
DT	Integration step size
IFLAG	= 0 Do not modify integration step size = 1 Halve or double step size as necessary
LOD	L/D ratio can be used instead of a lift coefficient table to calculate lift
ABETA	Ballistic coefficient (not necessary if CAO or drag table is supplied)
BALTRJ	= 0 Unguided trajectory = 1 Guided trajectory
T	Initial time
WEIGHT	Vehicle weight
AREF	Aerodynamic reference area
IOUT	= 0 Print out intermediate data = 1 Suppress all intermediate output

data may be suppressed if desired. Table 4-1-II describes the output data format and Table 4-1-III shows a sample output page.

4.1.3.4 Program PTRAJ Uses

Program PTRAJ is embodied as an impact point predictor in each of the programs used in the ADTC risk assessment methodology. In Programs DENGEN and RISK all of the I/O subroutines were stripped away and the impact point prediction algorithms and data bases were incorporated intact. PTRAJ also has uses as a stand-alone program in the ADTC risk assessment methodology. It serves as a tool to test the aerodynamic and performance descriptions of advanced weapon systems for later use in DENGEN and RISK. Additionally, PTRAJ serves as a tool to generate nominal flight profiles which are frequently required in risk assessment analyses.

4.1.4 Program DENGEN Overview

4.1.4.1 DENGEN Background

Program DENGEN calculates debris impact PDFs using a combination of Monte Carlo sampling, dynamic simulation, failure mode effects modeling and multivariate nonlinear regression techniques. Program DENGEN was developed to fill data and capability voids and the deficiencies identified in references 11, 12, and 13. The historical approach to the debris impact PDF problem was to assume that the debris would all be contained within the maximum energy boundary of the tested vehicle and within that boundary the debris would be normally distributed. Reference 12 showed by example that the debris distributions were not normally distributed, and reference 13 showed that the E_c calculations were affected adversely by the assumption of normality. Further, the maximum energy boundaries associated with advanced weapons and targets are so large that their usage would impose unrealistic constraints upon the design of weapon tests and also imply a complete lack of capability to control the locus of debris impacts through the use of an FTS.

Program DENGEN simulates the vehicle failure mode effects and accounts for the effects of FTS usage including debris types and geometry. The resulting debris impact PDFs, because they are convolved from numerous event distributions which themselves are abnormal, are generally abnormal, multimodal and asymmetrical.

4.1.4.2 Program DENGEN Computational Sequence

The primary purpose of Program DENGEN is to provide debris impact PDFs for use in Program RISK. These PDFs are calculated in DENGEN and stored on permanent disk files for later usage by Program RISK. Because there

Table 4-1-II

Explanation of Printout Heading Parameters

POSITION	TIME	X XDD	Y YDD	Z ZDD	XD XMT	YD	ZD
GUIDANCE		ALPHA ALPHAT	BETA SIGR	LOSP GAMMAV	LOSS PSIV	LOSPD	LOSYD
FORCES		FA MACH	FB VEL	FA1 Q	FX CN	FY CA	FZ LAT ACC

TIME	-	time from launch (sec)
X, Y, Z		X,Y,Z coordinates of vehicle (ft)
XD, YD, ZD	-	$\dot{X},\dot{Y},\dot{Z}$ rectangular components of vehicle velocity (ft/sec)
XDD, YDD, ZDD	-	$\ddot{X},\ddot{Y},\ddot{Z}$ rectangular components of vehicle acceleration (ft/sec/sec)
XMT	-	missile target separation distance (ft)
ALPHA, BETA	-	pitch and sideslip angles of attack (deg)
LOSP, LOSS	-	pitch and sideslip plane missile/target line-of-sight angles (deg)
ALPHAT, BETA	-	total angle of attack and effective roll angles (deg)
GAMMAV	-	flight path angle (deg)
PSIV	-	azimuth of velocity vector (deg)
FA, FB, FA1	-	forces along the A, B and A1 axes (lbs)
FX, FY, FZ	-	forces along the XYZ axes (lbs)
MACH	-	vehicle mach number (-)
VEL	-	vehicle speed (ft/sec)
Q	-	dynamic pressure (PSF)
CN	-	normal force coefficient

Table 4-1-II (Continued)

CA	-	axial force coefficient
LAT ACC	-	lateral acceleration (g's)

Table 4-1-III

Sample Output Data with Intermediate Print

T=78,ALT=50000,GUIDED, WITH INTER PRINT

POSITION	TIME	X	Y	Z	XD	YD	ZD
		XDD	YDD	ZDD	XMT		
GUIDANCE		ALPHA	BETA	LOSP	LOSS	LOSPD	LOSYD
		ALPHAT	SIGR	GAMMAV	PSIV		
FORCES		FA	FB	FA1	FX	FY	FZ
		MACH	VEL	0	CN	CA	LAT ACC
POSITION	123.00	-.14804E+05	.31008E+04	-.20846E+06	85.89	-1089.83	-450.92
		-6.88	3.34	35.81	.44035E+04		
GUIDANCE		-2.60	.03	3.90	-.01	-.61	-.00
		2.60	179.39	-80.38	-79.21		
FORCES		-1.434	.007	-.650	-.216	1.105	1.100
		1.05	1182.55	1435.53	.000453	.000999	.650
POSITION	123.50	-.14762E+05	.25563E+04	-.20868E+06	82.43	-1088.00	-432.94
		-6.92	3.69	36.00	.38155E+04		
GUIDANCE		-2.68	.03	3.60	-.01	-.61	-.00
		2.69	179.40	-67.16	-79.22		
FORCES		-1.436	.007	-.673	-.217	1.116	1.106
		1.04	1173.87	1437.69	.000468	.000999	.674
POSITION	124.00	-.14721E+05	.20128E+04	-.20889E+06	78.94	-1086.00	-414.81
		-6.98	4.01	36.27	.23216E+04		
GUIDANCE		-2.79	.03	3.30	-.01	-.59	-.00
		2.79	179.41	-67.95	-79.22		
FORCES		-1.438	.007	-.701	-.219	1.126	1.115
		1.03	1165.23	1439.45	.000487	.000999	.701

are generally several failure modes associated with a given weapon type, and because the PDF development process is iterative, it is generally best to develop PDFs for one failure mode at a time. DENGEN can consider multifailure modes simultaneously, but from a user point of view this is not recommended.

The macro level computational flow for Program DENGEN is shown in Figure 4-1-4. Essentially, the computational sequence involves the following steps:

1. Input all data to the program and perform mission-level data setup.

2. Setup failure mode particular data.

3. Monte Carlo sampling begins by selecting a random failure time from the failure time distribution.

4. Determine the vehicle state vector from the nominal trajectory for the failure time.

5. Determine the β dependent, failure mode dependent impact point.

6. If a destruct line violation occurred, determine the impact points for the debris.

7. Store the data for statistical processing.

8. If more samples are to be calculated, return to step 3. Otherwise, proceed.

9. Sort all data into bivariate histograms according to debris type.

10. Calculate means and variances as a function of sample size and also calculate event probabilities.

11. Filter the histogram data using a bivariate parabolic regression scheme.

12. Plot and store all data.

13. Setup update files so process can be continued if deemed necessary.

14. If additional failure modes are to be considered, return to step 2. Otherwise, terminate sequence.

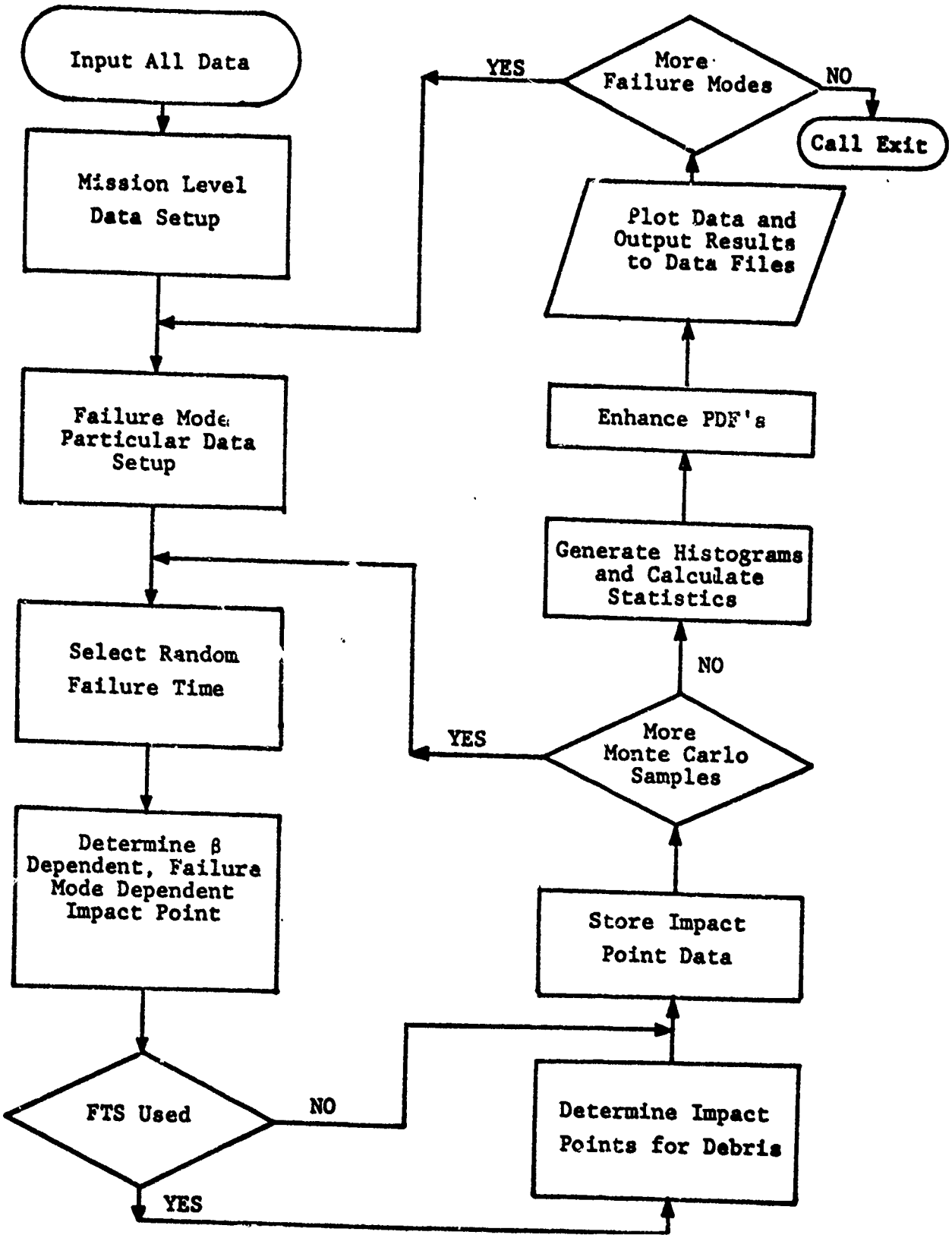

Figure 4-1-4. DENGEN Macro Flow Diagram

4.1.4.3 Program DENGEN I/O

4.1.4.3.1 DENGEN Input Data

The user furnished data for Program DENGEN are supplied to the program in the NAMELIST format. The required data consist of any array of failure mode data and a list of related data plus all of the data required by Program PTRAJ (see Table 4-1-I). The additional data required by DENGEN are described in Table 4-1-IV and the contents of the failure mode data array are shown in Table 4-1-V.

4.1.4.3.2 DENGEN Output Data

The output data for Program DENGEN consist of tabulated data, plotted data and permanent file data. The tabulated and plotted data provide the range safety analyst with a hard copy of the calculated results. The permanent file data are available for data set update and for use by Program RISK. Figures 4-1-5 through 4-1-7 provide examples of DENGEN plotted outputs.

4.1.5 Program RISK Overview

4.1.5.1 RISK Background

Program RISK is the final element in the ADTC risk assessment methodology as shown in Figure 4-1-1. This program was developed to be applicable to the broad spectrum of air-to-ground weapons types planned for testing at ADTC in the present to 1985 time frame.

Because of factors particular to ADTC, the risk assessment methodologies, which have been developed over a number of years and which have been employed at other national ranges, have been tailored to meet ADTC's particular needs. These ADTC-particular factors include:

1. the nonuniform and occasional high density distribution of population on and in the near vicinity of ADTC,

2. the irregular boundary of the ADTC land reservation,

3. the diversity of weapon types tested and the varied manners in which the performance and failure mode characteristics are described,

4. the nonlinear character of the advanced air-to-ground weapon trajectories, and

5. the size of the controlled air and ground space at ADTC relative to the range and maneuverability limits of the advanced weapons to be tested.

Table 4-1-IV

DENGEN Input Data Required in Addition to PTRAJ Data

NFM	- Total number of failure modes being considered
FMODE	- Array of failure mode defining type, effect, probability of occurrence, and FTS fragment types. Contents detailed in Table 4-1-V.
DLCLL	- Latitude and longitude of destruct line corner points
NDLCP	- Number of destruct line corner points
FTSREL	- Reliability of the FTS
NMCSMP	- Number of Monte Carlo points to be calculated for data sample
IPLOT	- Plot control flag
ENHANCE	- Data enhancement control flag
SEED	- Initial value for random number generator
INITFLG	- Flag specifying whether or not a previous data set is being updated
CAERO	- Aerodynamic coefficient modifier
CPROP	- Propulsion table modifier

Table 4-1-V

Failure Mode Data Array Structure

FMODE(20,10)

IFM = Failure mode subscript

NFM = Maximum number of failure modes

FMODE(1,IFM)		Guidance effect flag
	=1	normal guidance
	=2	ballistic $\alpha = \beta = 0$
	=3	hold last command
	=4	hard turn
	=5	seeker wandering
FMODE(2,IFM)		Propulsion effect flag
	=1	normal propulsion
	=2	thrust out
	=3	thrust variant
FMODE(3,IFM)	T_1	Initial failure time
FMODE(4,IFM)	T_2	Final failure time
FMODE(5,IFM)	Q_1	$= P(T_1)$ or σ
FMODE(6,IFM)	Q_2	$= P(T_2)$ or $\overline{m}$
FMODE(7,IFM)		Failure time distribution type
	=1	uniform
	=2	normal
	=3	trapizoidal
	=4	exponential
FMODE(8,IFM)		Symmetry flag
	=1	Yes
	=2	No
FMODE(9,IFM)		Number of FTS fragment types
FMODE(10,IFM)		W_T of fragment type 1
FMODE(11,IFM)		β of fragment type 1
FMODE(12,IFM)		W_T of fragment type 2

Table 4-1-V (Continued)

FMODE(13,IFM)	β of fragment type 2
FMODE(14,IFM)	W_T of fragment type 3
FMODE(15,IFM)	β of fragment type 3

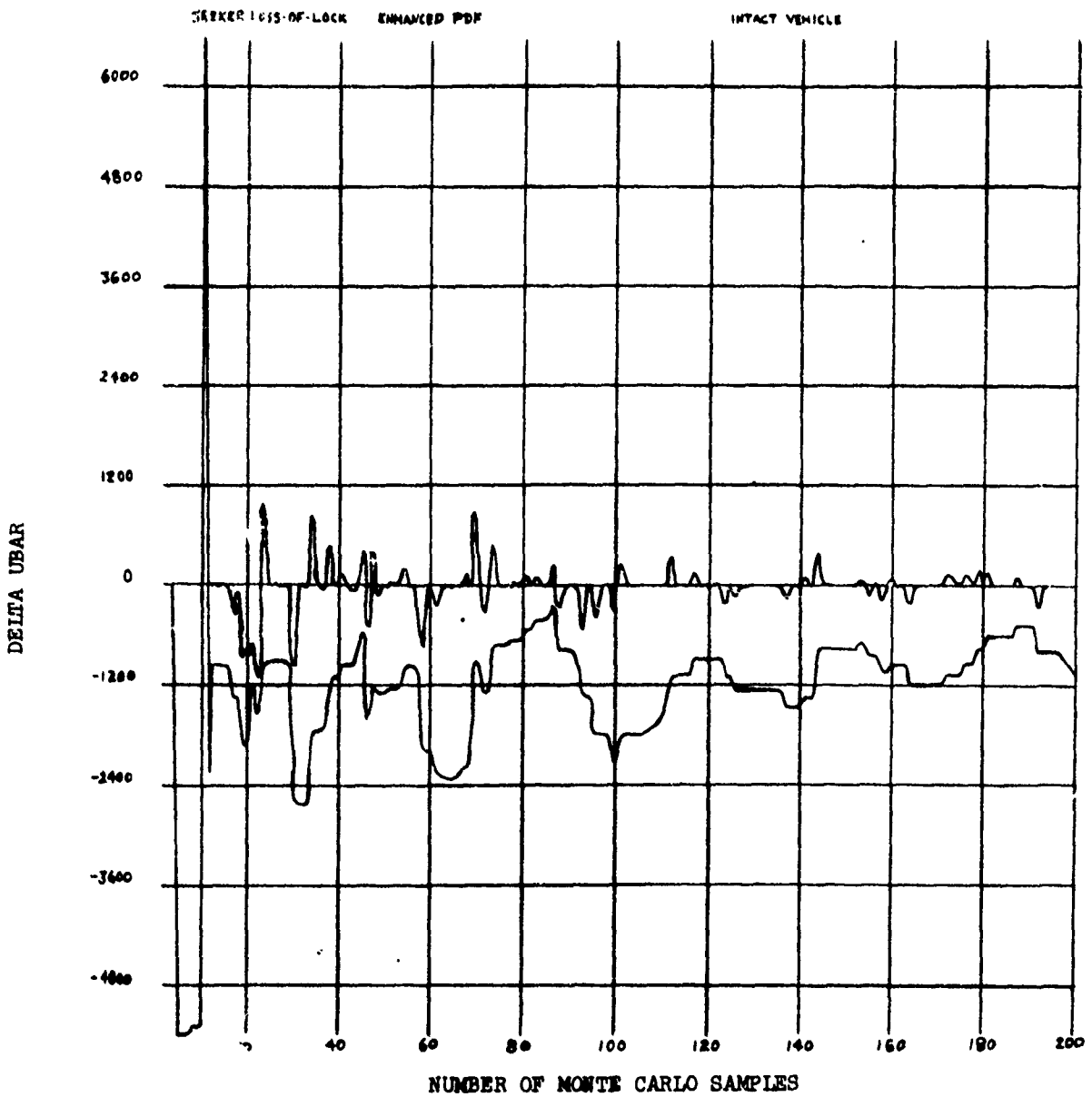

Figure 4-1-5

Sample DENGEN Output Showing Rate of Convergence of Pdf Mean and Standard Deviation for U Coordinate

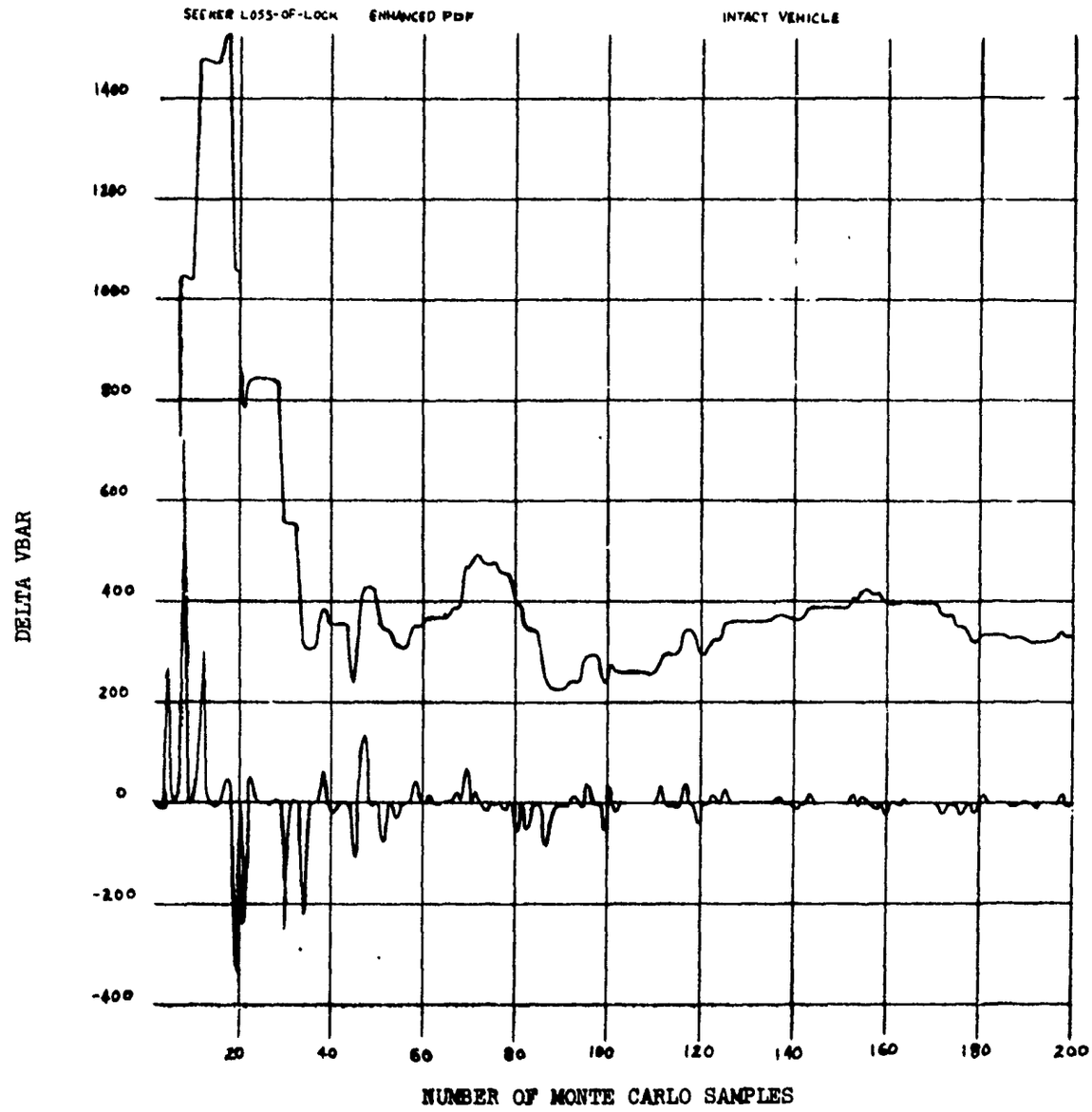

Figure 4-1-6

Sample DENGEN Output Showing Rate of Convergence of the Pdf Mean and Standard Deviation for V Coordinate

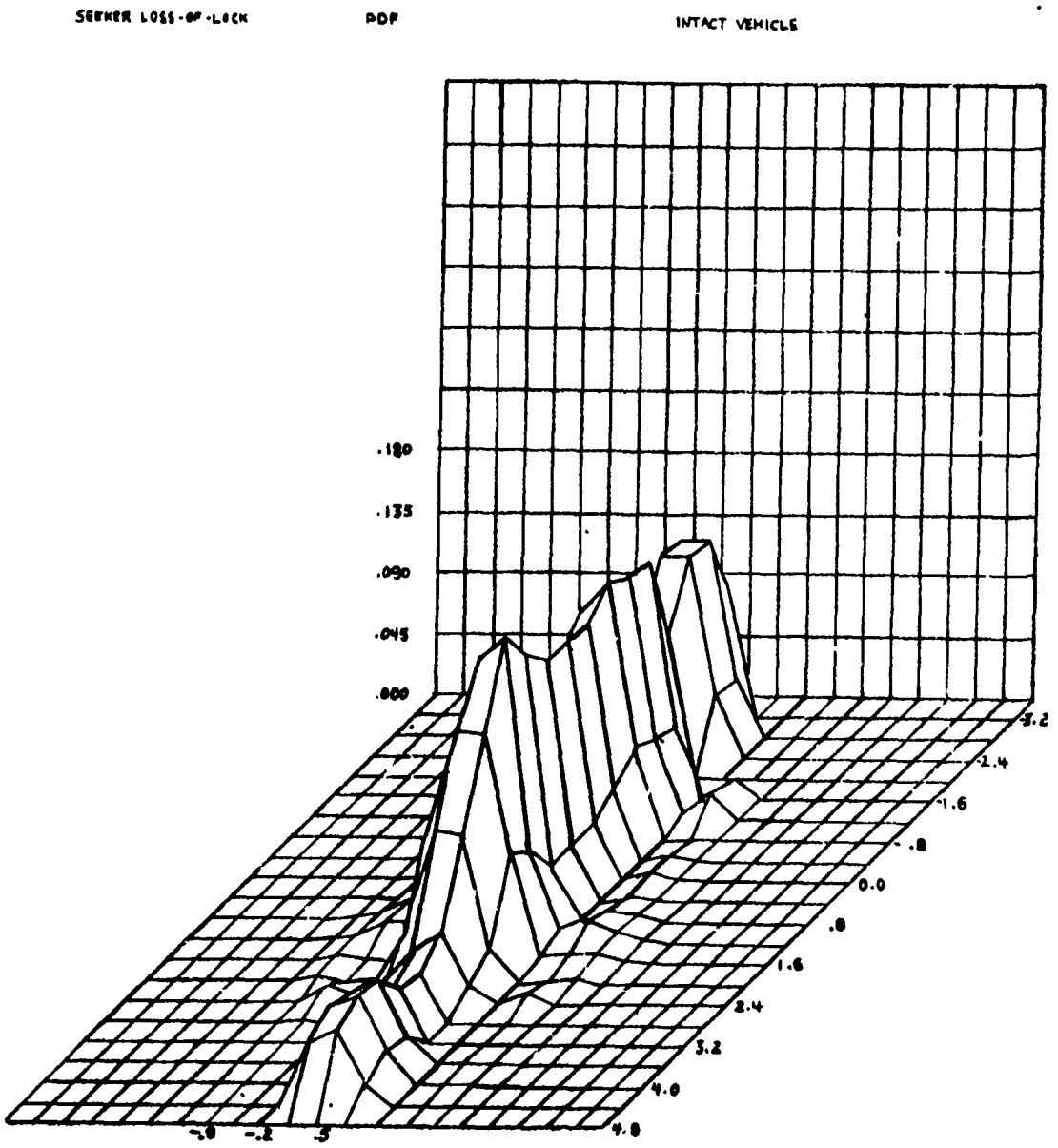

Figure 4-1-7

Sample DENGEN Output Showing Shape of Computed Pdf for Impacts of the Intact Vehicle

The inclusion of these factors along with the factors common to all test ranges requires numerous lengthy and repetitive calculations. These calculations are performed by Program RISK.

4.1.5.2 Program RISK Computational Sequence

As the final element in the ADTC risk assessment methodology, it is Program RISK that actually calculates the measures of risk, i.e., the casualty expectations associated with a given weapon test. Embodied in Program RISK is the logic necessary to perform the E_c calculations described in section 4.1.2.2.2 for air-to-ground weapon tests conducted at ADTC. To do this RISK requires the output of both Programs PTRAJ and DENGEN or comparable data from other sources.

Program RISK is a very general program and offers the range safety analyst a large number of options. The large number of user options available in RISK are necessary for RISK to be applicable to the wide variety of problems which arise at ADTC. These options enable the user to deal with the many weapon types considered at ADTC, the multitude of ways in which performance data are presented or not presented, and the general lack of available data or failure modes and effects. In addition, the user options enable the analyst to present the calculated results in varying degrees of detail, both plotted and printed, to meet any particular reporting requirements.

The macro level flow diagram for Program RISK is shown in Figure 4-1-8. The computational sequence shown involves essentially the following steps:

1. Input NAMELIST data to the program and perform initial data setup.

2. Input DENGEN data, if available, and skip to step 5. Otherwise, proceed.

3. Calculate the mean impact point for each failure mode.

4. Calculate the failure probability for each failure mode.

5. Calculate the debris hazard area and debris penetration categories for each failure mode.

6. Establish failure mode hazard area bounds.

7. From the master population library, select those population areas subjected to a possible hazard by each failure mode.

8. Calculate a conditional E_c for each of the selected population areas for each failure mode and debris type.

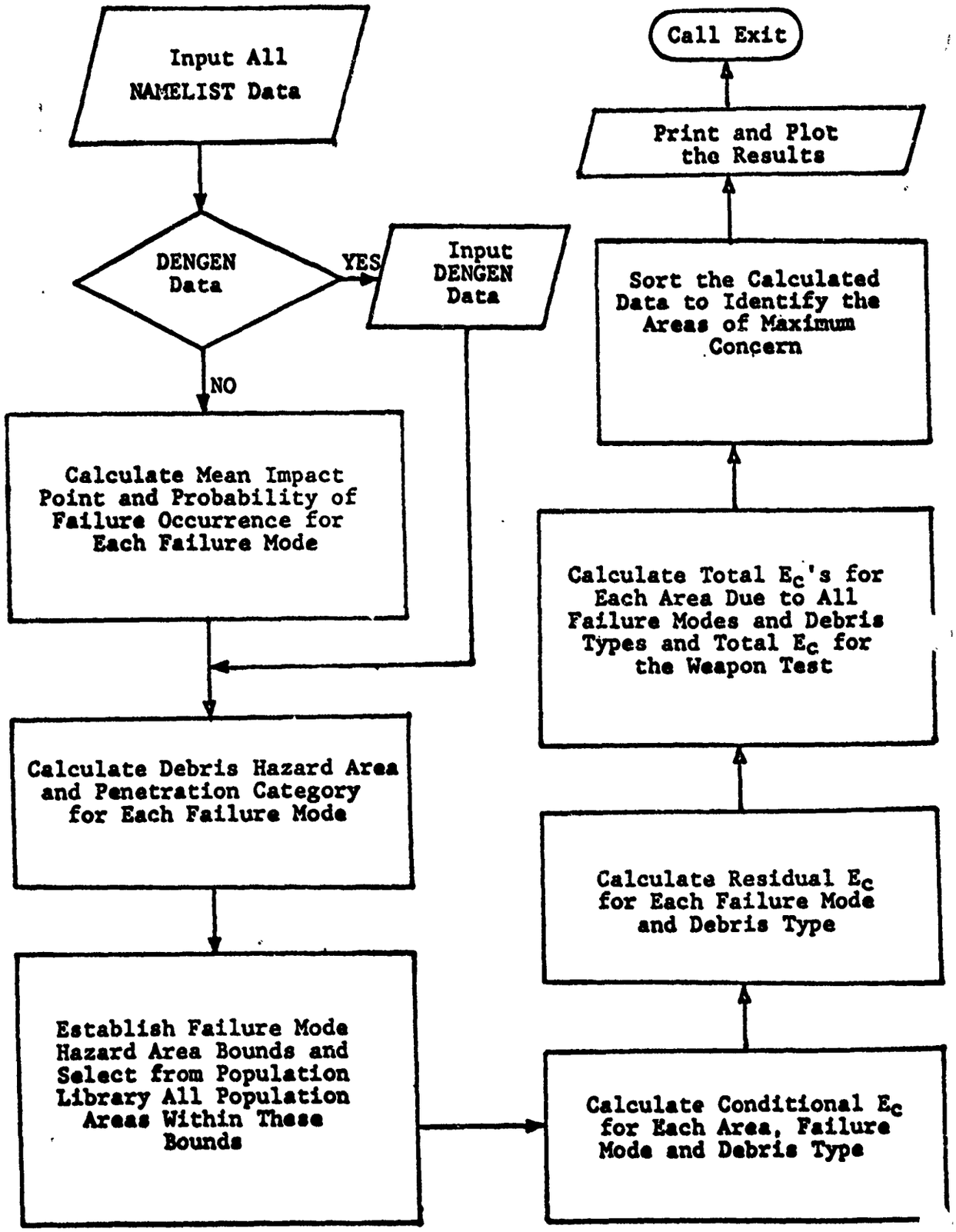

Figure 4-1-8. RISK Macro Flow Diagram

9. Calculate the E_c for the residual population, i.e., hunters, hikers, etc., for each failure mode and debris type.

10. Calculate the total E_c for each area, for each failure mode and each debris type, and then calculate the total E_c for the test.

11. Sort the data for final output and identify the areas of maximum concern.

12. Print and plot the calculated data.

These are the macro level functions performed by Program RISK. The details of the actual calculations are documented in reference 4.

4.1.5.3 Program RISK I/O

4.1.5.3.1 RISK Input Data

Program RISK requires data from a variety of sources. These include user supplied data; environmental, geographical and geophysical data from the risk assessment data library; population data from the Eglin and vicinity population library; and data from both PTRAJ and DENGEN. The PTRAJ and DENGEN data can be bypassed if comparable data is input as part of the user supplied data. These data include the nominal trajectory, the failure mode debris PDFs, the geographical location and orientation of the PDFs, and the probabilities of occurrence of the failure modes. The user supplied data is input to Program RISK in the NAMELIST format and these data are described in Table 4-1-VI. The structure of the option list parameter is shown in Table 4-1-VII and the structure of the failure mode array is shown in Table 4-1-VIII.

4.1.5.3.2. RISK Output Data

The program output data has two main parts: (1) the output of the input data and the output of the calculated results for the weapon test, and (2) an optional output consisting of computed intermediate data useful for verification of data consistency, case setup and evaluation of the details of the risk assessment calculations on a failure-mode-by-failure-mode basis.

The parameters output are described in Tables 4-1-IX and 4-1-X. The calculated results consist of: (1) the total expected casualty for the test, (2) the total conditional expected casualty for each failure mode along with the conditional probability of that failure occurring and (3) a list of the areas subjected to a hazard; ordered with the most endangered area appearing first and the least endangered area appearing last. These data are printed and plotted, and examples are shown in Table 4-1-XI, Table 4-1-XII and Figure 4-1-9.

Table 4-1-VI

RISK User Supplied Data

PVHIST	-	Vehicle position/velocity time history
PDTABI	-	Tabular debris impact PDFs. (can be supplied directly from DENGEN)
PLATI, PLONI	-	Latitude and longitude of PDF mean (can be supplied directly from DENGEN)
FMI	-	Failure mode data array (see Table 4-1-VIII)
IOPTION	-	Program Option Flags (see Table 4-1-VII)
NFM	-	Number of failure modes
THTAB	-	Thrust table
CLTAB	-	Coefficient of lift table
NTV	-	Number of points in thrust table
NLV	-	Number of points in lift table
LOD	-	L/D ratio
PHIORI, LAMORI	-	Latitude and longitude of position/velocity time history origin
PSIORI	-	Azimuth of position/velocity time history
EVALB	-	Array of latitude and longitude pairs defining a region to be evacuated.
ECLL	-	Lower limit of E_c to be considered for output
ALTF, RHORI	-	Vehicle altitude and horizontal distance to mean impact point (used only when a skip lock failure is selected)
PSEEK	-	Seeker viewing cone half angle
FUELWTO	-	Initial fuel weight
FUELFLO	-	Fuel flow rate
FUELTNT	-	Explosive equivalent of fuel in lbs of TNT

Table 4-1-VI (Continued)

WHDTNT	-	Explosive equivalent of warhead in lbs of TNT
ENFAC	-	Blast energy partition factor
PKE	-	Minimum fragment kinetic energy considered hazardous
STYPE	-	Seeker type
DATE	-	Date (day,month) for which hazard analysis is to be applicable.

Table 4-1-VII

Default Option Values

PARAMETER	VALUE	MEANING
IOPTION (1)	1	Use PHAZRD1
(2)	0	Skip input data printout.
(3)	1	Print intermediate debug data.
(4)	1	Print intermediate report data.
(5) thru (14)	1	Input impact latitude, longitude impact velocity orientation for probability density function for ith failure mode.
(15) thru (24)	0 0	Calculate PDF from standard bivariate normal statistical parameters.
(25)	1	Zero out wind table values.
(26)	0	No lift considered or else L/D is assumed input.
(27)	1	Plot output data

Table 4-1-VIII

Failure Mode Data Array Structure

Data is input in FMI(25,10) array
Data is stored in FM(10,25) array
FM(I,J)=FMI(J,I)

FM(IFM,1)	Failure Mode Name Code =1. Failure to Ignite =2. Initial Guidance Failure =3. Meander Guidance Failure =4. Terminal Guidance Failure =5. Seeker Loss of Lock =6. Skiplock Failure
FM(IFM,2)	Vehicle Casualty Area
FM(IFM,3)	Failure Mode Type =±1. discrete =±2. distributed > 0 tabular definition < 0 functional definition
FM(IFM,4)	Earliest time for IFMth failure
FM(IFM,5)	Latest time for IFMth failure
FM(IFM,6)	Probability of IFMth failure occurring > 0 use input value = 0 calculate from exponential model < 0 calculate from Weibull model
FM(IFM,7)	Impacting vehicle weight
FM(IFM,8)	Frontal Area (aerodynamic)
FM(IFM,9)	β of impacting vehicle
FM(IFM,10)	Explosive weight of warhead
FM(IFM,11)	Shape Factor =1. Flat Plate =2. Sphere =3. Cone
FM(IFM,12)	Fragment list indicator =-1 new fragment list

Table 4-1-VIII (Continued)

	=0 no fragment list =1 same list as before
FM(IFM,13)	Fuel burn flag =0 Burns to ground (or out) =1 Burns until failure
FM(IFM,14)	Number of warhead fragments
FM(IFM,15)	Weight of each fragment (lbs)
FM(IFM,16)	β of each fragment
FM(IFM,17)	Number of small fragments from vehicle
FM(IFM,18)	Weight of each small fragment
FM(IFM,19)	β of each small fragment
FM(IFM,20)	Number of large fragments from vehicle
FM(IFM,21)	Weight of each large fragment
FM(IFM,22)	β of each large fragment
FM(IFM,23)	Warhead casing wt (FM(IFM,14)=0)
FM(IFM,24)	Warhead casing thickness
FM(IFM,25)	Warhead casing inside diameter

Table 4-1-IX

Explanation of Calculated Output

$COMPILATION OF CASUALTY EXPECTATIONS$

TOTAL CASUALTY EXPECTATIONS

FROM ALL CAUSES = Total E_C for the Test

SUBTOTALS FROM LIBRARY ASSIGNED POPULATION	RESIDUAL POPULATION
Total E_C for Population Defined in Population Library	Total E_C Associated with Hikers/Hunters, etc.

CASUALTY EXPECTATION BY FAILURE MODE

Failure Mode Name for Failure #1

PROBABILITY OF FAILURE OCCURRING = Failure Probability for 1st Failure Mode.

CASUALTY EXPECTED IN LIBRARY ASSIGNED POPULATION	RESIDUAL POPULATION
E_C for Population Defined in Population Library due to this Failure Mode	E_C for Hikers, Hunters, etc due to this Failure Mode

Failure Mode Name for Failure #2

(Can be repeated for up to 10 failure modes)

Table 4-1-X

Explanation of Calculated Output for Each Hazarded Population Center

EXPECTED CASUALTY BY AREA IN DESCENDING ORDER OF IMPORTANCE

DESCRIPTORS	CASUALTY EXPECTATION	HAZARD PROBABILITY	AREA POP	COORDINATES S T	FAIL MODE
Name of the Area	E_C for Area	Hazard Probability	Number of People in Area	S and T Coordinates for Area	Failure Mode which Hazarded Area

Table 4-1-XI

```
***CASE7, 750LB BOMB, FRAGMENTATION, NO WIND, LOD=0, SKIP LOCK

 THE FOLLOWING RESULTS ARE VALID FOR
MONTH =   5
DAY   =   5
AT WHICH TIME RESIDUAL POPULATION ON THE RESERVATION
DUE TO HIKERS, HUNTERS ETC. IS ESTIMATED TO BE
  .92 PERSONS PER SQUARE MILE

                          $COMPILATION OF CASUALTY EXPECTATIONS$

                            TOTAL CASUALTY XPECTATIONS
FROM ALL CAUSES =   .87218E-02

SUBTOTALS FROM
LIBRARY ASSIGNED POPULATION       RESIDUAL POPULATION
         .87213E-02                   .48534E-06

                            CASUALTY EXPECTATION BY FAILURE MODE
 INITIAL GUIDANCE FAILURE
PROBABILITY OF FAILURE OCCURRING =  .43300E-01

CASUALTY EXPECTED IN
LIBRARY ASSIGNED POPULATION       RESIDUAL POPULATION
         .41277E-05                   .39649E-06

 SEEKER LOSS OF LOCK SKIP LOCK
PROBABILITY OF FAILURE OCCURRING =  .29400E-01

CASUALTY EXPECTED IN
LIBRARY ASSIGNED POPULATION       RESIDUAL POPULATION
         .87172E-02                   .88846E-07
```

Table 4-1-XII

EXPECTED CASUALTY BY AREA IN DESCENDING ORDER OF IMPORTANCE

DESCRIPTOR			CASUALTY EXPECTATION	HAZARD PROBABILITY	AREA POP	COORDINATES S	T	FAIL MODE
B-126	9400	B-75*	.22216E-02	.35985E-02	21.	50.	87.	2
SYSTEMS	M-42	B-70*	.19011E-02	.80859E-02	8.	53.	87.	2
	6300	B-1 *	.94021E-03	.26652E-02	12.	48.	86.	2
B-109A	9420	B-75*	.50513E-03	.57275E-02	3.	50.	88.	2
B-141	9313	B-70*	.46488E-03	.52712E-02	3.	49.	86.	2
	9417	B-1 *	.39668E-03	.33734E-02	4.	47.	87.	2
B-142	9425	B-75*	.37253E-03	.42241E-02	3.	46.	87.	2
B-130	9411	B-75*	.36608E-03	.62264E-02	2.	48.	88.	2
B-128	9406	B-75*	.36453E-03	.41333E-02	3.	45.	86.	2
B-118	9303	B-70*	.25619E-03	.43574E-02	2.	55.	85.	2
B-129	9410	B-75*	.20709E-03	.35221E-02	2.	50.	87.	2
B-127	9403	B-75*	.19639E-03	.33402E-02	2.	47.	87.	2
B-134	9422	B-75*	.17506E-03	.19850E-02	3.	47.	92.	2
B-109	9408	B-75*	.13019E-03	.14762E-02	3.	44.	86.	2
B-11	9407	B-75*	.13019E-03	.14762E-02	3.	44.	86.	2
	9306	B-1 *	.78350E-04	.26652E-02	1.	48.	86.	2
	6120	FLD6*	.82192E-05	.34948E-04	8.	50.	95.	2
	8982	B-76*	.37662E-05	.39207E-05	24.	37.	91.	2
WHSE	9461	C-80A*	.18031E-05	.26038E-05	16.	101.	94.	1
	9462	C-80A*	.11270E-05	.26038E-05	10.	101.	94.	1
VALPARAISO			.15099E-06	.10965E-07	318.	81.	85.	1
COMM.	8721	C-52N*	.12736E-06	.14713E-05	2.	101.	90.	1
VALPARAISO			.12363E-06	.16223E-07	176.	82.	85.	1
PRISON CAMP		*	.11034E-06	.57819E-08	450.	79.	85.	1
	8708	C-52N*	.98047E-07	.22653E-05	1.	100.	91.	1
NICEVILLE			.74576E-07	.17223E-06	10.	88.	85.	1
NICEVILLE			.73538E-07	.17983E-06	10.	87.	85.	1
NICEVILLE			.73937E-07	.16868E-06	10.	89.	85.	1
NICEVILLE			.70706E-07	.16329E-06	10.	90.	85.	1
	8712	C-52N*	.56648E-07	.65418E-06	2.	102.	91.	1
C-131	8705	C-52*	.56648E-07	.65418E-06	2.	102.	91.	1
VALPARAISO			.55972E-07	.73446E-08	176.	80.	85.	1
NICEVILLE			.56024E-07	.10398E-06	10.	86.	85.	1
C-135	9537	*	.23576E-07	.27236E-06	2.	101.	98.	1
NICEVILLE			.19646E-07	.45372E-07	10.	85.	85.	1
NICEVILLE			.13947E-07	.32210E-07	10.	84.	85.	1
NICEVILLE			.10069E-07	.23253E-07	10.	83.	85.	1
VALPARAISO			.95034E-08	.48773E-08	45.	79.	85.	1
C-132	9434	*	.38213E-08	.44144E-07	2.	104.	95.	1
C-102	8728	C-52*	.38826E-09	.44852E-09	20.	102.	85.	1
C-101	8702	C-52*	.19757E-09	.22823E-08	2.	100.	85.	1

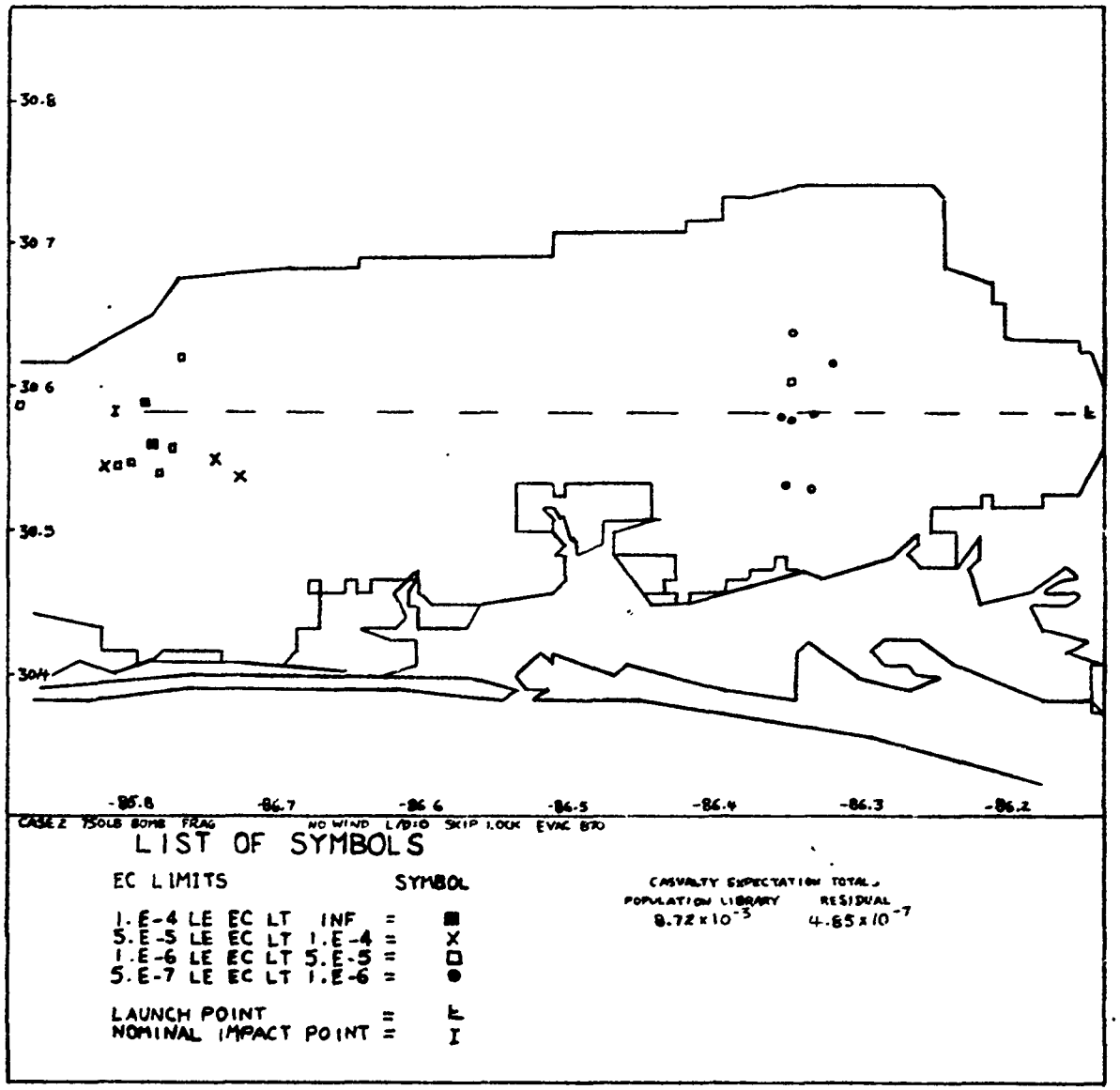

Figure 4-1-9. E_C Map for Sample Test Case 2

4.1.6 Risk Assessment Program Capabilities and Limitations

4.1.6.1 Applicable Weapon Types

Programs PTRAJ, DENGEN and RISK have been designed for applicability to the broad spectrum of air-to-ground weapon types planned for testing at ADTC in the 1975-1985 time frame. These weapons will possess advanced systems to enable them to fly preprogrammed flight paths with gliding and/or thrusting legs, sense their target, and actively guide to impact. These weapons will be subject to failure modes in any of their main systems. The occurrence of these failure modes during a test can result in a hazard to the population in the vicinity of ADTC. Although there is no way to describe all of the possible critical failure modes for current and future weapon types, the gross failure modes and their effects can be described. These failure mode effects are modeled in programs DENGEN and RISK, and they are of two types:

1. Propulsion System Failures - failure to ignite or thrust deviation.

2. Guidance System Failures - seeker wandering, hold last guidance command, hard turn, ballistic, or skip lock.

Structural failures, if identifiable, can be modeled as guidance failures, i.e., a broken vehicle will tumble and can be treated as a high β ballistic object; a bent fin can be treated as a hold last command guidance failure.

4.1.6.2 Program Assumptions and Limitations

The phenomena associated with the behavior of a failed weapon system are not well understood nor are there sufficient data available to study or completely model this behavior. The assessment of the risks associated with the testing of a weapon system requires that the impacts of the debris associated with a failure of the system be determinable. The determination of debris impact points in turn requires knowledge of the behavior of the failed weapon system. The consequence of this is that in the development of a comprehensive risk assessment methodology some behavioral assumptions were made and some performance limitations were imposed to fill the technology and data voids associated with the phenomena of failed weapon system behavior.

In the realm of lethal or hazardous effects generated by debris impacts there exist considerable data both theoretical and empirical. These data are generally for particular weapons against particular targets and, as a consequence, the methods and data have been extrapolated and generalized to apply to the broad class of structures on and in the vicinity of ADTC.

Finally, there were some operational limitations imposed to facilitate the modeling of some aspects of the risk assessment problem. These limitations were imposed only when there would be no impact on the accuracy of the computed results and when there would be a benefit in terms of lesser computer resource requirements, ease of data handling, a simplification of modeling mathematics, or an opportunity to include multiple user options within a single computing format.

The following is a list of assumptions and limitations that pertain to the ADTC risk assessment methodology:

1. All buildings are square and the people within are uniformly distributed.

2. The impact PDFs are constant over the area and in the near vicinity of buildings.

3. A hazard exists to all population exposed to a 2-psi overpressure or to fragments with a kinetic energy greater than 33 ft-lbs, and at least 30-psi overpressure is required to pose a hazard to sheltered population when the building is not directly hit.

4. The energy generated at impact is proportioned between cratering, plastic deformation of the vehicle, the generation of overpressure and the generation of fragments.

5. At impact, no more than three classes of fragments are generated.

6. The use of the FTS will generate no more than three types of debris in addition to the intact vehicle.

7. The probability of occurrence of each of the vehicle failure modes can be estimated from either reliability data or historical data.

8. The weapon has no more than 10 failure modes (can be increased if necessary). When FTS is used, each debris category is treated as a separate failure mode.

9. All of the random processes which affect the vehicle process or after-failure performance are either uniform or normal. Time of failure is an exception and it is functionally modeled over a closed interval.

10. If a seeker loss-of-lock failure occurs, it is assumed that the weapon will home on any building within its visual cone

at the time of failure. The probability of impacting the building is the same as impacting within the ellipse formed by projecting the seeker visual cone upon the ground.

11. A 3-DOF model is used to predict impact point locations, and it is assumed that the physical, aerodynamic, and performance data are available or can be estimated for use in the 3-DOF model.

12. If a vehicle stalls, it is assumed to tumble and is treated as a low β ballistic object.

13. The vehicle destruct boundary is a closed polygon with no more than 10 corner points (an arbitrary limit that can easily be extended if necessary). The vehicle launch point must be interior to this polygon.

14. The location of the target must be included as the last point in the vehicle position/velocity time history.

15. There are a number of program specific limitations such as the number of data items permissible in a given data table. These program-specific items are detailed in the individual program documents.

References

1. "A Guided Vehicle Impact Predictor for Use in Statistical Models-Program PTRAG" (ER-EOO-031, Science Applications, Inc., Eglin Operations Office, Ft. Walton Beach, FL, 30 September 1976).

2. "Program for Generating Debris Impact Probability Density Functions (Program DENGEN)" (ER-EOO-034, Science Applications, Inc., Eglin Operations Office, Ft. Walton Beach, FL, December 1976).

3. "Impact Probability Density Function Enhancement" (ER-ESD-042, Science Applications, Inc., Eglin Systems Division, Ft. Walton Beach, FL, 23 September 1977).

4. "Risk Assessment Program: Phase II" (ER-EOO-025, Science Applications, Inc., Eglin Operations Office, Ft. Walton Beach, FL, April 30, 1976).

5. "Population Library Update II" (ER-EOO-015, Science Applications, Inc., Eglin Operations Office, Ft. Walton Beach, FL, June 26, 1975).

6. Baker, Wilfred E., Explosions in Air. University of Texas Press, 1973.

7. Kornhauser, M., Structural Effects of Impact. Spartan Books, Inc., 1964.

8. Meteorological Working Group, Inter-Range Instrumentation Group, Reliability of Meteorological Data, Range Commanders Council, Document 110-71, March 1971.

9. Parks, L. D., P2020 Land Range Ballistic Trajectory Program. ADTC/TSX, 25 January 1973.

10. SAFET3 Range Safety Analysis Program (TD-72-0078-A2, Software Directorate, Federal Electric Corporation, Vandenberg AFB, CA, June 1973).

11. "Missile Safety Study" (Missile Testing Safety Study Committee, Eglin AFB, FL, August 1971).

12. "Techniques of Impact Density Estimation for Range Safety Usage" (ER-EOO-009, Science Applications, Inc., Eglin Operations Office, Ft. Walton Beach, FL, July 22, 1974).

13. "Sensitivity of Range Safety Calculations to Selected Impact Distributions" (ER-EOO-013, Science Applications, Inc., Eglin Operations Office, Ft. Walton Beach, FL, 25 April 1975).

14. "A Quantitative Approach to ADTC Range Safety" (ER-EOO-019, Science Applications, Inc., Eglin Operations Office, Ft. Walton Beach, FL, June 27, 1975).

15. "Quantitative Operational Risk Criteria and Guidelines" (ER-EOO-028, Science Applications, Inc., Eglin Operations Office, Ft. Walton Beach, FL, 30 June 1976).

16. "Quantitative Operational Shipping Surveillance and Clearance Criteria and Guidelines" (ER-EOO-026, Science Applications, Inc., Eglin Operations Office, Ft. Walton Beach, FL, May 26, 1976).

17. "Operational Quantitative Guidelines to ADTC Range Safety" (ER-EOO-021, Science Applications, Inc., Eglin Operations Office, Ft. Walton Beach, FL, June 15, 1975).

18. "Gulf Shipping Density" (ER-EOO-008, Science Applications, Inc., Eglin Operations Office, Ft. Walton Beach, FL, April 25, 1975).

19. "Impact Predictors for Range Safety at ADTC" (ER-EOO-014, Science Applications, Inc., Eglin Operations Office, Ft. Walton Beach, FL, June 19, 1975).

20. "Debris Centerline Development: Debris Triangle" (ER-EOO-018, Science Applications, Inc., Eglin Operations Office, Ft. Walton Beach, FL, June 30, 1975).

21. "Debris Centerline Development: Impact Point Location" (ER-EOO-033 (Draft), Science Applications, Inc., Eglin Operations Office, Ft. Walton Beach, FL, undated).

22. "Land Range Flight Termination Risk Assessment for ADTC Weapon Tests" (ER-EOO-027, Science Applications, Inc., Eglin Operations Office, Ft. Walton Beach, FL, 30 June 1976).

4.2 KWAJALEIN MISSILE RANGE (KMR) RISK ANALYSIS TECHNIQUES

4.2.1 General

Performance of risk analyses at KMR is intended to satisfy one or more of the following applications: to serve as limiting criteria; to provide a measure of safety solution adequacy, for comparative purposes; and to provide documented evidence of the depth of analysis performed in development of a safety solution. In most cases a preliminary estimate of the risk level is obtained using simplified models that assume only one impacting piece, no abnormal missiles and bivariate Gaussian distributions. Depending upon the level of risk indicated and the nature of the program being evaluated, i.e., guided or unguided missile, a more thorough risk analysis might be undertaken. The four applications of the results of the analyses are discussed in more detail in the following paragraphs.

4.2.1.1 Limiting Criteria

Results of a risk analysis are used for establishing or limiting the risk that will be accepted for a given test or series of tests. The use of actual risk values is preferred over that of stating an acceptable criterion based on the term sigma since the usual connotation of sigma is associated with the normal distribution of a single variable, i.e., $3\sigma = 99.7\%$. It should be noted that an acceptable risk is influenced by many other elements, i.e.; national need, confidence level, etc., and therefore an acceptable risk for all tests cannot be established.

4.2.1.2 Measure of Safety Solution Adequacy

Risk analyses are used not only in determining the constraints that must be placed on a proposed test but to evaluate the residual risk after the constraints are imposed. In this manner a determination can be made as to the degree of protection that has been gained through imposing various safety restrictions, i.e., flight termination systems (FTS), and a judgment can be made as to the worth of the restriction. Again, the number of restrictions and the resulting decrease in residual risk must be weighed against the impact on the proposed test or tests and a threshold established based on all factors affecting the test.

4.2.1.3 Comparative Purposes

Risk analyses are used to compare the residual risk resulting from alternative safety scenarios. In this manner the scenario can be chosen which provides the lowest residual risk and the fewest restrictions on a proposed test. It is important to note than when using risk analyses for comparative purposes, the same model and assumptions must be used in each evaluation.

4.2.1.4 Documented Evidence of Safety Evaluation

Documentation of risk analyses provides reference data that is invaluable in the event of a safety incident. In addition it provides an excellent source of reference material for future evaluations of similar programs.

4.2.2 Risk Analysis Models

4.2.2.1 General

As stated previously, a preliminary estimate of the risk associated with a particular test is usually obtained using simplified models which provide a quick-look approximation. If the risk calculated appears to be excessive, more detailed analysis is then performed using more rigorous models. The simplified models currently being used are limited to the evaluation of normal missiles only, assume bivariate Gaussian dispersion distributions (either circular or elliptical) and only a single impacting piece. The more rigorous models have the capability of analyzing situations considering both normal and abnormal missiles, safety system effects and wind contributions to debris drift and impact. Each of these models is discussed in the following paragraphs.

4.2.2.2 Circular Dispersion Model

The circular dispersion model calculates the probability of impact (P_I) on a given area given the following:

- location of the nominal impact point of the object producing the hazard,
- distance from the nominal impact point to the near and far side of the area of interest,
- circular dispersion about the nominal impact point, and
- size of the area of interest.

The geometry for this model is shown in Figure 4-2-1 along with the equation used for computing P_I. This algorithm is currently programmed on a Hewlett Packard 65 calculator and the program instructions are given in Figure 4-2-2. This model assumes bivariate Gaussian distributed dispersions, normal missiles and a single impacting object.

4.2.2.3 Elliptical Dispersion Model

When the impact dispersion of an object cannot be closely approximated by a circle, a model employing an elliptical bivariate Gaussian

CIRCULAR DISPERSION MODEL

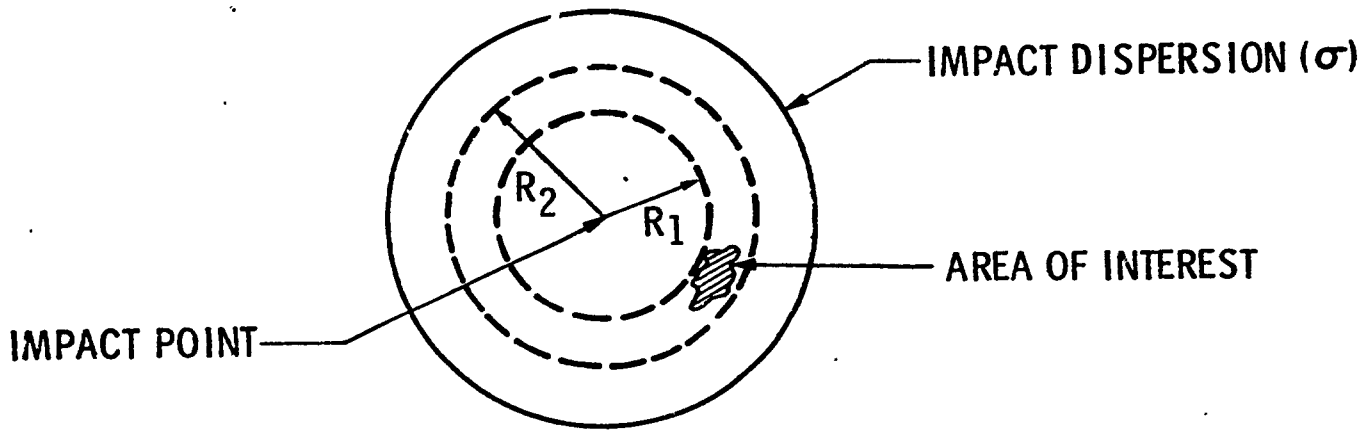

$$P_I = \left[e^{\frac{-R_2^2}{2\sigma^2}} - e^{\frac{-R_1^2}{2\sigma^2}} \right] \left[\frac{\text{AREA OF INTEREST}}{\text{AREA IN RING}} \right]$$

Figure 4-2-1

HP-65 Program Form

Title CIRCULAR DISPERSION MODEL - Figure 4-2-2 Page 1 of 2

SWITCH TO W PRGM PRESS f PRGM TO CLEAR MEMORY

KEY ENTRY	CODE SHOWN	COMMENTS
LBL	23	STORE R1
A	11	
STO 1	33 01	
RTN	24	
LBL	23	STORE R2
B	12	
STO 2	33 02	
RTN	24	
LBL	23	STORE σ
C	13	
STO 3	33 03	
RTN	24	
LBL	23	STORE AREA
D	14	
STO	33	
9	09	
RTN	24	
LBL	23	CALCULATE P_I
E	15	
DSP	21	CHANGE TO SCIENTIFIC
02	02	NOTATION
RCL 1	34 01	R_1
f^{-1}	32	
$\sqrt{x}$	09	R_1^2
STO 4	33 04	
RCL 2	34 02	R_2
f^{-1}	32	
$\sqrt{x}$	09	R_2^2
STO 5	33 05	
RCL 3	34 03	σ
f^{-1}	32	
$\sqrt{x}$	09	σ^2
2	02	
×	71	$2\sigma^2$
STO 6	33 06	
RCL 4	34 04	R_1^2
RCL 6	34 06	$2\sigma^2$
÷	81	$R_1^2/2\sigma^2$
CHS	42	$-R_1^2/2\sigma^2$
f^{-1}	32	
LN	07	e to the $-R_1^2/2\sigma^2$
STO 7	33 07	
RCL 5	34 05	R_2^2
RCL 6	34 06	$2\sigma^2$
÷	81	$R_2^2/2\sigma^2$
CHS	42	$-R_2^2/2\sigma^2$
f^{-1}	32	
LN	07	e to the $-R_2^2/2\sigma^2$
RCL 7	34 07	
g X⇄Y	35 07	

KEY ENTRY	CODE SHOWN	COMMENTS
−	51	$e^{-R_1^2/2\sigma^2} - e^{-R_2^2/2\sigma^2}$
STO 8	33 08	
RCL 2	34 02	R_2
f^{-1}	32	
$\sqrt{x}$	09	R_2^2
RCL 1	34 01	R_1
f^{-1}	32	
$\sqrt{x}$	09	R_1^2
−	51	$R_2^2 - R_1^2$
g	35	
π	02	π
×	71	$\pi(R_2^2 - R_1^2)$
RCL	34	
9	09	Area
g X⇄Y	35 07	
÷	81	$\text{Area}/\pi(R_2^2 - R_1^2)$
RCL 8	34 08	
×	71	$\text{Exp}\ [\text{Area}(R_2^2 - R_1^2)]$
RTN	24	

REGISTERS	
R_1	R_1
R_2	R_2
R_3	σ
R_4	Scratch
R_5	Scratch
R_6	Scratch
R_7	Scratch
R_8	Scratch
R_9	Area

LABELS	
A	R_1
B	R_2
C	σ
D	Area
E	Calc.
0	
1	
2	
3	
4	
5	
6	
7	
8	
9	

FLAGS	
1	
2	

TO RECORD PROGRAM INSERT MAGNETIC CARD WITH SWITCH SET AT W PRGM

HP-65 User Instructions

Title CIRCULAR DISPERSION MODEL - Figure 4-4-2 (Continued) Page 2 of 2

Programmer Johnny G. Allen Date 1978

CIRCULAR DISPERSION MODEL

R_1	R_2	σ	Area	Calc

STEP	INSTRUCTIONS	INPUT DATA/UNITS	KEYS	OUTPUT DATA/UNITS
1	Enter Program			
2	Input Radius 1		A	ft
3	Input Radius 2		B	ft
4	Input Sigma		C	ft
5	Input Area		D	ft^2
6	Calculate Probability of Impact		E	-
7	Input New Data in Steps 2, 3, 4, and/or 5 for new problem - then Step 6			

HEWLETT PACKARD

distribution is used for a preliminary approximation of the risk level. This model is more flexible than the circular model in that distances from the impact point to the area of interest are calculated and provisions are made to vary the dispersions so that the model can be used for parametric studies during test planning. The geometry upon which this model is based is shown in Figure 4-2-3. The model is currently being run on a CDC 7600 and copies of the program are available upon request. Inputs required are:

- latitude and longitude of the nominal impact point,
- semi-major and semi-minor axes of the impact dispersion,
- latitude and longitude of the center of the area of interest, and
- size of the area of interest.

Assumptions used in developing this model are bivariate Gaussian distributions and a single impacting piece.

4.2.2.4 Risk Contour Model

This model is used when preliminary estimates from the models discussed earlier indicate a marginal risk or when a detailed analysis is desired. The model was developed to handle both normal and abnormal missiles, winds, and effects caused by activation of the missile destruct system. The total model consists of three separate computer programs which are run sequentially, i.e., the output of the first is the input to the second, etc.

The purpose of this model is to generate contours of constant impact probability per square foot. These contours are typically used to estimate the risk of impacting fragments in selected areas. An example of the results is shown in Figure 4-2-4 for a SPRINT missile launch from Meck Island in the Kwajalein Atoll.

4.2.2.4.1 Footprint Generator Program

This program utilizes a nominal trajectory, wind data and malfunction turn information to determine the impact points or footprints for a specified range of ballistic coefficients having nominal and 1-sigma winds, 1-sigma malfunction turns and 1-sigma dispersion. The output consists of five impact points for each specified time point on the trajectory and ballistic coefficient combination. These points provide the foundation for the construction of a 1-sigma wind impact ellipse and a 1-sigma malfunction turn ellipse which are computed in the Impact Probabilities Analysis Program. The output is in the form of punched cards.

ELLIPTICAL DISPERSION MODEL

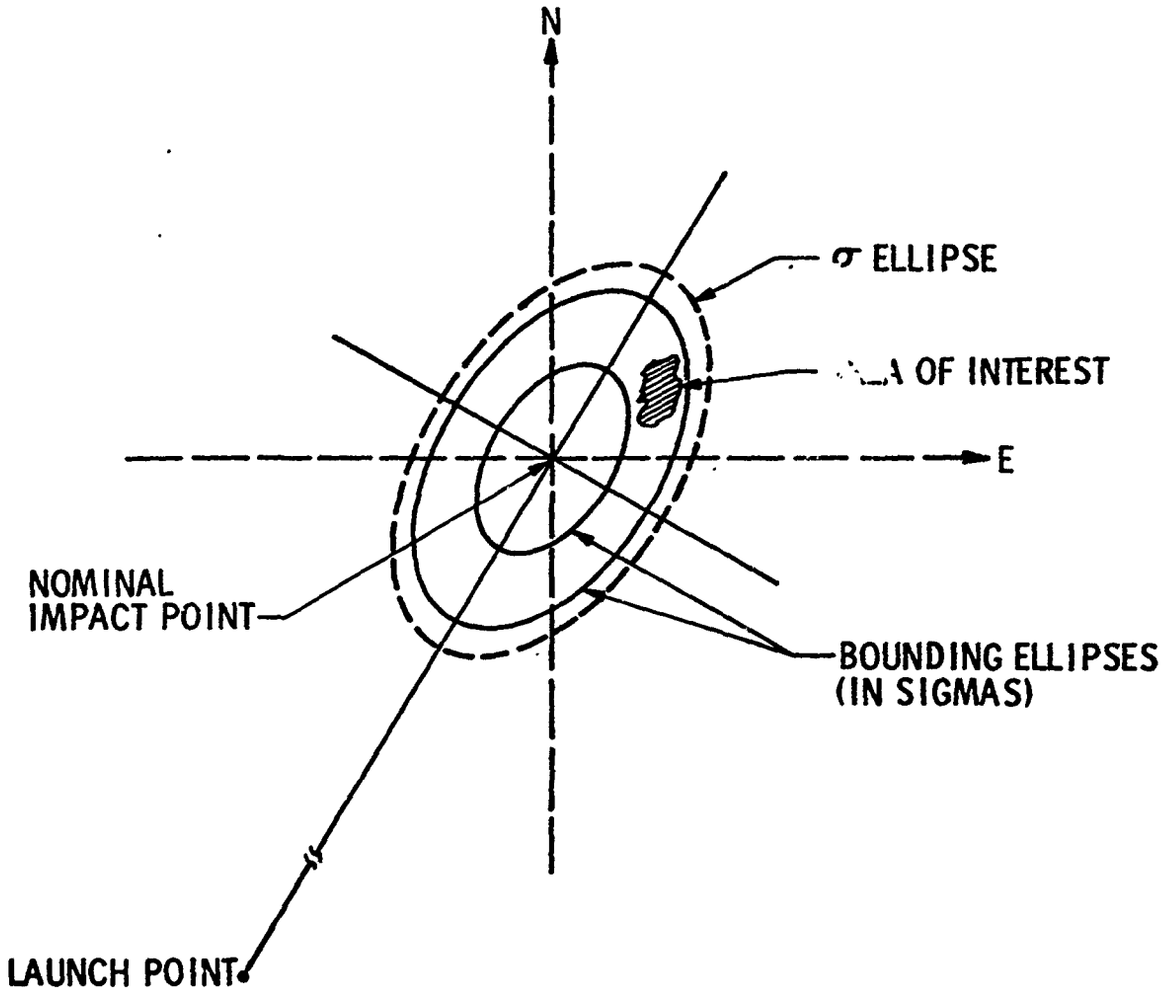

Figure 4-2-3

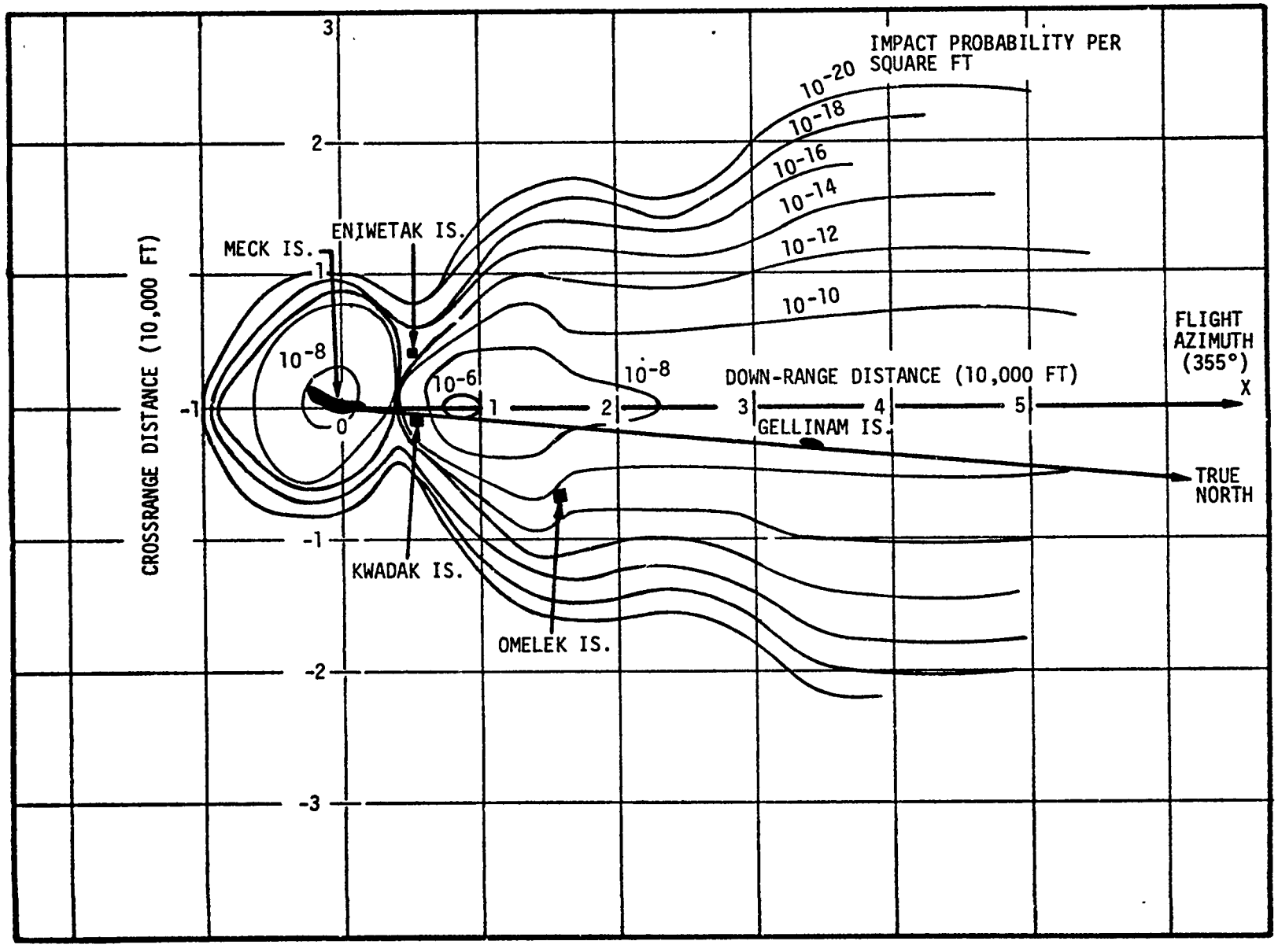
IMPACT PROBABILITY PER SQUARE FT
10-20
10-18
10-16
10-14
10-12
10-10
10-8
10-6
10-8
MECK IS.
ENIWETAK IS.
KWADAK IS.
OMELEK IS.
GELLINAM IS.
CROSSRANGE DISTANCE (10,000 FT)
DOWN-RANGE DISTANCE (10,000 FT)
FLIGHT AZIMUTH (355°)
X
TRUE NORTH
3
2
1
0
-1
-2
-3
1
2
3
4
5

Figu 4-2-4

4.2.2.4.2 Impact Probability Analysis Program

The purpose of this program is to compute the probability of impacting at least one piece of debris at each point on a specified grid. The computed probability at each grid point is output on tape which is used by the third program of this model to produce contour plots of constant probability. Input data is read from the punched cards produced by the Footprint Generator Program. This data is converted into 1-sigma ellipses which are combined with failure probability data to yield impact probability.

The program is divided into two parts. First, an evaluation of "close-in" (normally the general vicinity of the launch point) impact probabilities is performed. When this phase is completed, the "far-out" region is evaluated. Finally, in the close-in region the computation at each grid point is performed for the time span specified up to some value t_{max}. In the far-out region the computation is performed only for those times at which a nominal impact may occur near the downrange axis. This choice was made to reduce the time required for computation.

The computed (and plotted) impact probability is per unit area. To determine the impact probability, the probability per unit area is multiplied by the size of the area of interest. This will yield the approximate probability that at least one fragment impacts within the area of consideration. These programs are currently being run on a General Electric 615 computer at the Ford Aerospace and Communications Corporation, Aeronutronic Division. It is anticipated that considerable effort would be required to adapt this model for use on other computer systems.

4.3 PACIFIC MISSILE TEST CENTER (PMTC) RISK ANALYSIS MODELS

4.3.1 Hazard Analysis for TOMAHAWK Cruise Missile Inland Tests

4.3.1.1. Introduction

The following material is from "Hazard Analysis for TOMAHAWK Cruise Missile Inland Tests" prepared for PMTC by J. H. Wiggins Corp., Redondo Beach, California. In compiling this material, Wiggins Corp. used a computer program which calculates risk to population centers, vehicles and aircraft along the missile route. As seen in subparagraph 4.3.2.2, this computer program may be used to determine the hazards produced by any vehicle which flies along a predetermined route and whose probability of failure is known.

4.3.1.2 Hazard Computation Models

The models used to compute the impact hazards and the air collision hazards for the cruise missile are described in the following sections. These models are general in nature and, thus, could be used to analyze the hazards for any airborne vehicle flying a predefined flight path.

4.3.1.2.1 Impact Hazards Model

Impact hazards are the hazards to populated locations, roads or other critical locations on the ground due to the potential impact of debris from an airborne vehicle. The hazards are expressed in terms of probabilities of impact and casualty expectations. They are computed for each vehicle mode of failure which can result in impacting debris and for each fragment resulting from the failure. The model developed to compute these hazards is designed to analyze a single fragment (resulting from a given failure mode) at a time. If, however, multiple fragments have a common impact distribution due to a failure anytime during flight, the hazards resulting from these fragments can be analyzed simultaneously. Similarily, if multiple failure modes will result in common fragments and corresponding fragment impact distributions, these failure modes can be treated as a single failure mode with a failure rate (probability of failure per second) equal to the sum of the individual failure rates.

The impact hazards model is developed assuming that the following data are known (refer to Figure 4-3-1).

1. The locus of the mean impact point for a fragment(s) from a failed vehicle as a function of the flight time at which the failure occurred. The locus is approximated as piecewise linear and defined by specifying the coordinates (latitude and longitude) of the end points of the linear segments.

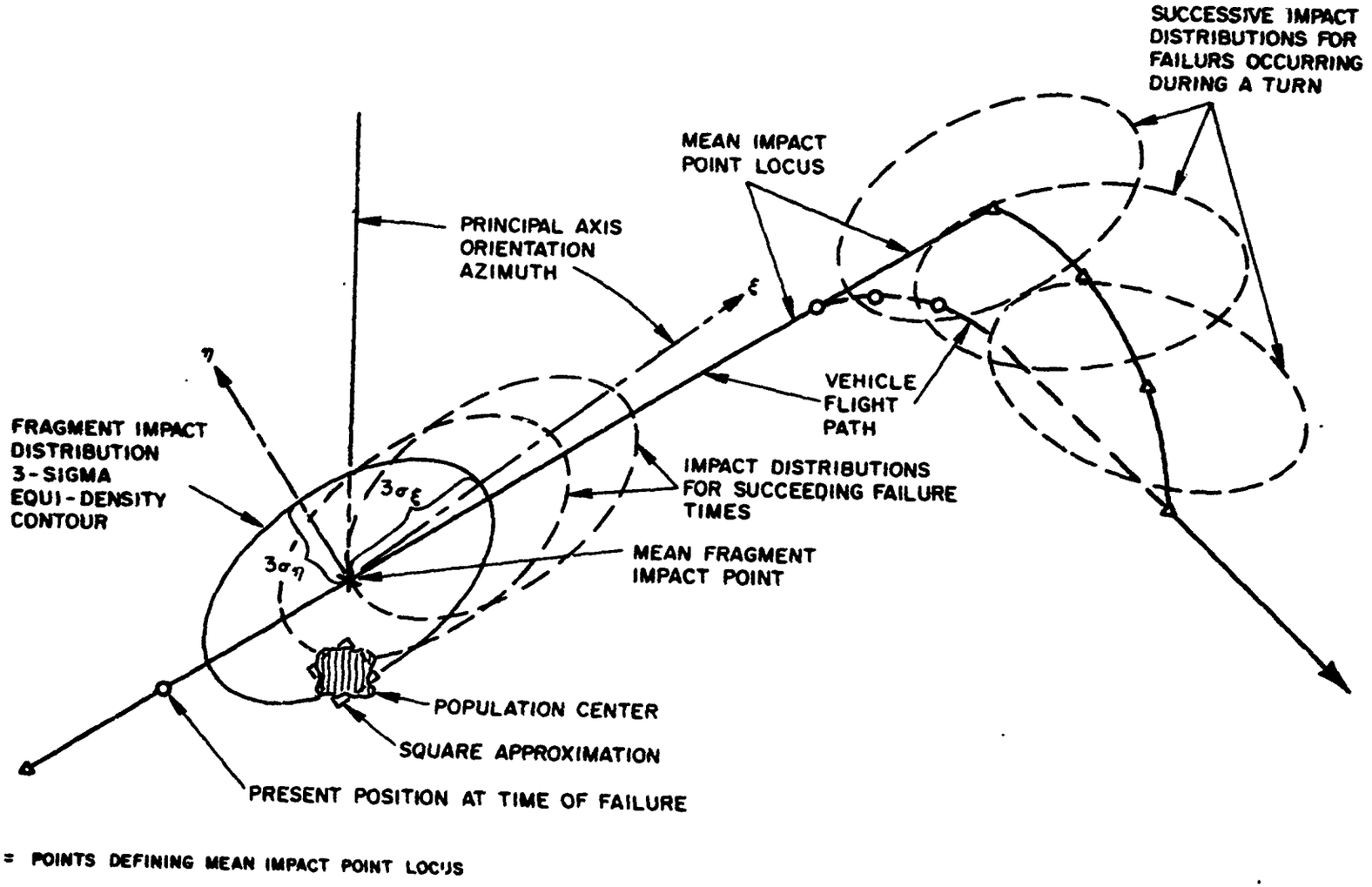

Figure 4-3-1. Impact Hazards Model

2. The impact distribution for the fragment(s) defined, as a function of flight time, in terms of the principal 1-sigma impact uncertainties ($\sigma\xi$, $\sigma\eta$) and the orientation of the principal ξ axis (a bivariate normal impact distribution is assumed).

3. The vehicle failure rate as a function of flight time for the failure mode(s) being considered.

4. The casualty area for the impacting fragment(s) as a function of flight time. For multiple fragments the sum of the individual casualty areas is used.

5. The size (land area), location (coordinates of the centroid) and population of critical locations.

6. The width, traffic density (occupants per nmi) and the coordinates of the end points for segments of roads. (Each road is assumed to be straight.)

To compute the hazards, the total vehicle flight time is segmented into a series of short time intervals with each interval represented by an intermediate flight "failure time." The fragment impact distribution for each failure time is weighted according to the probability of a failure occurring during the corresponding time interval. The failure times are closely spaced so that the fragment impact distributions for successive failure times overlap sufficiently (as depicted in Figure 4-3-1) to simulate the actual continuous distribution. The hazards are computed for each failure time, for each critical center, and for each road. The total hazards for a given critical center or road are obtained by summing the results over all failure times. A functional flow diagram of the computations is shown in Figure 4-3-2. The computations for a given failure time are described in further detail in the following paragraphs.

4.3.1.2.1.1 Impact Probability

For a given failure time, the latitude and longitude of the mean fragment impact point are obtained by interpolation of the mean impact point locus data. The orientation of the impact distribution principal ξ-axis (see Figure 4-3-1) and the principal impact uncertainities ($\sigma\xi$, σ_η) are also obtained using linear interpolation. The impact distribution is assumed to be bivariate normal and, thus, the impact probability density function (PDF) is given by

$$P(\xi,\eta) = \frac{1}{2\pi\sigma_\xi\sigma_\eta} \exp\left[-\tfrac{1}{2}\left(\xi^2/\sigma_\xi^2 + \eta^2/\sigma_\eta^2\right)\right] \qquad (1)$$

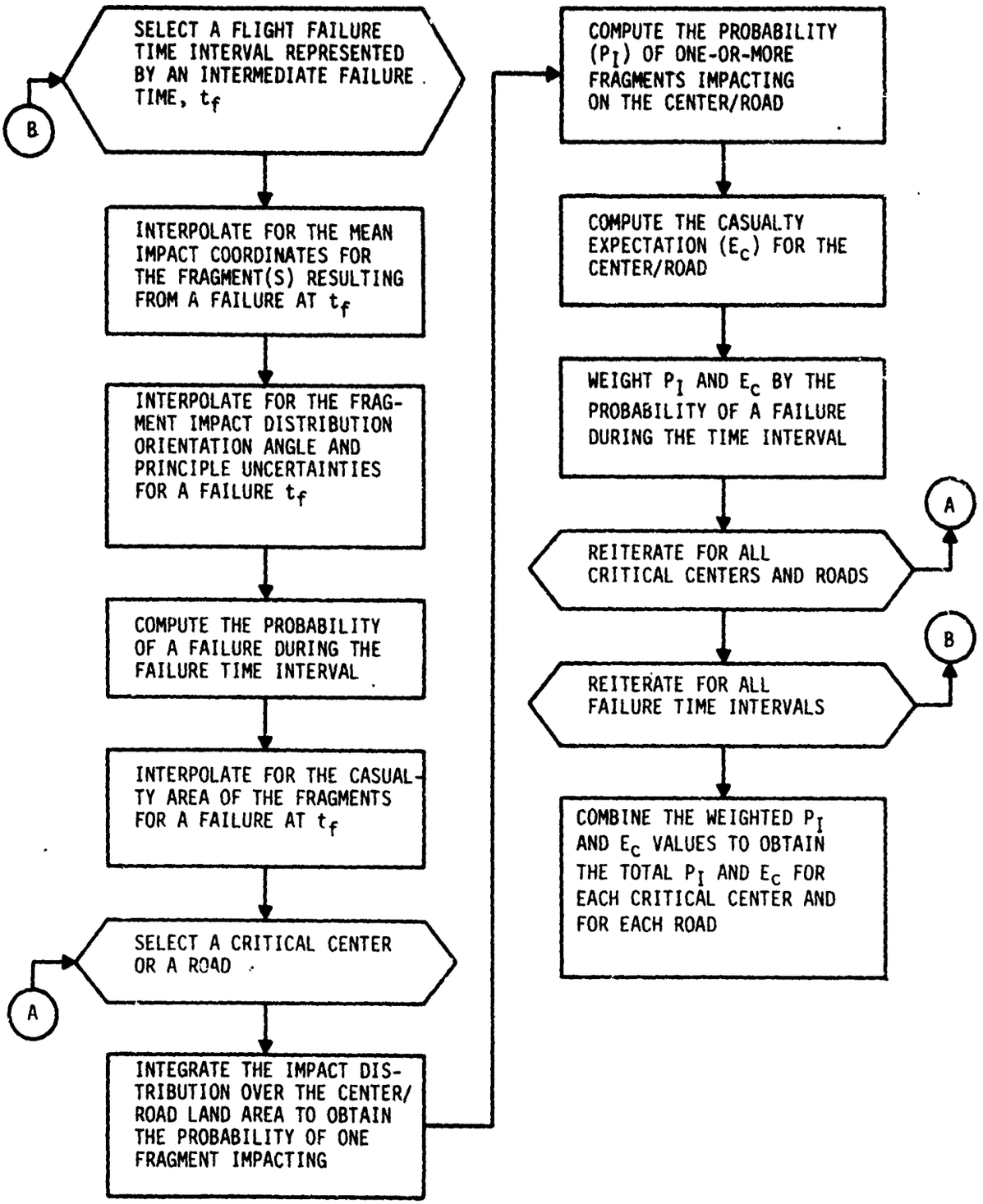

Figure 4-3-2. Impact Hazards Model Functional Flow Diagram

The conditional probability of one fragment impacting on a given critical center, given that a failure has occurred, is obtained by integrating the PDF over the land area of the center. To perform this integration, the critical center is assumed to be square with sides parallel to the principal ξ-η coordinate axes.

The conditional probability of one fragment impacting on a road segment is computed by defining the impact probability density along the length of the road. Since the fragment impact PDF is assumed to be bivariate normal, this conditional density will be normally distributed as shown in Figure 4-3-3.

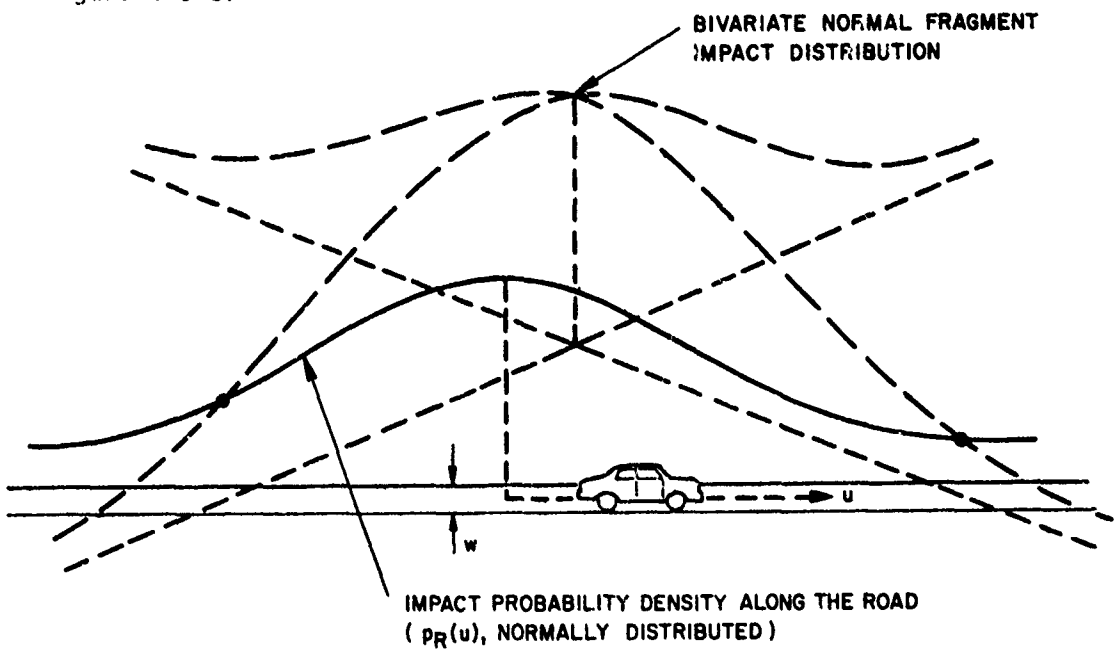

Figure 4-3-3. Impact Probability Computation for Roads

It is assumed that the density is constant over the width (w) of the road. The conditional impact probability is given by

$$P_I = w \int_{u_1}^{u_2} P_R(u)\,du \qquad (2)$$

where

P_R (u) is the impact probability density along the road,

u_1, u_2 are the u coordinates of the ends of the road segment.

If multiple impacting fragments are to be considered, the probability of impact becomes the probability of one or more fragments impacting a critical center or a road. This probability is given by

$$P_{In} = 1 - \left(\bar{1} - P_I\right)^n \qquad (3)$$

where

P_I is the conditional probability of impact for one fragment

n is the number of fragments.

The impact probabilities discussed thus far have been conditional probabilities based on the assumption that a failure has occurred. These probabilities must be weighted by the probability of occurrence of a failure during the current flight time interval. This failure probability is obtained by integrating the vehicle failure rate over the flight time interval. Total impact probabilities are computed by summing the weighted values over all flight time intervals.

4.3.1.2.1.2 Casualty Expectation

The casualty expectation for a critical center or a road is equal to the weighted probability of one fragment impacting times the expected number of casualties given impact as given by

$$E_C = \frac{P_I A_C}{A} N \qquad (4)$$

where

P_I = probability of one fragment impacting the critical center or the road (weighted by the probability of a failure during the time interval)

A_C = casualty area of the fragment(s)

A = land area of the critical center or road

N = number of people in the center or on the road

4.3.1.2.2 Aircraft Collision Model

The purpose of the air collision model is to provide an estimate of the probability of a collision between the cruise missile and an aircraft. It is assumed for this analysis that no evasive action is taken by either the pilot of the aircraft or the remote "pilot" of the missile.

To compute the probability of collision, the flight path of the vehicle is considered in segments over which the missile heading, speed and altitude, and the aircraft traffic (across the flight path segment) are reasonably constant. The collision probability is computed for each segment and the results are summed over all segments.

Consider a flight path segment of length D as illustrated in Figure 4-3-4.

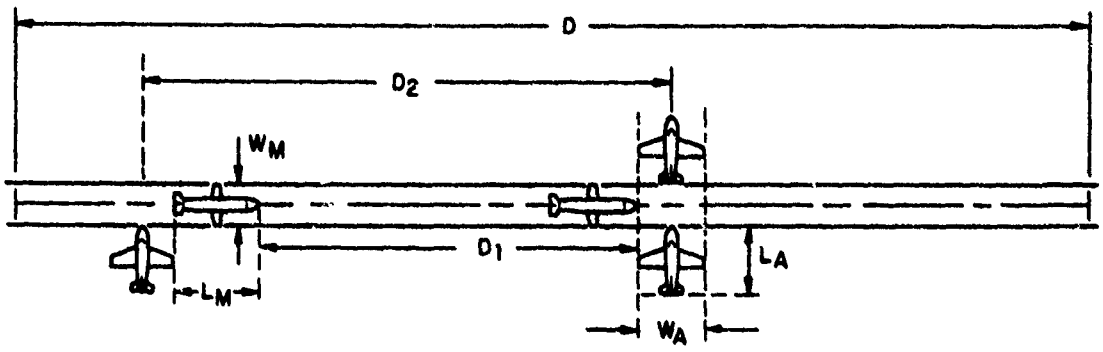

Figure 4-3-4. Air Collision Model Geometry

Let the space occupied by the missile and by a typical aircraft be approximated by the boxed-in regions defined by the length, width and height of the vehicles. Let

L_M = length of the missile

W_M = width of the missile (wing span)

H_M = height of the missile (including fins)

L_A = length of a typical aircraft

W_A = width of a typical aircraft (wing span)

H_A = height of a typical aircraft (including fin and landing gear)

V_M = speed of the missile

V_A = average speed of an aircraft in the direction orthogonal to the missile flight path segment

F_A = frequency of aircraft crossing the missile flight path

Aircraft will be treated as if they are heading in a direction orthogonal to the missile flight path segment at speed V_A. The actual aircraft heading will not significantly affect the collision probability unless the heading is nearly parallel to the missile heading.

The probability, P(D), of a collision while the missile traverses a segment can be expressed as follows:

$$P(D) = P(C) \cdot P(I|C) \cdot P(A) \tag{5}$$

where

P(C) = probability of an aircraft crossing the segment during passage of the missile

P(I/C) = probability of collision given an aircraft crossing and assuming both vehicles are at the same altitude

P(A) = probability of the two aircraft being sufficiently close in altitude to collide.

Assuming that the frequency of aircraft is small enough, the probability of a crossing can be approximated by

$$P(C) = \frac{\text{missile traversal time}}{\text{time between aircraft}} \tag{6}$$

$$= \frac{D/V_M}{I/F_A}$$

Referring to Figure 4-3-4, it is seen that the time (T_A) that any part of an aircraft is in the collision zone is given by

$$T_A = \frac{W_M + L_A}{V_A} \tag{7}$$

The distance traveled by the missile during this time is

$$D_1 = T_A V_M \tag{8}$$

The portion of the flight path segment through which the centroid of the aircraft could pass and be struck by the missile is seen to be of length D_2 (refer to Figure 4-3-4)

where

$$D_2 = L_M + W_A + D_1 \tag{9}$$

The ratio of this distance to the length of the flight path segment represents the probability of the aircraft crossing at a point where it would be struck if both vehicles were at the same altitude. Thus,

$$P(I|C) = \frac{D_2}{D} \tag{10}$$

In order to compute the probability of the vehicle altitudes being sufficiently close, it is assumed that the probability distributions for the altitudes of the two vehicles are normally distributed with specified means and uncertainties. Let

$p_A(h)$ = normal density function for aircraft altitude

$p_M(h)$ = normal density function for the missile altitude

Let the altitudes of the missile and the aircraft be specified by the altitudes of their respective centroids. Referring to Figure 4-3-5, it is seen that the aircraft altitude would have to be within the region $(H_M + H_A)$ about the missile for a collision to result.

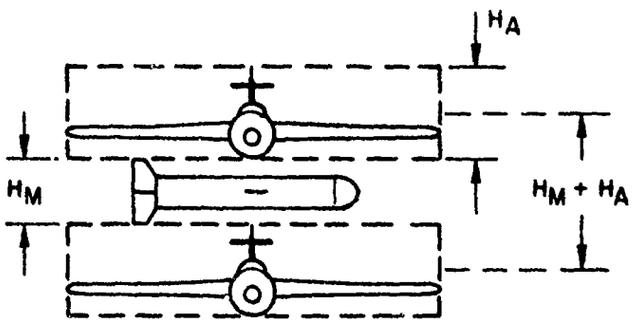

Figure 4-3-5. Altitude Collision Geometry

Consider the missile altitude to be within an increment of altitude, dh. The corresponding probability of the vehicle altitudes being sufficiently close to result in a collision is approximated by

$$p_M(h)dh\ p_A(h)\ (H_M + H_A)$$

Summing over all altitude increments gives the result

$$P(A) = (H_M + H_A)\int_0^\infty p_A(h)\ p_M(h)dh \tag{11}$$

Using equations 6 through 11 with equation 5 gives the collision probability relation

$$P(D) = F_A \left[\frac{W_M + L_A}{V_A} + \frac{L_M + W_A}{V_M} \right] (H_M + H_A) \int_0^\infty p_A(h) p_M(h) dh \qquad (12)$$

4.3.1.3 REQUIRED DATA

The data used in computing the impact and air collision hazards are presented in this section.

4.3.1.3.1 Impact Hazards Data

The data used for the computation of the hazards to critical centers and roads are presented in the following paragraphs.

4.3.1.3.1.1 Impact Distribution

A dispersion analysis was performed by General Dynamics to determine the limiting impact ranges for fragments resulting from various types of failure of the cruise missile. All types of single failures which would result in the abnormal impact of missile debris were included. The impact ranges are expressed in terms of downrange (x) and crossrange (y) distances from the position of the missile at failure. The downrange direction is defined as the direction of the missile horizontal velocity just prior to a failure. The limiting impact ranges account for all sources of impact dispersion except that the crossrange dispersion does not account for guidance system drift. This drift contribution will be accounted for later.

The limiting impact ranges account for all impacting fragments such that the impact points for all fragments lie within the region defined by the limiting values. Since dispersion data were not developed separately for each impacting fragment, the impact distribution is assumed to be the same for all fragments. A bivariate normal impact distribution is assumed using the limiting impact ranges as 3-sigma values. The parameters defining the distribution are the downrarge distance ($\bar{D}$) from the missile position at failure to the mean impact point of the fragments and the downrange (σ_{DR}) and crossrange (σ_{CR}) 1-sigma impact uncertainties. These are computed as follows:

$$\bar{D} = \frac{X_{min} + X_{max}}{2} \qquad (13)$$

$$\sigma_{DR} = \frac{X_{max} - X_{min}}{6} \tag{14}$$

$$\sigma_{CR} = \frac{y_{max}}{3} \tag{15}$$

where

X_{min}, X_{max} = minimum and maximum downrange distance to impact,

Y_{max} = maximum crossrange distance to impact.

Using the data developed by General Dynamics, the impact distribution parameters were computed for each failure mode. These are presented in Table 4-3-I where failure modes having the same impact distribution have been grouped together. Results are presented for both start of cruise (SOC) and end of cruise (EOC) missile mass properties. The values for the loss of RF carrier failure mode are based on X_{max} values which differ from those given in the General Dynamics study in that the distance traveled by the missile (on track) for the assumed 30-second delay between loss of carrier and flight termination was excluded. This was done since the missile would be performing normally (barring a second failure) up to the time of termination and, thus, vehicle "failure" does not actually occur until activation of the termination system. The revised X_{max} values are 1.040 for SOC and 0.897 for EOC.

By reviewing the parameters presented in Table 4-3-I, it is seen that the values do not have large variations over the various failure modes or in going from SOC to EOC. This is the case in particular for σ_{CR} which is the most significant parameter in computing the impact hazards. Thus, a conservative approach was used wherein the maximum values for the three parameters were assumed to apply to all failure modes and flight times (SOC to EOC). Thus,

$$\begin{aligned} \bar{D} &= 1.46 \text{ nmi} \\ \sigma_{DR} &= 0.40 \text{ nmi} \\ \sigma_{CR} &= 0.44 \text{ nmi} \end{aligned} \tag{16}$$

This allows for the computation of the impact hazards for all failure modes simultaneously and as a result, greatly reduces the computations required.

As mentioned earlier, the crossrange impact uncertainty does not include the effect of guidance system drift. The maximum drift rate for the

Table 4-3-I. Failure Mode Impact Dispersion Data

NUMBER	FAILURE MODE(S)	PROBABILITY[1] OF OCCURRNECE ($\times 10^3$)	IMPACT DISTRIBUTION PARAMETERS (NMI)					
			SOC			EOC		
			MEAN[2]	σ_{DR}	σ_{CR}[3]	MEAN[2]	σ_{DR}	σ_{CR}[3]
1	3 Fins Hardover	.08	1.23	.31	.31	1.46	.40	.27
2	3 Fins Nulled	.02	1.23	.33	.40	1.06	.18	.16
3	V-Fin Hardover V-Fin No Control	.46	.81	.26	.44	.66	.21	.41
4	R/L Fin Hardover	.19	1.23	.31	.32	1.36	.38	.39
5	R/L Fin Nulled	.05	1.36	.30	.30	1.38	.34	.26
6	R/L Fin No Control	.74	1.29	.33	.32	1.36	.38	.39
7	3 Fins No Control Rapid Loss of Thrust Loss of Power Inlet Closes	3.38	1.23	.33	.40	1.46	.40	.27
8	Gradual Loss of Thrust	1.79	1.37	.34	.30	1.22	.30	.25
9	Erroneous Turn	2.19	1.22	.32	.34	1.03	.30	.37
10	Loss of RF Carrier	.10	.87	.06	.27	.74	.05	.26
	TOTAL	9.00						
		Maximum	1.37	.34	.44	1.46	.40	.41

DR = Downrange
CR = Crossrange

1. Based on a one-hour mission
2. Downrange distance ($\bar{D}$) from vehicle position at failure to debris mean impact
3. Does not include guidance system drift

missile is 1.0 nmi per hour. Because the drift error of the missile is corrected periodically at TERCOM updates, the maximum drift that can occur is a function of the maximum time between updates. This time is estimated to be 0.5 hour. Thus, the maximum crossrange drift is 0.5 nmi. This is assumed to be a 3-sigma dispersion. Since the drift contribution is relatively small, it is assumed that this maximum drift dispersion is applicable throughout flight. Combining the drift effect with the crossrange uncertainty of equation 16 gives the result

$$\sigma_{CR} = \left[(.44)^2 + \left(\frac{0.5}{3}\right)^2 \right]^{\frac{1}{2}} = 0.47 \text{ nmi} \tag{17}$$

The locus of the mean impact point for the fragments is computed from the flight path of the missile (position versus flight time) and the distance $\overline{D}$. The mean impact point coordinates corresponding to a given flight time are obtained using the relations

$$\overline{\lambda} = \lambda + \frac{D \sin\alpha}{R_E \cos\phi} \tag{18}$$

$$\overline{\phi} = \phi + \frac{D \cos\alpha}{R_E} \tag{19}$$

where

$\overline{\phi}, \overline{\lambda}$ = latitude and longitude, respectively, of the mean fragment impact point (radians),

ϕ, λ = latitude and longitude, respectively, of the vehicle position at the time of failure (radians),

α = azimuth of the downrange direction (measured clockwise from north),

R_E = local radius of the earth (nmi).

The resulting mean impact point locus is presented in Tables 4-3-II through 4-3-IV for the nominal and alternate flight path from Naval Weapons Center (NWC) to Dugway Proving Ground (DPG) and the nominal and alternate flight path segment from Vandenberg AFB (VAFB) to NWC.

4.3.1.3.1.2 Failure Probability

The probability of occurrence for the various types of vehicle failure has been estimated by General Dynamics. The results are reflected in

Table 4-3-II. Mean Impact Point Locus - NWC to DPG - Nominal Flight Path

FLIGHT TIME (SEC.)	MEAN IMPACT POINT		DOWNRANGE AZIMUTH (Deg.)
	LATITUDE (Deg.)	LONGITUDE (Deg.)	
0.0	35.5289	-117.5978	10.00
157.6	35.8126	-117.5353	10.00
159.0	35.8508	-117.5038	35.00
175.4	35.8756	-117.4743	47.00
359.8	36.1407	-117.1242	47.00
375.0	36.1703	-117.1066	20.00
389.1	36.2007	-117.1035	9.00
405.8	36.2350	-117.1133	343.0
855.3	37.1422	-117.4485	343.0
880.1	37.1949	-117.4399	10.0
897.2	37.2205	-117.4025	37.00
910.1	37.2377	-117.3764	54.00
1016.4	37.3717	-117.1513	54.00
1034.2	37.3856	-117.1073	71.00
1047.9	37.3878	-117.0709	83.00
1627.5	37.5329	-115.5456	83.00
1641.9	37.5131	-115.5110	102.0
1660.1	37.4669	-115.4733	130.0
1840.6	37.2298	-115.0923	130.0
1870.4	37.2179	-115.0358	100.0
1892.0	37.2233	-114.9786	82.00
1956.3	37.2443	-114.8106	82.00
1971.2	37.2654	-114.7783	64.00
1942.4	37.2917	-114.7490	45.00
2424.1	37.9589	-113.9536	45.00
2438.5	37.9920	-113.9482	23.00
2457.9	38.0339	-113.9497	.50
2775.3	38.7020	-113.9347	.50
2793.7	38.7368	-113.9070	25.00
2806.0	38.7567	-113.8856	39.00
2822.6	38.7724	-113.8436	59.00
2918.9	38.8804	-113.6235	59.00
2939.6	38.9212	-113.5975	28.00
2961.4	38.9691	-113.6000	0.00
3222.7	39.5192	-113.6000	0.00
3234.9	39.5434	-113.5839	15.00
3246.3	39.5636	-113.5658	27.00
3260.1	39.5812	-113.5337	48.00
3281.8	39.6112	-113.4887	48.00
3295.6	39.6202	-113.4515	65.00
3313.7	39.6234	-113.4009	82.00
3326.8	39.6314	-113.3669	82.00
3340.1	39.6532	-113.3386	57.00
3355.5	39.6780	-113.3109	42.00
3372.7	39.7154	-113.3018	15.00
3565.6	40.1065	-113.1588	15.00

THIS PAGE IS BEST QUALITY PRACTICABLE
FROM COPY FURNISHED TO DDC

Table 4-3-III. Mean Impact Point Locus - VAFB to NWC - Nominal Flight Path

FLIGHT TIME (SEC.)	MEAN IMPACT POINT		DOWNRANGE AZIMUTH (Deg.)
	LATITUDE (Deg.)	LONGITUDE (Deg.)	
0.0	34.7	-120.5704	90.
858.4	34.7	-118.3724	90.
887.7	34.7329	-118.3059	58.
917.5	34.7928	-118.2747	20.4
1038.8	35.0328	-118.1687	20.4
1052.8	35.0514	-118.1370	37.25
1064.5	35.0673	-118.1149	54.1
1281.0	35.3343	-117.6639	54.1
1302.4	35.3757	-117.6374	31.55
1320.0	35.4139	-117.6328	10.
1376.3	35.5289	-117.5978	10.

Table 4-3-IV. Mean Impact Point Locus - VAFB to NWC - Alternate Flight Path

FLIGHT TIME (SEC.)	MEAN IMPACT POINT		DOWNRANGE AZIMUTH (Deg.)
	LATITUDE (Deg.)	LONGITUDE (Deg.)	
0.0	34.4372	-120.4792	45.00
171.6	34.6922	-120.1691	45.00
165.3	34.6999	-120.1330	66.00
207.3	34.7000	-120.0754	90.00
872.4	34.7000	-118.3724	90.00
901.7	34.7329	-118.3059	58.00
931.5	34.7928	-118.2747	20.40
1052.7	35.0328	-118.1687	20.40
1066.7	35.0511	-118.1367	38.05
1078.5	35.0659	-118.1138	58.00
1324.7	35.3379	-117.5747	58.00
1344.4	35.3758	-117.5496	31.00
1368.8	35.4293	-117.5494	3.00
1416.3	35.5293	-117.5484	3.00

THIS PAGE IS BEST QUALITY PRACTICABLE
FROM COPY FURNISHED TO DDC

Table 4-3-I. In obtaining the probability values of Table 4-3-I, it was assumed that the probability for a 1-fin hardover, 1-fin nulled or 1-fin no control failure was equally distributed among the left, right and vertical fins. The probability of occurrence for the loss of RF carrier failure mode was computed based on a carrier reliability of 0.9999. The probability of occurrence per second (failure rate) for each mode of failure is assumed to be constant over all segments of flight. Since the probabilities of occurrence are based on a 1-hour mission, the failure rate for all failures is

$$\text{Rate} = \frac{.009}{3600} = 2.5\ \text{E-6 failures/second} \tag{20}$$

4.3.1.3.1.3 Impacting Fragments

Eight fragments, three of which are considered to be nonhazardous, result from a recovery or termination of the cruise missile. The nonhazardous fragments which would not be expected to cause significant injury are the pilot chute, main chute and a .03-pound lead slug. The remaining five fragments are listed in Table 4-3-V together with the corresponding weights, projected areas and casualty areas.

Table 4-3-V. Hazardous Impacting Fragments

ITEM	WT (LBS)	PROJECTED AREA (A_p)	CASUALTY AREA (A_c)
1. Recovery Compartment Cover with Thruster Pistons and Risers	24.	3.8 FT^2	13.9 FT^2
2. Aft Compartment Cover	1.6	1.1	8.0
3. Steel Piston	.08	Negligible	3.4
4. Steel Piston	.08	Negligible	3.4
5. Missile and Main Chute	--	41.9	68.0
			Σ=96.7

The casualty area (A_c) for each fragment is computed using the relation

$$A_c = \pi \left[\sqrt{\frac{A_p}{\pi}} + r_p \right]^2 \qquad (21)$$

where

r_p is the radius of the area occupied by a person (assumed to 1.0 feet).

It was assumed that the fragments do not break up, bounce or scrape along the ground upon impact. The total casualty area for the fragments is 96.7 square feet.

4.3.1.3.1.4 Population Centers and Roads

Tables 4-3-VI and 4-3-VII illustrate the type of data on population centers and roads near the missile flight path which the computer program uses.

4.3.1.3.2 Aircraft Collision Hazards Data

The data used in the computation of the aircraft collision hazards are presented in the following paragraphs.

4.3.1.3.2.1 Air Traffic

The low altitude air traffic crossing the missile flight path is presented in Table 4-3-VIII. The air traffic data are presented for segments of the flight path over which the aircraft speed, expected heading, altitude distribution, and aircraft frequency (aircraft/unit/time) can be assumed to be constant.

4.3.1.3.2.2 Vehicle Dimensions

The dimensions of the cruise missile and the estimated dimensions for a typical general aviation aircraft are presented in Table 4-3-IX.

4.3.1.3.2.3 Missile Parameters

The speed of the missile is 0.7 mach which, based on an altitude of 5000 feet ASL, is equal to 768.1 feet/second. The missile altitude is assumed to have a mean of 5000 feet AGL and a 1-sigma uncertainty of 33 feet. The uncertainty was based on a maximum altitude error in a terrain following mode of 100 feet. The maximum error was assumed to represent a 3-sigma dispersion.

Table 4-3-VI. Population Centers

POPULATION CODE	AREA SQ. N.MI.	LATITUDE DEGREES	LONGITUDE DEGREES	POPULATION	POPULATION NAME
1210001	4.	35.317	-117.960	80	CANTIL
1410002	10.	35.370	-117.620	655	RED MTN
1210003	2.	35.362	-117.687	60	SALTDALE
1210004	1.	35.407	-117.790	9	GARLOCK
1210005	10.	35.653	-117.693	21977	RIDGECREST,CHINA LAK
1210006	4.	35.603	-117.818	800	INYOKERN
1410007	10.	35.725	-117.377	1989	WESTEND,ARGUS,SEARLE
1510008	2.	35.893	-117.383	60	HOMEWOOD CANYON
1510009	1.	35.670	-117.878	20	PEARSONVILLE
1510010	4.	35.935	-117.908	20	LITTLE LAKE
1510011	4.	36.265	-117.208	10	WILDROSE
1510012	4.	36.267	-117.592	150	DARWIN
1510013	1.	36.342	-117.467	5	PANAMINT SPRINGS
1510014	4.	36.480	-116.880	250	DEATH VALLEY-WINTER
1510015	1.	36.59[illegible]	-116.942	1	BEATTY JCT
1510016	1.	36.608	-117.140	125	STOVE PIPE WELLS-WIN
1510017	2.	36.767	-117.565	30	TEAKETTLE JCT-CAMPS
1510018	2.	37.010	-117.300	45	SCOTTYS CASTLE
2210019	10.	37.025	-116.750	60	RTE95-ROADSIDE
1510020	2.	37.092	-117.607	25	MTN-CAMPERS
2310021	1.	37.112	-118.690	10	CARP
2310022	1.	37.147	-118.365	6	MINES
2210023	5.	37.250	-117.085	22	SCOTTYS JCT
2310024	4.	37.375	-118.165	302	ALAMO,ROADSIDE
2310025	1.	37.352	-118.535	12	EIGIN
1510026	1.	37.367	-117.988	35	DEEP SPRINGS
2110027	1.	37.355	-117.350	3	GOLD-POINT
2110028	1.	37.455	-117.700	9	MINES
2110029	1.	37.458	-117.498	10	LIDA
2310030	1.	37.467	-118.197	3	ASH-SPRINGS
2110031	1.	37.495	-117.183	5	LIDA-JCT
2310032	1.	37.498	-118.067	5	BEAVER-DAM
2310033	1.	37.513	-118.250	13	BARCLAY
2310034	10.	37.557	-115.230	37	MIRO FARMS-RANCHES
2310035	4.	37.610	-114.513	916	GALIENTE
2310036	1.	37.652	-115.033	9	TEMPIUTE
2110037	2.	37.707	-117.233	234	GOLDFIELD

THIS PAGE IS BEST QUALITY PRACTICABLE
FROM COPY FURNISHED TO DDC

THIS PAGE IS BEST QUALITY PRACTICABLE
FROM COPY FURNISHED TO DDC

Table 4-3-VII. Road Locations

Road Name	Begin Latitude	Begin Longitude	End Latitude	End Longitude	Width Feet	Density People/k
1017	35.000	-120.426	35.000	-120.515	70.	16.
1016	34.887	-120.410	35.000	-120.426	70.	16.
1015	34.745	-120.276	34.887	-120.410	70.	23.4
1014	34.585	-120.005	34.708	-120.276	70.	23.4
1013	34.490	-120.227	34.675	-120.150	70.	24.8
1012	34.415	-119.563	34.490	-120.227	70.	104.0
1011	34.340	-119.490	34.415	-119.563	70.	104.0
0011	34.515	-120.218	34.525	-120.325	30.	6.6
0012	34.525	-120.325	34.760	-120.515	30.	6.6
0013	34.665	-120.440	34.950	-120.020	30.	6.6
0014	34.760	-120.515	34.815	-120.440	70.	14.0
1501	34.500	-119.795	34.585	-120.005	30.	15.4
1502	34.440	-119.795	34.500	-119.795	30.	15.4
1751	34.950	-120.415	34.770	-120.110	30.	3.5
1752	34.770	-120.110	34.640	-120.045	30.	3.5
1753	34.850	-120.250	35.025	-120.119	30.	3.5
1061	35.000	-120.426	35.025	-120.119	30.	1.0
1062	35.080	-120.020	34.940	-119.665	30.	1.0
1063	34.940	-119.665	34.940	-119.457	30.	1.0
1064	35.550	-119.400	35.550	-118.975	30.	1.0
0591	34.533	-119.300	34.585	-119.250	30.	1.4
0592	34.583	-119.250	34.610	-119.375	30.	1.4
0593	34.610	-119.373	34.690	-119.350	30.	1.0
0594	34.690	-119.350	34.940	-119.525	30.	1.0
0595	34.940	-119.457	35.085	-119.390	30.	1.4
1381	35.080	-119.630	34.875	-119.330	30.	4.4
1382	34.875	-119.330	34.795	-118.825	30.	4.4
1383	34.775	-118.800	34.780	-118.175	30.	4.4
1384	34.825	-119.000	34.720	-119.110	30.	4.4
1385	34.720	-119.110	34.693	-119.350	30.	4.4
0053	35.080	-116.987	34.905	-119.925	70.	49.4
0054	34.905	-119.925	34.775	-118.795	70.	49.4
0051	34.775	-118.795	34.345	-118.550	70.	49.4
1501	34.366	-119.692	34.458	-119.195	30.	1.4
1502	34.458	-119.195	34.560	-119.045	30.	1.4
1261	34.560	-119.045	34.437	-118.605	30.	1.4
1262	34.437	-118.405	34.413	-118.485	30.	1.4
[illegible]	34.345	-118.550	34.313	-118.245	70.	16.[illegible]
0144	34.515	-118.205	34.500	-118.115	70.	16.[illegible]
0145	34.500	-118.115	34.782	-118.177	70.	16.[illegible]
[illegible]	34.782	-118.177	35.027	-118.163	70.	29.4
0143	35.210	-118.040	35.050	-118.176	30.	10.3
0581	35.228	-118.550	35.102	-118.370	70.	9.[illegible]
0582	35.102	-118.370	35.127	-117.945	70.	18.[illegible]
0583	35.120	-118.205	35.027	-118.165	70.	35.4
0584	35.050	-118.176	35.010	-117.915	70.	18.[illegible]
0585	35.010	-117.915	35.010	-117.655	70.	3.[illegible]
0586	35.010	-117.435	34.985	-117.465	70.	3.[illegible]
0181	34.585	-118.135	34.585	-118.045	30.	16.[illegible]
0182	34.585	-118.045	34.582	-118.000	30.	16.[illegible]
0183	34.582	-118.000	34.515	-117.925	30.	16.[illegible]
1304	35.127	-117.945	35.010	-117.915	30.	20.[illegible]
0954	35.150	-117.40	34.950	-117.520	70.	3.[illegible]
1447	35.35	-117.65	35.127	-117.945	30.	18.
0541	35.21	-118.04	35.40	-118.0	30.	10.[illegible]
0542	34.40	-118.0	35.70	-117.68	30.	10.[illegible]
0561	35.68	-118.03	35.61	-117.92	30.	0.[illegible]

Table 4-3-VIII. Air Traffic Data (Low Altitude)

	AIR LANE	WIDTH (n.mi.)	AIRCRAFT ALTITUDE (FT.) MEAN	AIRCRAFT ALTITUDE (FT.) 1σ UNCERTAINTY	AIRCRAFT FREQUENCY (No./HR.)
	1	8	5700	1633	0.5
	2	15			0.6
	3	35			1.5
MMC TO RPB	4	32			0.5
	5	11			0.75
	6	11			0.76
	7	6			0.5
	8	5			0.5
	9	3			2.0
YAFB TO MWB	10	6			2.0
	11	2			2.0
	12	3			2.0
	13	4			2.0
	BETWEEN AIRLANES	-			.01 per n.mi. of Missile Flight Track

THIS PAGE IS BEST QUALITY PRACTICABLE
FROM COPY FURNISHED TO DDC

Table 4-3-IX. Vehicle Dimensions

	MISSILE	AIRCRAFT
Length (ft.)	18.2	30
Width (Wingspan) (ft.)	8.6	30
Height (Including Fins) (ft.)	3.5	10

4.3.2 Safety Hazard Analysis Program (SHAZAM)

4.3.2.1 Introduction

The launching of missiles of the Polaris family from the broad ocean areas into target areas located in the vicinity of island groups can present a range safety problem for inhabited islands near the line of flight. Because previous computer programs for hazard evaluation were intended primarily for hazards in the vicinity of the launch area or those associated specifically with the impact area, it has been necessary to develop a new approach designed specifically for evaluating hazards accompanying second stage flight malfunctions of Polaris missiles. A computer program was structured to treat individually the various failure modes associated with the Polaris vehicle. These include combinations of pitch, yaw and roll associated with angular accelerations and angular velocities of the malfunctioning vehicle as well as specific malfunctions affecting reentry body deployment. This report represents a final version of SHAZAM which incorporates numerous improvements in accuracy and utility over earlier versions. The range safety philosophy which establishes the basis of the program maintains that a malfunctioning missile will be allowed to continue its flight to burnout unless its filtered instantaneous impact point (IIP) trace intersects an abort wall. In SHAZAM, burnout is assumed either to occur at a specified time

after malfunction or at the normal time of burnout of the rocket motor. Upon abort-wall impingement, the vehicle is either destructed or thrust terminated, depending upon the type of wall encountered.

In addition to evaluating the hazards associated with a specific flight test, SHAZAM can be employed in multiple runs to determine the appropriate abort-wall geometry which will provide optimal protection to populated islands, while giving a good missile a high probability of achieving its mission without abort.

4.3.2.2 Computer Program Description

4.3.2.2.1 Scope

This program is intended for evaluating the hazards associated with flights of the Polaris missiles relative to malfunctions which manifest themselves when the missile is outside the sensible atmosphere. The hazards can result from reentry of a failed vehicle or from command abort of a vehicle, the IIP of which violated an abort wall. The program is general enough in concept and operation that it could be used for vehicles other than those specified above with appropriate choices of input parameters.

The dimensionality of the program is as follows:

- Trajectory points - 60 trajectory points may be input, but the first N (specified) trajectory data points input are used only for initializing the filter employed in the abort logic.

- Time blocks - 15 failure time blocks are permissible.

- Failure modes - five distinct crossrange failure modes are built into the program. Three correspond to angular acceleration type malfunctions including roll-pitch-yaw, pitch-yaw and yaw; the remaining two correspond to the angular velocity type malfunctions, pitch-yaw and yaw. The program also will accomodate three distinct reentry vehicle failure modes.

- Failure cases - ten crossrange failure cases are permissible, to be comprised of any mix of the above five failure modes. One downrange failure mode accommodates all contributors to downrange failures.

- Fragments - 16 fragment classes are allowable for command destruct of a vehicle. Sixteen fragment classes are also allowed for a thrust-terminated vehicle plus an additional three for the thrust termination ports. For reentry breakup following burnout,

the 16 fragment classes in the thrust termination list are utilized.

- Reentry vehicles - the program can handle up to three reentry vehicles.

- 3-sigma guidance - 2 points are input to define the 3-sigma guidance deviations from the nominal locus of impact points.

- Abort walls - ten open or closed abort walls may be input, each being defined by a maximum of ten points.

- Population centers - a maximum of 100 locations can be input, defined by name, land area, population and geodetic coordinates.

- PAGM timeblocks - a maximum of 20 timeblocks can be input defining the probability of abort of a good missile over a specified timeblock.

The program provides, as output, the impact loci and corresponding standard deviations for each failure mode of the nonaborted vehicle. In addition it provides the probability of impact associated with each population library location and within a 1-nautical mile border about the location, and the casualty expectation based upon injury and lethality criteria.

Output options include the following:

- Printout of input data without program execution.

- Suppression of all abort logic.

- Specification of malfunction interval for no abort to reduce program run time.

- Printout of point of impingement of the filtered IIP locus with the abort wall and associated fragment impact ellipse parameters for selected fragments, walls or failure modes.

- Card output of vehicle position and velocity during a malfunction turn.

- Generation and printout of vehicle IIP during a failure turn for specified malfunction times and failure modes.

4.3.2.2.2 Operational Instructions

4.3.2.2.2.1 Console/Restoring

All options for the program are under programmed control. Therefore, sense switches, indicators and other console operations are not necessary. The program has no restart capability.

4.3.2.2.2.2 Magnetic Tape Setup

Logical Assignment	Mode	Density	Physical Assignment	Purpose
5	BCD	High	A2	System Input
6	BCD	High	A3	System Output
*10	BCD	High	A5	Tape Option
13	BCD	High	B5	Card Output
33	BIN	High	B5	TWRT Input

*The tape option applies only when standard flight data which will be used with multiple runs is input from a tape. Abort wall, filter and PAGM data are then input as cards. The population library may be input from cards as an option.

4.3.2.2.3 Sequence of Operations

The process of generating hazards due to failed or aborted vehicles is performed by the computer program through the following series of sequential steps:

1. Input data is loaded, subjected to any necessary transformations and then output.

2. The filter which simulates the tracking radar data-smoothing filter is initialized by the first N trajectory points as determined by linear interpolation between these input points, where N is specified on input.

3. A failure mode is selected and a mean malfunction turn is started.

4. Impact points are generated from the filtered data of the mean malfunction turn. The mirror images of the impact points are created on both sides of the nominal vacuum IIP.

5. If no abort wall is intercepted by the filtered impact locus, a mean vehicle burnout impact point is generated at approximately

1-second intervals in time of malfunction. A 1-sigma burnout impact point is also generated for the purpose of determining the standard deviation about the mean burnout impact point. The time of malfunction is then incremented in preparation for the next malfunction turn.

6. If an a abort wall is intercepted by the filtered locus, the subsequent search for intercept is limited to that side of the nominal IIP and steps 7 through 12 apply. For a yaw-pitch-roll failure, the standard deviation is based upon burnout time standard deviation. For other failures it is based upon standard deviation in yaw rate or acceleration.

7. The time of malfunction, corresponding to first intercept of that wall, is saved.

8. A malfunction turn vacuum IIP is generated, based upon the time of wall interception by the filtered locus plus the abort reaction time.

9. A second impact point is generated by incrementing the trajectory by an additional time interval equal to the computer cycle delay time. The midpoint between the two impact points along with other impact ellipse parameters are determined.

10. Malfunction time is incremented and another abort wall impact point is generated. This process is repeated until either the filtered impact locus moves beyond the abort wall, or some point on the filtered locus is found to be downrange of the most uprange point defining the next adjacent abort wall on the same side of the nominal IIP. If the latter situation occurs, a search by the filtered locus is immediately initiated for this adjacent wall as well as the primary wall. If the adjacent wall is intercepted, the search for the primary wall is terminated. If the adjacent wall is not intercepted, the search continues for the primary wall until the filtered locus can no longer reach that wall. In either case the last malfunction time is saved.

11. The hazards associated with that abort wall for the selected failure mode are assessed by development of a composite 1-sigma impact ellipse for each malfunction time and each fragment which incorporates radar tracking uncertainty, guidance standard deviation, computer cycle time delay and fragment dispersion. If the abort wall is designated as a thrust termination wall, an additional ellipse is generated for thrust termination port fragments. The ellipse centers are next corrected to account for atmospheric drag effects. Adjacent, overlapping ellipses form a hazard band associated with that abort wall. Hazards are then evaluated for locations near these ellipses.

12. Locations are checked to determine if they lie within the area protected from no-abort failures by the abort wall. If so, they are appropriately tagged as protected locations.

13. The program now returns to the malfunction time corresponding to first intercept of the abort wall and proceeds to search on the opposite side of the nominal IIP for intercept of another abort wall until the time of malfunction corresponding to first miss of the previous abort wall is reached. From that point a simultaneous search for abort walls on either side of nominal is initiated.

14. The process outlined in steps 4 through 13 is repeated until the time of malfunction reaches the time of fuel depletion.

15. The hazards associated with the burnout impact loci are then evaluated. The magnitude of such hazards to locations which are protected by the abort walls is reduced by the probability of a successful abort. These hazards are added to those generated from the abort ellipses. The program then returns to the nominal trajectory point corresponding to the first malfunction turn.

16. The program selects the next failure mode and initiates a malfunction turn, proceeding as in steps 3 through 13. The hazards produced by this failure mode are summed with those produced by previous failure modes taking into account the failure mode occurrence probability. This process is continued until all failure modes have been considered.

17. The hazards associated with downrange failures and abort of a good missile are evaluated and added to the other hazard contributions.

18. Finally the hazards associated with reentry vehicles and impact of the second stage are included in the summation.

19. The program outputs not only the impact probabilities and casualty expectations, but also the points of filtered locus - abort wall intersection, the impact ellipses for selected abort walls, failure modes and fragments, and the burnout impact loci and standard deviations.

4.4 SPACE AND MISSILE TEST CENTER (SAMTEC)

4.4.1 Launch Area Risk Analysis

The SAMTEC launch and near launch areas at Vandenberg AFB are so situated that many risk assessment considerations associated with the launch of a missile or space booster must be undertaken. Local towns of Santa Maria, Lompoc, Vandenberg Village and Mission Hills in addition to on-base population and major population centers such as Los Angeles and San Diego are potential risk centers. Extending almost the entire length of Vandenberg AFB is the Southern Pacific Railroad. This major rail transportation system, as well as sea traffic lanes less than 30 miles offshore, and nearby air traffic lanes are additional risk centers.

With the number and variety of missile launches from SAMTEC and the large number of potential risk centers influenced by these launches, a risk assessment model which evaluates missile performance factors against these risk centers is required. Under contract with the J. H. Wiggins Corp., SAMTEC has developed the Launch Risk Analysis (LARA) program - a comprehensive, computerized missile launch risk assessment model. The following discussion of the LARA program is taken from a paper presented to the Proceedings 1977 Annual Reliabilty and Maintainability Symposium by representatives of J. H. Wiggins Corp.

The basic requirements of a launch risk analysis are: (1) define the impact probability distributions for impacting vehicle debris which account for all significant sources of impact uncertainty, (2) compute the corresponding probabilities of one or more fragments impacting specified critical centers (land areas, generally populated) and the expectation of casualties for each center. The concept is illustrated in Figure 4-4-1.

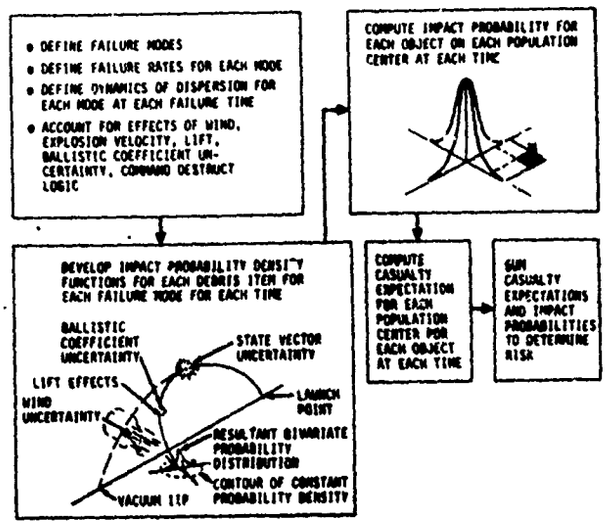

Figure 4-4-1. Risk Computation

To properly describe the problem and solution, it is necessary to define the basic factors which must be contemplated. They are:

1. All significant events which can result in the impact of launch vehicle debris must be considered. This includes the normal jettisoning of hardware such as depleted motor cases and all modes of vehicle failure which will result in the abnormal impact of vehicle debris. The basic vehicle failure modes which are considered are malfunction turns and premature thrust termination. Malfunction turns cover all abnormal vehicle turns from a gradual turn off course to a tumble turn.

2. The vehicle dynamic behavior following a malfunction turn failure must be assessed to statistically define the resulting perturbation in the vehicle state vector from the time of failure to the time when steady state conditions are reached or the vehicle breaks apart. This analysis must include the effect of a flight termination system (FTS), if one is employed.

3. The fragments resulting from the breakup of a vehicle must be defined and accounted for. Breakup may result from the activation of an FTS or may be due to excessive airloads.

4. The impact distribution for each fragment must include the effects of initial state vector uncertainty and the effects of the atmosphere on the fragment during free fall. State vector uncertainty results from normal vehicle guidance and control uncertainties, malfunction turn dynamics and destruct-induced fragment-velocity perturbations.

5. The lethality of each impacting fragment must be defined in terms of the size of the land area endangered by the fragment and the ability of the fragment to penetrate different classes of structures.

6. All endangered critical centers must be defined in terms of their location, size and population. The population must be distributed according to various levels of sheltering.

The launch risk analysis is accomplished by segmenting the vehicle trajectory into short time intervals. Hazards for each time interval are computed for each mode of failure assuming the failure occurred at a single representative time point within the interval. The results are weighted according to the probability that the particular failure mode will occur during the time interval. The procedure is delineated in the flow diagram, Figure 4-4-2. Successive failure times are spaced sufficiently close so that the successive impact distributions for each impacting fragment overlap sufficiently to simulate the actual continuous distribution.

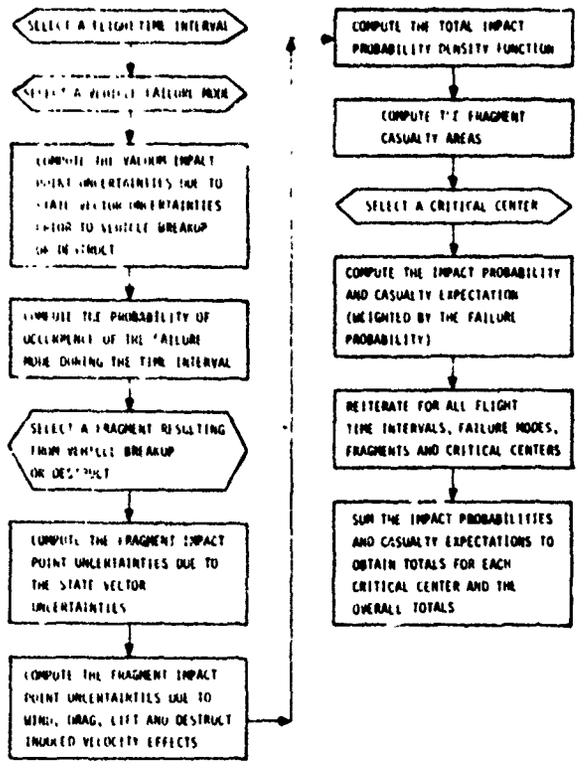

THIS PAGE IS BEST QUALITY PRACTICABLE
FROM COPY FURNISHED TO DDC

Figure 4-4-2. Launch Risk Analysis Procedure

One of the primary requirements of a launch risk analysis is the computation of fragment impact data as a function of flight time. The impact data for a fragment are the coordinates (latitude and longitude) of the nominal impact point together with data required in the analysis of fragment lethality (time of fragment free fall, impact velocity components, decrease in the size of a burning solid propellant fragment during free fall). The nominal impact point for a fragment is defined as the impact point corresponding to an initial state vector of the vehicle at the time of a failure. The mean impact point for a fragment is computed from the nominal point by applying the mean perturbations resulting from the various sources of impact uncertainty.

Since data are required for a very large number of impacting fragments (each fragment, failure mode and failure time combination), it is necessary to employ a rapid and accurate technique for computing these data. If the impact data were computed for each impact by numerically integrating the impact trajectory, the computation time would become excessive. To overcome this problem an interpolation technique was

developed which greatly reduces the required number of integrated impact computations. Integrated impact data are computed for a set of appropriately spaced vehicle flight times and fragment ballistic coefficients (β). The impact data for any particular failure time and fragment (defined by its β value) are obtained by first interpolating versus flight time, followed by an interpolation versus β. Simple linear interpolations can be used for the fragment lethality data item while cubic interpolations are required for the impact coordinates.

In addition to the computation of nominal impact data, a method is required to predict fragment impact points corresponding to relatively small perturbations in initial state vector, or equivalently, to perturbations in the vacuum impact point. To accomplish this, the concept of the "debris centerline" is used. The debris centerline (different versions of which are given in references 1 and 2) is defined as the locus of impact points for fragments having varying ballistic coefficients which correspond to a specified initial state vector. What is required is a transformation from a known centerline, such as the centerline defined by the nominal impact points, to the perturbed centerline corresponding to a perturbed vacuum impact point. The required transformation is depicted in Figure 4-4-3.

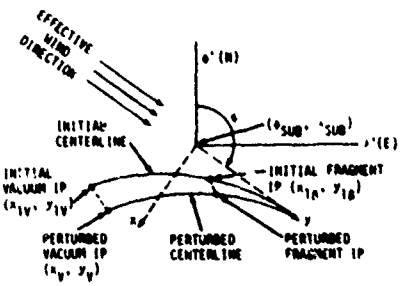

Figure 4-4-3. Centerline Transformation

The $\lambda' - \phi'$ coordinate system is an east-north system originating at the sub-vehicle point (ground projected position of the vehicle at the time of failure) when

$$\lambda' = (\lambda - \lambda_{SUB}) \cos \phi_{SUB} \qquad (1)$$

$$\phi' = \phi_{SUB} \qquad (2)$$

λ, ϕ are the longitude and latitude of impact and λ SUB, ϕ SUB are the longitude and latitude of the sub-vehicle point. The xy coordinate system is defined by the "effective wind direction" which is defined as the direction from the sub-vehicle point to the impact point for a fragment which becomes immediately embedded in the wind, i.e., a fragment having a very low ballistic coefficient. The direction is defined by its azimuth angle, y. The y axis is oriented along the effective wind direction, and the x axis is 90° clockwise from y. The transformation from the $\lambda' - \phi$ system to the x-y system is

$$x = \lambda' \cos \psi - \phi' \sin \psi \tag{3}$$

$$y = \lambda' \sin \psi + \phi' \cos \psi \tag{4}$$

The empirical centerline transfomation relations are

$$\lambda'_\beta = \frac{1}{x_{1V}} \left[\{(y_V - y_{1V}) \cos \psi - x_V \sin \psi\} x_{1\beta} + x_{1V} \sin \psi \, y_{1\beta} \right] \tag{5}$$

$$\phi'_\beta = \frac{1}{x_{1V}} \left[\{(y_V - y_{1V}) \cos \psi - x_V \sin \psi\} x_{1\beta} + x_{1V} \cos \psi \, y_{1\beta} \right] \tag{6}$$

Thus, given the vacuum and fragment impact points for a reference initial condition and the vacuum impact point for a perturbed initial condition, the perturbed impact point for any fragment can be predicted. The transformation provides sufficient accuracy whenever the nominal centerline is well defined.

Fragment impact uncertainties come from four basic sources: (1) uncertainty in the vehicle state vector at vehicle breakup or destruct, (2) uncertainty in any destruct velocity imparted to the fragment by a destruct system, (3) uncertainty in the atmospheric environment during free fall, and (4) uncertainty in the fragment aerodynamic lift and drag. The models associated with these uncertainties are presented in the following paragraphs. Since the sources of uncertainty are independent, e.g., wind uncertainty is independent of explosion velocity uncertainty, the effects of each uncertainty source are developed separately and then combined to produce the total impact uncertainties.

4.4.1.1 Vehicle State Vector Uncertainty

The vehicle state vector uncertainty contribution to the impact distribution is developed based on the assumption that the perturbations in fragment impact points caused by variations in initial velocity (from the expected velocity) can be linearly related. Since the impacts will be assumed to be normally distributed, the probability distributions are fully characterized by the first two moments. The impact covariance (defining the impact uncertainties) is calculated as shown in equation 7.

$$\left[\Sigma_{DC}\right] = \left[\frac{\partial(D,C)}{\partial(V_1,V_2,V_3)}\right] \left[\Sigma_V\right] \left[\frac{\partial(D,C)}{\partial(V_1,V_2,V_3)}\right]^T \tag{7}$$

Position uncertainty can be ignored because of the relatively small influence compared to velocity uncertainty. The mean perturbation in the fragment impact point is obtained from the mean initial velocity perturbations $[\overline{\Delta V}]$ as shown in equation 8.

$$\begin{Bmatrix} \overline{\Delta D} \\ \\ \overline{\Delta C} \end{Bmatrix} = \left[\frac{\partial(D,C)}{\partial(V_1,V_2,V_3)}\right] \begin{Bmatrix} \overline{\Delta V_1} \\ \overline{\Delta V_2} \\ \overline{\Delta V_3} \end{Bmatrix} \tag{8}$$

where

D,C = downrange and crossrange impact coordinates

V_1, V_2, V_3 = velocity components in a Cartesian coordinate system

$\left[\Sigma_{DC}\right]$ = impact covariance matrix

$\left[\Sigma_V\right]$ = initial velocity covariance matrix

The partial derivatives (referred to as miss coefficients) can be computed by perturbing the ballistic equations for a vacuum trajectory. These vacuum miss coefficients are then scaled to account for the effect of drag on an object. The scaling coefficients are determined using the centerline transformation relations (equations 5 and 6).

The first source of initial velocity uncertainty to be considered is that due to guidance and performance variations of the vehicle. Frequently the effects of these variations are specified directly in terms of vacuum impact uncertainties. If these variations are defined in terms of uncertainties in the vehicle velocity vector, the uncertainties can be transferred to impact uncertainties using equation 7.

The most significant source of vehicle velocity uncertainty is the malfunction turn behavior of the vehicle. The turn can range from a gradual turn to a tumbling turn depending upon the effective angle of the thrust vector relative to the vehicle axis. The orientation of the tumble plane is assumed to be completely random and the angle of the thrust vector misalignment can be expressed in terms of a probability density function (PDF) ranging from zero to a specified maximum for the particular gimbal system. The entire procedure for the development of the malfunction turn impact PDF is shown in Figure 4-4-4.

The procedure accounts for the violations of destruct lines which modify the basic impact dispersions due to flight termination (abort). Figure 4-4-5 shows an ellipse representing the impact uncertainty of the vacuum impact point of a missile due to vehicle initial velocity uncertainties (including the guidance and performance contribution). Normal range safety practice uses a real-time vacuum instantaneous impact point (VIIP) to determine whether a missile is malfunctioning. If this VIIP crosses a destruct boundary the missile is destroyed. The impact distribution as shown indicates that there is a probability that the VIIP will violate the destruct bounds. By integrating the PDF over the regions defined by the destruct bounds (Regions I, II and III), the probability of no destruct bound violation and the probability of violation for each destruct bound are computed. Three corresponding modes of failure are defined as follows:

- Left Mode (Region I): Vehicle VIIP violates the left destruct bound.
- Right Mode (Region II): Vehicle VIIP violates the right destruct bound.
- Center Mode (Region III): No destruct line violation occurs.

New vacuum impact means and uncertainties are computed for each of the three modes. For the center mode these are computed by integrating the original distribution over Region III. The mean and uncertainties for the left and right modes are developed based on the distribution of the VIIP position as it crosses a destruct line (defined by the intersection of the destruct line with the original impact distribution), the expected velocity of the IIP as it crosses the destruct line, and the mean uncertainty for the time delay between destruct line violation and actual vehicle destruct.

The impact distributions for fragments for each of the modes are obtained from the vacuum distributions using the centerline transformation relations to relate vacuum impact perturbations to fragment impact perturbations.

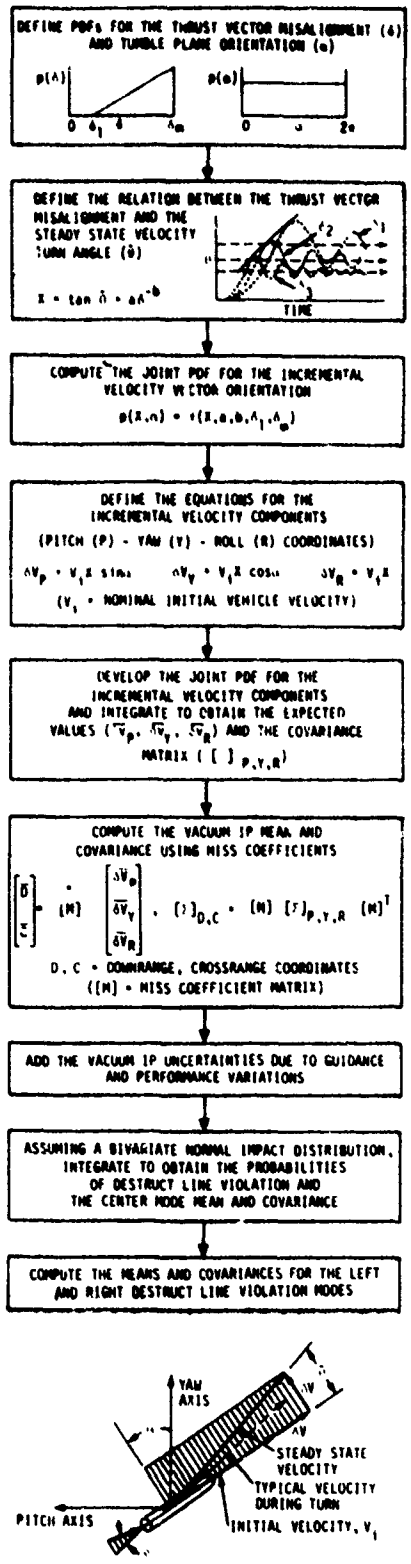

Figure 4-4-4. Development of the Malfunction Turn Impact Distributions

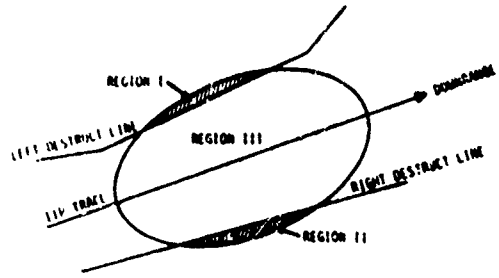

Figure 4-4-5. Malfunction Turn Vacuum IIP Distribution

4.4.1.2 Destruct Induced Velocity

Most launch vehicles have a system which will halt powered flight upon command of a range safety controller. Typical destruct systems cut open the casing of the vehicle to relieve chamber pressure and halt thrust. This is done by explosive charges which usually produce a conflagration of flying propellant and vehicle fragments. The fragment velocities are estimated based on ground tests and flight experience and expressed in terms of a velocity covariance. The velocity covariance for each fragment is transformed to an impact covariance as in equation 7.

4.4.1.3 Wind Uncertainty

The winds through which fragments fall can be approximated by a profile of winds, piecewise linear in altitude and direction, blowing horizontally. Statistical models of wind can be developed by selecting a set of altitudes and establishing mean values for the wind velocity components at these altitudes. Wind uncertainties can be described by a covariance for the wind components for all altitudes. The wind uncertainty is derived from several sources including variability in wind measurement and change in the wind from the time of measurement to the time of launch.

The effect of wind uncertainty on fragment impact points can be determined by computing influence coefficients relating horizontal translation in a wind field - between two altitude levels - to wind velocity components. The influence coefficients are computed based on a fragment having a ballistic coefficient of 1 psf and falling embedded in the wind at terminal vertical velocity. The impact dispersions are found to approximately vary inversely with ballistic coefficient. The impact covariance for a fragment having ballistic coefficient β is thus computed as follows:

$$\left[\Sigma_W\right] = \frac{1}{\beta}\,[C]\left[\Sigma_U\right][C]^T \qquad (9)$$

where

$[\Sigma_w]$ is the impact covariance matrix due to wind,

$[C]$ is the matrix of influence coefficients, and

$[\Sigma_u]$ is the wind covariance matrix.

4.4.1.4 Fragment Ballistic Coefficient Uncertainty

The ballistic coefficient ($\beta = W/C_DA$) of a particular fragment is difficult to predict because of the uncertainties in weight (W), drag coefficient (C_D) and cross-sectional area (A). The effect of these uncertainties is to produce a curvilinear monovariate fragment impact uncertainty along debris centerline. This dispersion may be adequately characterized by the impact points associated with the lower bound, the mean and the upper bound estimates of the fragment β. The impact distribution is approximated by a bivariate normal distribution "fitted" to these three fragment impact points.

4.4.1.5 Fragment Lift Effects

Another source of fragment impact point uncertainty is aerodynamic lift. A spherically shaped object will fall without any lift effect, but irregular shaped, tumbling objects will have random lift vectors. It has been established that for initial altitudes up to about 60,000 feet, the 1σ impact dispersion due to lift ($\sigma\ell$) is approximately proportional to the initial fragment height. The proportionality constant ranges from 0.01 for blunt objects to 0.05 for flat panel-like objects. The impact dispersion does not increase appreciably for altitudes greater than 60,000 feet. Since the dispersion due to lift is random in direction, the impact covariance matrix becomes

$$\left[\Sigma_L\right] = \begin{bmatrix} \sigma_\ell & 0 \\ 0 & \sigma_\ell \end{bmatrix} \tag{10}$$

The total impact uncertainties for a given fragment due to a given mode of failure occuring at a particular flight time are obtained by combining the uncertainties resulting from the various error sources. This is done by expressing the impact covariance matrices for all error sources

in a common orthogonal reference coordinate system and summing them. The resulting covariance matrix is of the form

$$\left[\Sigma_R\right] = \begin{bmatrix} \sigma_\varepsilon^2 & \sigma_{\varepsilon\eta} \\ \sigma_{\varepsilon\eta} & \sigma_\eta^2 \end{bmatrix} \tag{11}$$

Based on the central limit theorem, the impact PDF is assumed to be bivariate normal, giving a PDF as follows:

$$P(\xi,\eta) = \frac{1}{2\pi\left|\Sigma_R\right|^{1/2}} \exp\left(\tfrac{1}{2}\begin{Bmatrix}\xi\\ \eta\end{Bmatrix}^T \begin{bmatrix}\Sigma\\ R\end{bmatrix}^{-1} \begin{Bmatrix}\xi\\ \eta\end{Bmatrix}\right) \tag{12}$$

This PDF is centered at the mean impact point for the fragment computed by shifting the nominal fragment impact point by the sum of the mean impact perturbations resulting from the impact error sources. The conditional probability of impact for the given fragment on a given critical center, given that the failure has occurred, is computed by integrating the PDF over the critical center land area.

The probability of one or more of the fragments, resulting from the given failure mode, impacting on the critical center is given by

$$P_n = 1 - \prod_{i-1}^{n}\left(1 - P_i\right) \tag{13}$$

where

n is the number of fragments and

P_i is the conditional probability of impact for the i<u>th</u> fragment.

The probability of one or more impacts is weighted according to the probability of occurrence of the failure mode during the time interval. The total probability of impact for a given criitcal center is obtained by summing the weighted probabilities of one or more impacts over all modes of failure and over all failure time intervals.

Before proceeding to the computation of casualty expectation, it is necessary to define the various categories of impacting fragments and the lethality of these fragments to persons in various levels of sheltering.

4.4.1.6 Fragment Categories

Impacting launch vehicle fragments are divided into the following categories: inert pieces of vehicle structure, pieces of solid propellant (solid or liquid) which are non-explosive, and fragments which contain propellant and which can explode upon impact. Definition of the fragments which will result from each type of vehicle failure are model inputs. The fragment list may vary for different segments of flight, such as for each stage of flight. For fragments which consist of or contain propellant, and which originate from a current operating booster motor, the size and weight of the fragment at vehicle breakup are adjusted according to the propellant consumed by normal operation prior to the failure. For fragments consisting of or containing burning propellant during free fall, the amount of propellant consumed prior to impact must be computed. For contained propellant the weight of propellant consumed is computed as the product of a specified consumption rate (pounds/second) and the time of free fall. For uncontained solid propellant fragments, the amount of propellant consumed is computed based on specified burn rate versus atmospheric pressure (P) relations of the form

$$\frac{dr}{dt} = AP^B \quad \frac{\text{feet}}{\text{second}} \tag{14}$$

where

dr/dt is the linear rate of burn and

A and B are constants dependent on the propellant type.

The propellant consumption for each propellant type is computed as part of the impact data for fragments.

4.4.1.7 Casualty Area

The casualty area of an impacting fragment is defined to be the surface area about the fragment impact point within which a person would become a casualty. The point location of both the fragment and a person are defined by their respective centroids. Casualties may result from a direct hit, from a bouncing fragment, from a collapsing structure resulting from an impact on a building or other shelter, or from the overpressure pulse created by an explosive fragment.

Consider first the casualty area of a non-explosive fragment falling vertically and impacting in the open. Let the projected area of the fragment be A_p and approximate the area occupied by a person as a circle

of radius r_p. Assuming a circular fragment projected area, the fragment casualty area is given by the relation

$$A_c = \pi \left(\sqrt{\frac{A_p}{\pi}} + r_p \right)^2 \tag{15}$$

Since some impacting fragments would not be expected to cause significant injury due to low impact velocity and/or low fragment weight, the casualty area may be reset to zero for these fragments. The impact kinetic energy can be used as a criterion to determine whether the fragment would be expected to cause injury. Threshold kinetic energy values from 35 to 50 ft-lb have been used.

The basic casualty area expressed above should be modified to account for bouncing or scraping upon impact and for the effect of any horizontal component of impact velocity. The effect of a horizontal velocity component is to increase the hazarded area due to the horizontal travel of the fragment while falling from the height at which a person could first be struck.

The casualty area for a fragment which explodes upon impact is made up of two components as follows: (1) the overpressure zone created by the explosion, and (2) the casualty areas of propellant and hardware fragments thrown out by the explosion which impact outside of the overpressure zone. The casualty area contribution resulting from the fragments thrown out by the explosion is generally insignificant relative to the overpressure zone contribution and can be ignored. The casualty area due to the overpressure zone is determined by the minimum overpressure level which would be injurious to a person. The casualty area is the area of the circle whose radius is equal to the distance from the explosion at which the overpressure level has dropped to the specified level. This radius (r_o) is given by the Kingery-BRL equation (reference 3).

$$r_o = K_o \, (fW_p)^{1/3} \tag{16}$$

where

fW_p is the weight of TNT which will generate an equivalent explosion,

W_p is the weight of propellant contained in the fragment at impact,

K_o is a factor obtained from the Kingery-BRL chart (a function of the specified overpressure level).

Thus far the casualty area computations have not accounted for the sheltering provided to persons located in structures. To do this, all sheltering is classified into predefined levels. It is assumed that the population of each critical center can be divided into the expected number of people who are unprotected and the number who are protected by each level of sheltering. People who are located on the lower floor(s) of buildings may be classified into higher levels of sheltering than those located on the upper floor(s). For non-explosive fragments, the casualty area to shelterd persons is computed as follows:

$$A^*_C = KP_pA_c \tag{17}$$

Where

A_c is the casualty of the fragment to unprotected persons (falling vertically and without bounce),

K is a factor to account for the increase in the casualty area due to collapsing structure, and

P_p is the probability that the fragment will penetrate the structure.

The penetration probability (P_p) is based on the impact kinetic energy of the fragment and on the bounding values for the kinetic energy required to penetrate the structure.

The effect of sheltering on the casualty area for explosive fragments is accounted for by changing the minimum overpressure level upon which the overpressure zone is based. The overpressure level used is that which would be expected to severely damage or collapse the sheltering structure.

The casualty expectation for a given critical center is the number of injuries or deaths expected to result within that center from a launch. To compute the casualty expectation for a center due to a given failure mode and flight time interval, consider the center as being segmented into sub-areas (A_i) within which the population is afforded a constant level of sheltering.

Let P_{I_i} = Probability of a given fragment impacting into sub-area A_i (weighted by the probability of the failure mode occurring during the time interval)

A_{c_i} = Casualty area of the fragment for the shelter level of A_i

N_i = Number of people in A_i

The casualty expectation for sub-area A_i is the probabilty of the fragment impacting in A_i times the expected number of casualties given impact. Assuming that the population in A_i is uniformly distributed, the casualty expectation (references 4 and 5) is given by

$$E_{C_i} = P_{I_i} \frac{A_{c_i}}{A_i} N_i \tag{18}$$

For the critical center sufficiently small so that the fragment impact probability density over the land area (A) is reasonably uniform, the casualty expectation becomes

$$E_{c_i} = P_I \frac{A_i}{A} \frac{A_{c_i}}{A_i} N_i = P_I \frac{A_{c_i}}{A} N_i \tag{19}$$

where

P_I is the probability of the fragment impacting anywhere on the center.

The casualty expectation for the entire critical center is obtained by summing the E_{c_i} over all sub-areas. The total casualty expectation for the center is obtained by summing the individual E_c over all fragments, failure modes and flight times.

The risk assessment model has been implemented on an IBM 360/65 computer system at SAMTEC.

4.4.2 Target Planning Optimization/Countour Plot

The Target Optimization Program (TARGOP) and its associate Contour Plot Program (CONTUR) are designed to produce information which can be used to select the best test missile target point in the sense of minimizing risk to life and property in the greater target area. These programs were developed by the J. H. Wiggins Corp. under the direction of SAMTEC/SEY.

Given a description of the pieces expected to impact and the associated impact uncertainty, the program combines such data with information about the critical centers (usually populated areas) in the target region to compute impact probability (P_I), unsheltered casualty expectation (E_{cu}), sheltered casualty expectation (E_{cs}), and balanced risk (R_C).

The quantities are computed in such a way that the threat of a particular impacting object to a particular center is obtained for all centers. Total probabilities are also computed which represent the total risk from all of the impacting objects to all centers. The most dangerous objects and the most threatened centers are determined.

A convenient procedure for analyzing the results is used; one in which equi-probable contours are plotted for the input grid. Along the E_{cu} contours, the values of E_{cu} are constant. Any one contour represents the locus of all potential target points that result in an unprotected casualty expectation of the magnitude specified. With such a display, the optimum target point is readily determined. Contours of constant sheltered casualty expectation would show the improvement, provided all people were in available shelters. Balanced risk contours would show the casualty expectation weighted with "reaction" factors.

TARGOP is an extremely valuable and useful tool in the planning phase of a missile test program. It serves as a measure of when to recommend the use of shelters, when to evacuate if the threat is relatively high, or when evacuation is not necessary because of a low threat. Further, the specific centers requiring notification can be identified well in advance so that sufficient time is available to modify plans and reduce risks.

Functionally, the data inputs to TARGOP are of three types: debris characteristics, population center characteristics and geographical data used in plotting. The procedure for TARGOP usage is illustrated in Figure 4-4-6.

Data concerning the impacting fragments associated with normal flight and up to seven failure modes must be supplied. This data is subdivided into three groups: (1) physical characteristics, (2) impact points and (3) uncertainties in the impact point data. The number of fragments and probability of occurrence of each event (normal flight or failure mode) must also be entered.

Population center characteristics in terms of position, area and population residing in various levels of shelter for each center must be supplied. Geographical data must be supplied defining the area for risk contour plotting and for informational background display. Additionally, special symbol plotting may be utilized to denote any special interest locations such as ship locations or temporary shelters.

TARGOP is basically a hazards analysis program that has two significant features: (1) it retains information on the effect of any fragment on any population center and (2) it rapidly produces many hazards analyses over a grid of target points. Figure 4-4-7 is a flowchart of TARGOP.

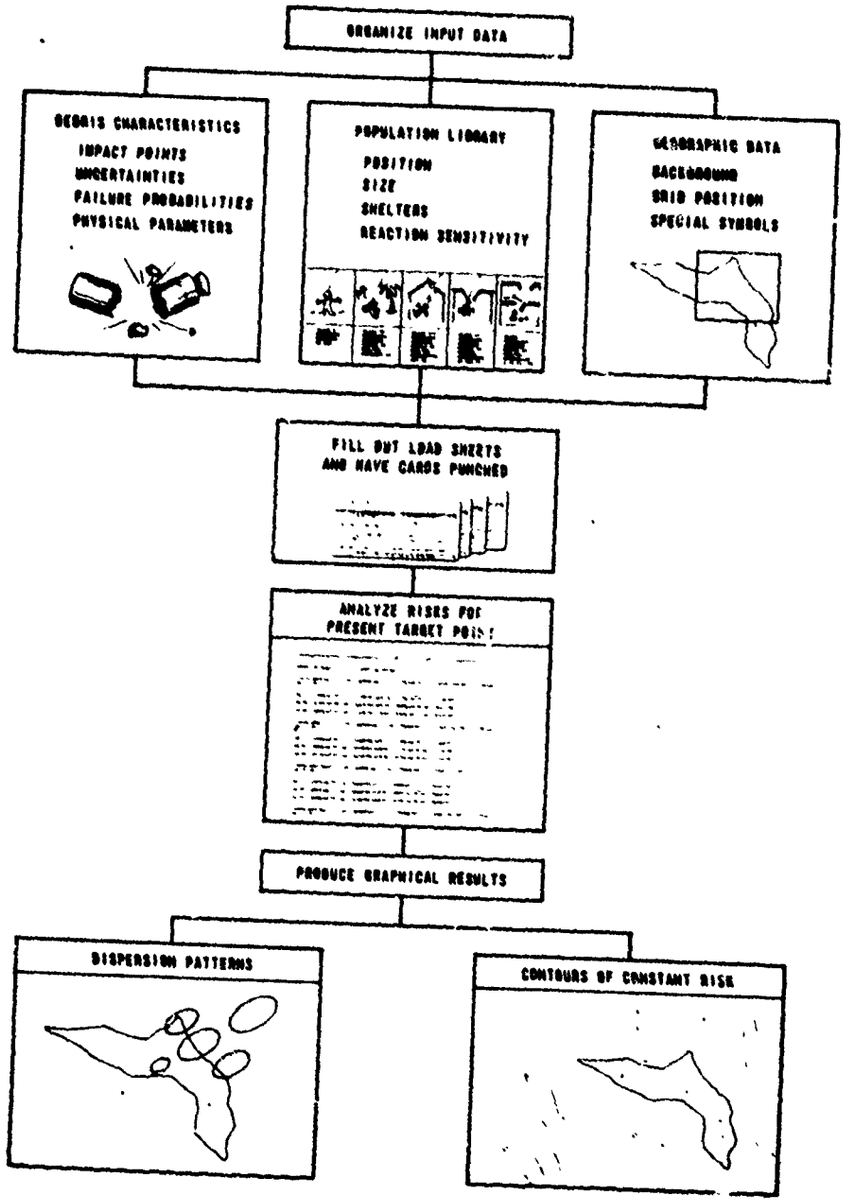

Figure 4-4-6. Procedure for TARGOP Usage

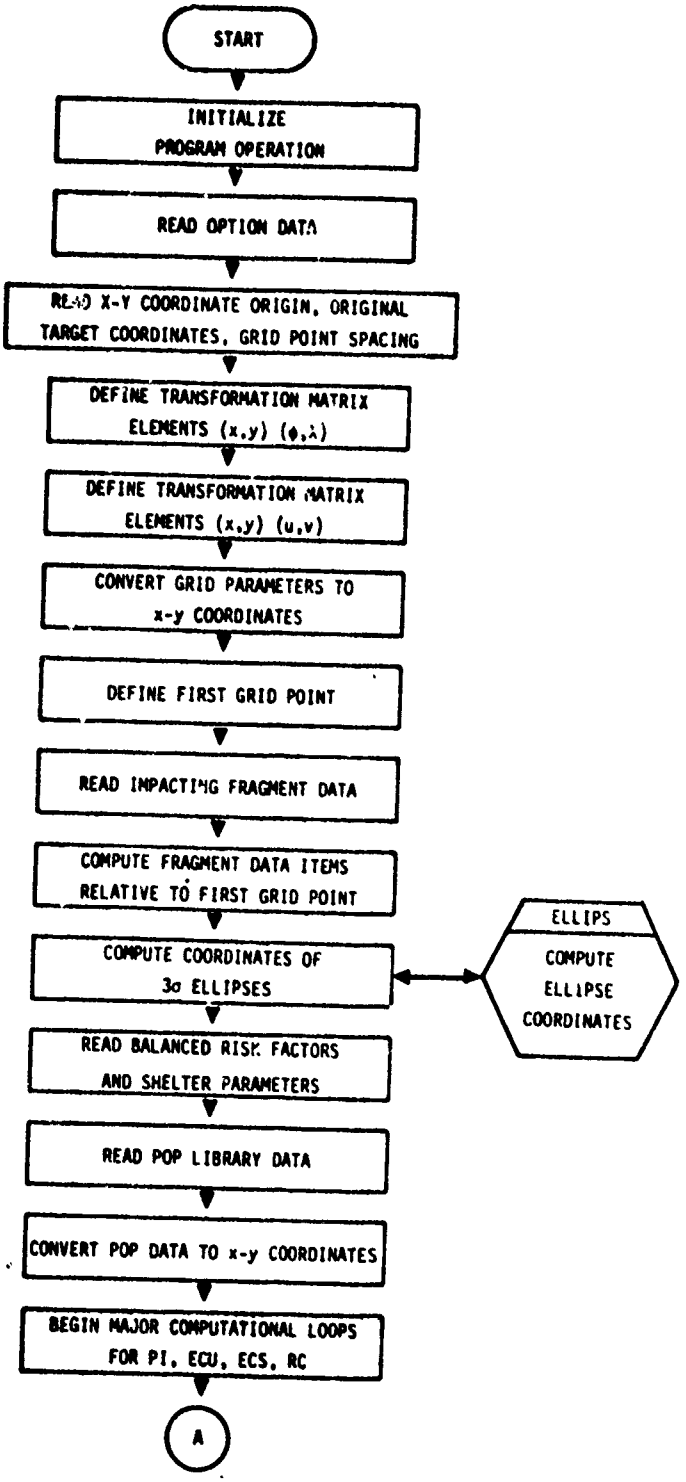

Figure 4-4-7. TARGOP Flowchart

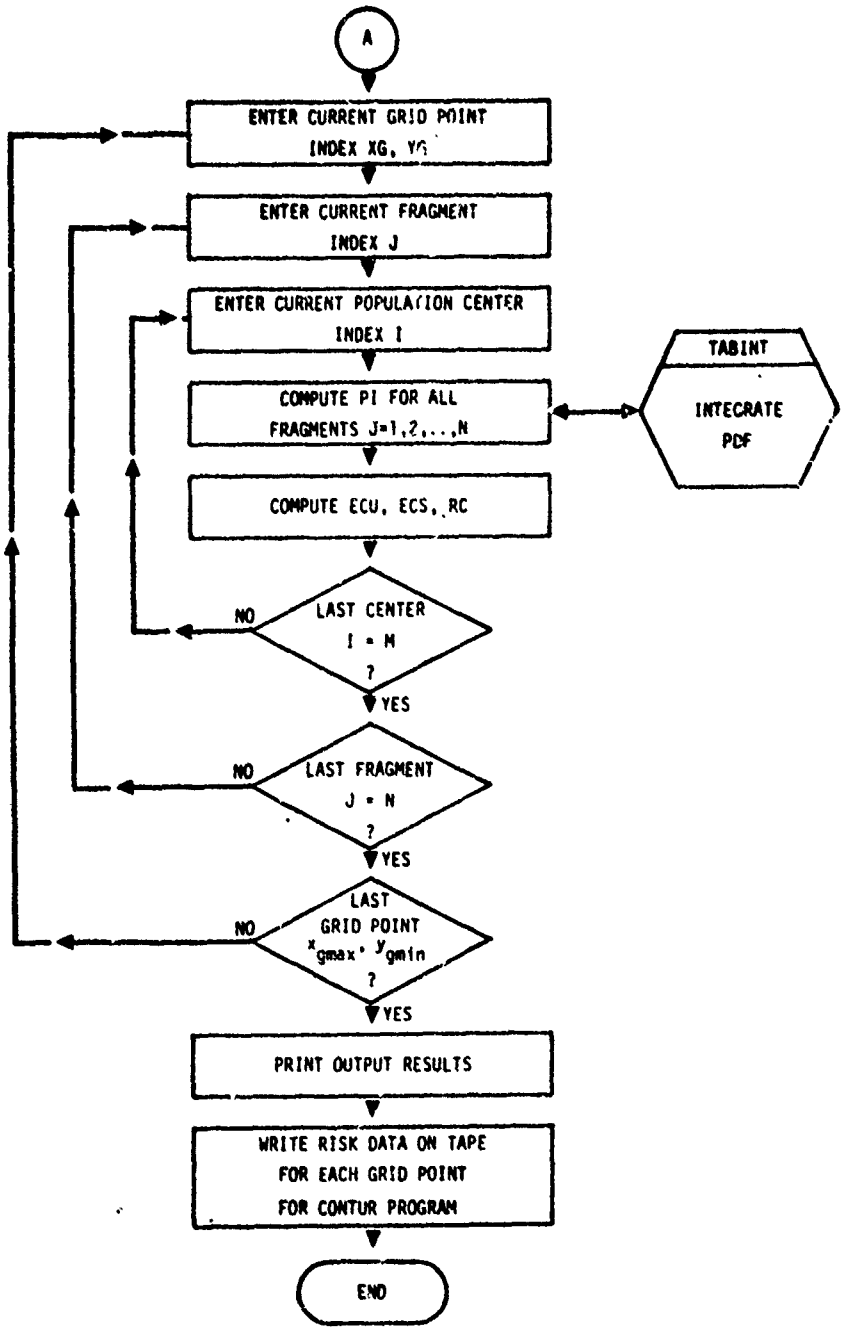

Figure 4-4-7 (Cont.). TARGOP Flowchart

After computing the coordinates of the first grid point and transforming the population center data and fragment data to the x, y topocentric coordinate system, TARGOP selects the first fragment and computes the risks for each population center, storing the result. It then selects the second fragment and repeats the computation of risk for each population center, storing the results for each fragment. This process is repeated until all fragments in the debris list have been covered. Having completed the computations for the first grid point, the second grid point coordinates are computed and the whole process defined above is repeated until all 625 grid points (maximum) have been covered. The data is then written onto a tape for automatic processing by the CONTUR Program.

In the event that analysis of only a single grid point is required, the computation process discussed above is performed twice. The first time reverses the computation, i.e., the first population center is selected and risks are computed for each fragment. Again, subtotals for each population center are retained. By so doing, one obtains:

1. The total risk produced by all fragments on any specific population center of interest.

2. Total risk for a given fragment on all population centers. The dual computation procedure is not employed when performing a full grid analysis.

The TARGOP grid data is passed to the CONTUR Program and the CONTUR execution is performed automatically. The CONTUR flowchart is presented in Figure 4-4-8. CONTUR is a computer graphics program written for the purpose of generating two-dimensional plotter drawings from "risk surface" information. The program takes the risk data defined on a grid and produces contour curves. CONTUR fits a smooth curve through a string of grid cells representing the contour line. These strings of curves are linked together in chains and associated with continuous "topographic elevation lines." A third order polynominal is used to fit contour lines to coordinate points. First, the program assumes that the "altitude" change between any two nodes is linear and finds all points along the lines between points that are contour elevations. It then pairs points that are within the same cell - in the same column and row area - and, finally, it connects these pairs of points (line segments) in a line which is then plotted. The CONTUR procedure is known as a "localized cubic spline procedure" having the unique feature that only two rows in the grid are processed at a time, obviating the need to read into core the whole grid. As used with TARGOP, CONTUR is limited to 25 columns and 25 rows.

All TARGOP modeling calculations are accomplished in one of three basic coordinate systems. In a global sense a spherical Earth is assumed. In

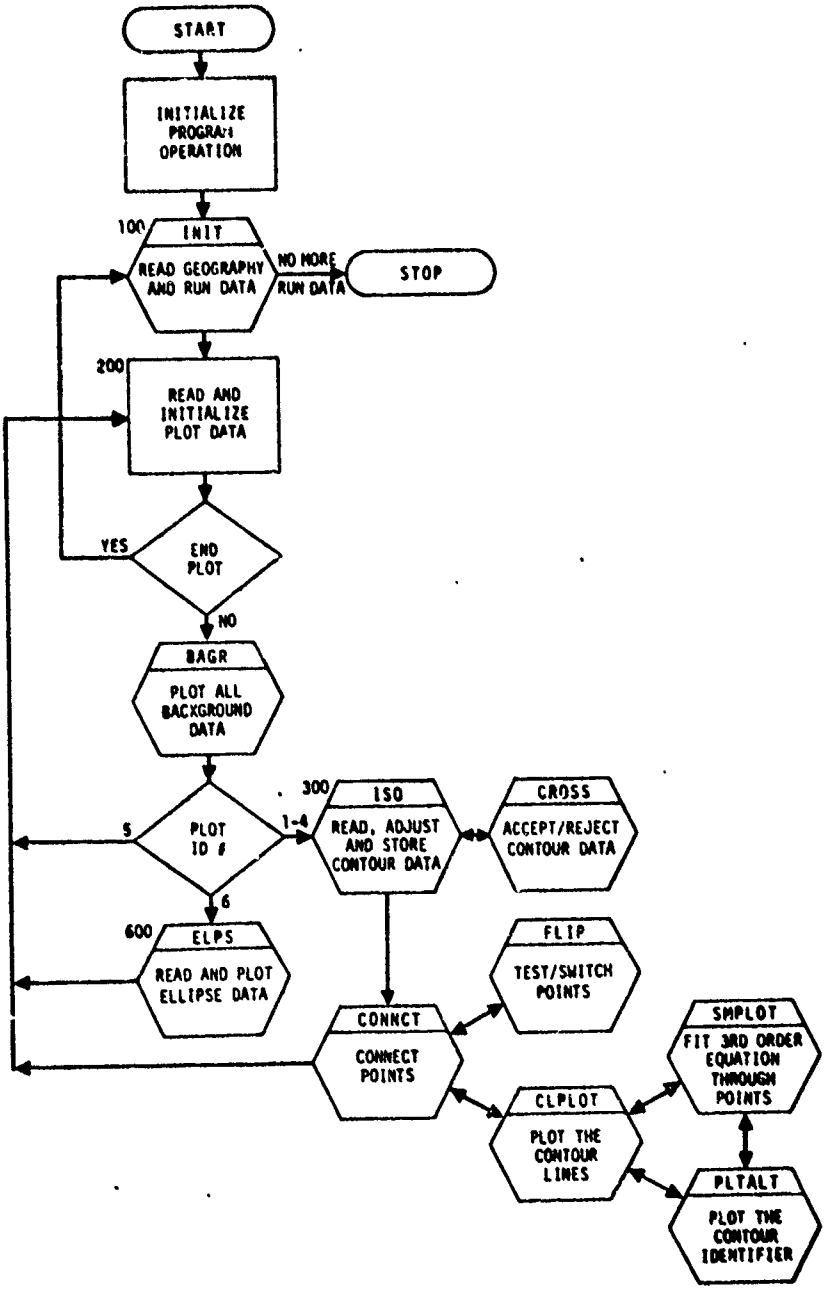

Figure 4-4-8. CONTUR Flowchart

a local sense, a flat Earth is considered appropriate. The basic x-y topocentric coordinate system shown in Figure 4-4-9 has its origin at the arbitrary point λ_0, ϕ_0. The u-v uprange/crossrange system has its origin at the point x_j, y_j.

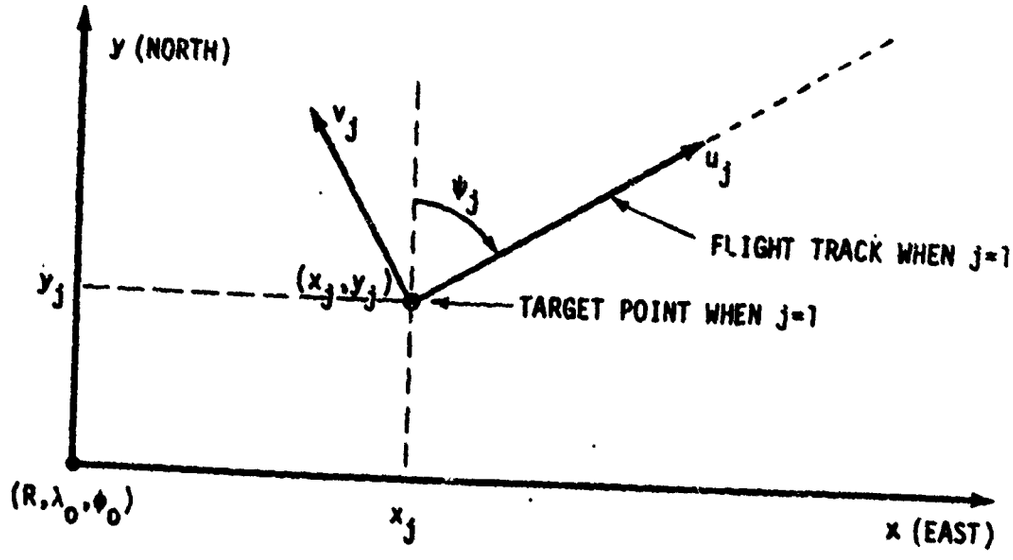

Figure 4-4-9. Relevant Coordinate Systems

Longitude and latitude are related to x and y coordinates through the matrix relationship.

$$\begin{Bmatrix} x \\ y \\ z \end{Bmatrix} = R \begin{bmatrix} -\sin\lambda_0 & \cos\lambda_0 & 0 \\ -\cos\lambda_0 \sin\phi_0 & -\sin\lambda_0 \sin\phi_0 & \cos\phi_0 \\ \cos\lambda_0 \cos\phi_0 & \sin\lambda_0 \cos\phi_0 & \sin\phi_0 \end{bmatrix} \begin{Bmatrix} \cos\lambda\cos\phi - \cos\lambda_0\cos\phi_0 \\ \sin\lambda\cos\phi - \sin\lambda_0\cos\phi_0 \\ \sin\phi - \sin\phi_0 \end{Bmatrix} \quad (20)$$

where

z is measured upward from the Earth's surface.

Expanding equation (20), it is shown that

$$x = R \cos\phi \sin(\lambda - \lambda_0) \tag{21}$$

and

$$y = R\,[\sin\phi\cos\phi_0 - \sin\phi_0\cos\phi\cos(\lambda - \lambda_0)] \tag{22}$$

Now if $\Delta\lambda = \lambda - \lambda_0$ and $\Delta\phi = \phi - \phi_0$ are small, i.e., less than 10°, then it is reasonable to assume that

$$\sin(\lambda - \lambda_0) = \Delta\lambda \tag{23}$$

$$\cos(\lambda - \lambda_0) = 1$$

$$\sin(\phi - \phi_0) = \Delta\phi$$

Then equations 21 and 22 reduce to

$$x = R\Delta\lambda \cos\phi \tag{24}$$

$$y = R\Delta\phi, \tag{25}$$

which are familiar expressions for relating increments of longitude and latitude to nautical mile distances east and north. The approximations in equation 23 are reasonable because the normal range of values is less than 4°.

Uprange and crossrange coordinates are related to x and y coordinates through the matrix relationship

$$\begin{Bmatrix} x \\ y \end{Bmatrix} = \begin{bmatrix} \sin\psi_j & -\cos\psi_j \\ \cos\psi_j & \sin\psi_j \end{bmatrix} \begin{Bmatrix} u_j \\ v_j \end{Bmatrix} + \begin{Bmatrix} x_j \\ y_j \end{Bmatrix} \tag{26}$$

The angle ψ_j is measured clockwise from north and is commonly referred to as the "back azimuth" because it is the reentry azimuth minus 180°.

As noted earlier, there are three groups of debris data required to adequately describe the target area risk situation. They are physical characteristics, impact points and impact uncertainties

Impact kinetic energy, weight, ballistic coefficient, impact velocity and lethal area comprise the physical characteristic group but not all of these items need be specified. In all cases, lethal area is required.

The purpose of the other items is to compute kinetic energy. If the kinetic energy is already known for a fragment, the weight ballistic coefficient and impact velocity are not needed.

If the impact kinetic energy is unknown, the program will compute it in two possible ways. If the weight and impact velocity are specified by the user, the kinetic energy is computed as

$$K.E. = \frac{1}{2} mV^2 = \frac{1}{2} \frac{W}{g} V^2 \tag{27}$$

where

W = weight

V = impact velocity

g = gravitational acceleration

If the weight and ballistic coefficient are specified by the user, the kinetic energy is computed as

$$K.E. = \frac{W\beta}{\rho g} \tag{28}$$

where

W = weight

β = ballistic coefficient

ρ = air density at sea level

g = gravitation acceleration

Impact point data is comprised of the coordinates of impact points and the back azimuth of the path the fragment traveled prior to impact. The impact points may be given optionally in latitude and longitude or in uprange and crossrange distances from the target point. The data for a particular fragment may be in either form, independent of the form used for any other fragment.

The TARGOP model has been extended to handle normal, exponential and uniform PDFs for fragment impact uncertainties. Also, these distributions may be mixed uprange and downrange, and have different variances

uprange and downrange. The crossrange distribution is assumed normal. The forms of the distributions are presented below.

The integral of the probability density function over the population center area represents the probability that the fragment will impact somewhere on the population center.

The general form for the normal density function is given by

$$f(u) = \frac{1}{\sqrt{2\pi}\,\sigma} \exp\left[-\frac{1}{2}\left(\frac{u-\mu}{\sigma}\right)^2\right], \; -\infty \leq u \leq +\infty \tag{29}$$

where

σ = standard deviation

μ = mean

u = uprange coordinate

If the distribution is about the impact point of the fragment, $\mu = 0$.

The exponential density function is a less common distribution, but important in modeling fragment debris from missile failures. The general form is given by

$$f(u) = \lambda e^{-\lambda u}, \; u > 0 \tag{30}$$

$$= 0 \quad , \; u \leq 0$$

where

$1/\lambda$ = standard deviation

λ = mean of distribution

The uniform distribution is also useful in modeling fragments emanating from missile failure. The general form is

$$f(u) = 1/\;(b-a) \quad , \; a \leq u \leq b \tag{31}$$

$$= 0 \text{ elsewhere}$$

There is no central tendency with this form of PDF. The key statistics of the uniform distribution are

$$\left.\begin{aligned} \mu &= \frac{b+a}{2} \\ \sigma &= \frac{(b-a)}{\sqrt{12}} \end{aligned}\right\} \quad , \quad b>a \tag{32}$$

Each of the nominal flight fragments usually has a corresponding 3σ ellipse such as that illustrated in Figure 4-4-10.

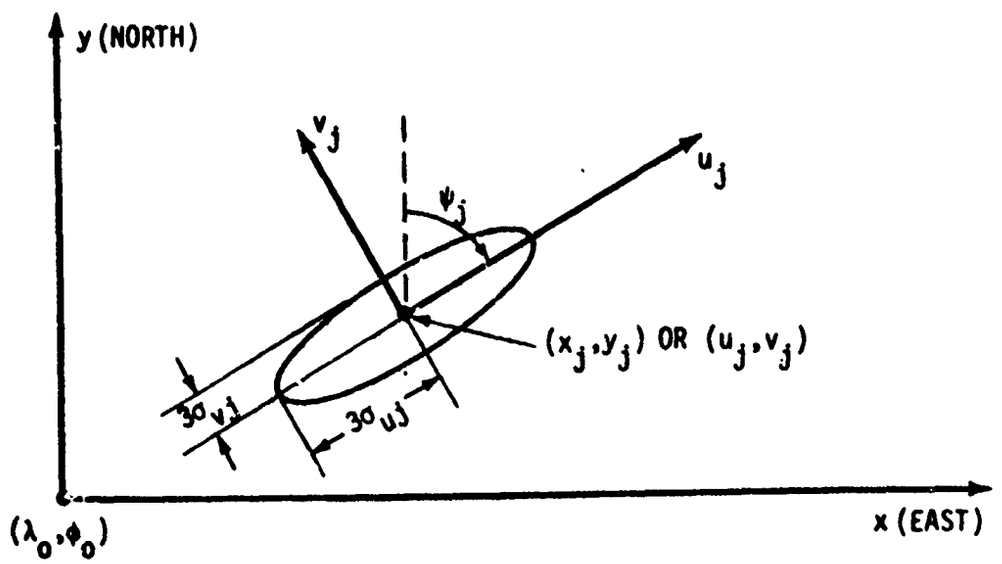

Figure 4-4-10. 3σ Uncertainty Ellipse for jth fragment

It is useful to display the total "footprint" of impacting debris by plotting each of the ellipses on a background of the target area. The required equations for plotting these ellipses are developed below. Figure 4-4-11 illustrates the normal PDF.

The equation for the 3σ ellipse of the jth fragment is

$$(u_j)^2 / (3\sigma_{uj})^2 + (v_j)^2 / (3\sigma_{vj})^2 = 1 \tag{33}$$

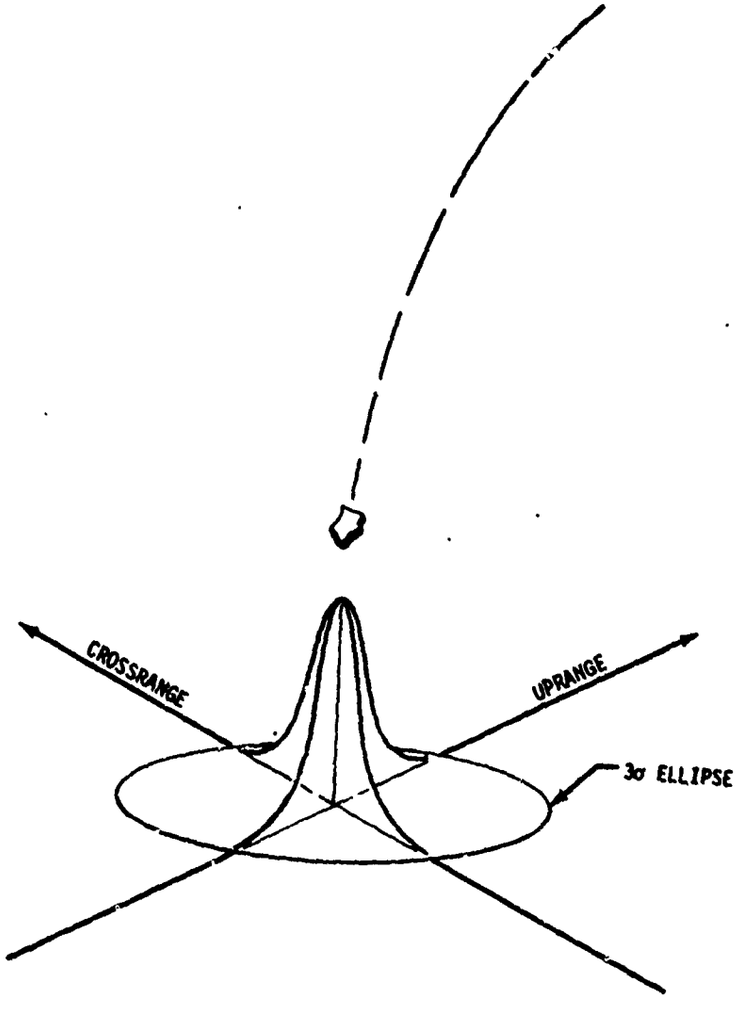

Figure 4-4-11. Bivariate Normal Distribution for Nominal Flight Fragment Impact Uncertainty

where

u_j, v_j are the uprange/crossrange coordinates of the jth fragment impact points, and

σ_{uj}, σ_{vj} are the standard deviations in the corresponding directions.

Figure 4-4-10 shows these relationships graphically. It is 99.5 percent probable that the jth piece would land within the ellipse in Figure 4-4-11 where the center is the nominal impact point.

To obtain points on the perimeter of the ellipse, a parameter $\bar{k}$ is introduced, and the equation for the ellipse, equation 33, is rewritten in the parametric form

$$u_j^2 = 9\bar{k}^2\sigma_{uj}^2 \tag{34}$$

$$v_j^2 = 9\,(1-\bar{k}^2)\,\sigma_{vj}^2 \tag{35}$$

The u_j and v_j values can then be directly computed as follows:

$$\frac{u_j}{\sigma_{uj}} = \pm\, 3\bar{k} \tag{36}$$

$$\frac{v_j}{\sigma_{vj}} = \pm\, 3\sqrt{1-\bar{k}^2} \tag{37}$$

where

$$0 \leq \bar{k} \leq 1 \tag{38}$$

To save computer time, the coefficients $(\pm 3\bar{k})$ and $(\pm\, 3\sqrt{1-\bar{k}^2})$ have been precomputed for 49 values of k. The values of k were chosen so that the points are not equally spaced, but are closer together when u_j and v_j are near zero. This means the plotted ellipses should be fairly smooth, even in the areas of expected high curvature.

A TARGOP user may specify different 1-sigma values uprange and downrange. If so, TARGOP will use the larger of the two as the 1-sigma value to be used in plotting. The (u, v) coordinates of each point on an ellipse are obtained by multiplying the precomputed coefficients by σ_{uj} and σ_{vj}, respectively. Letting n denote the point number, the corresponding (x,y) coordinates are then given by

$$\begin{matrix} x_j \\ y_j \end{matrix}^{n} = \begin{matrix} \sin\psi_j & -\cos\psi_j \\ \cos\psi_j & \sin\psi_j \end{matrix} \begin{matrix} u_j \\ v_j \end{matrix}^{n} + \begin{matrix} x_j \\ y_j \end{matrix} \qquad (39)$$

where

(x_j, Y_j) is the center of the ellipse - the impact point for the fragment.

Information required for the centers is integrally related to the method used for computing E_{cs}, sheltered casualty expectation (discussed later). Two approaches are optionally available in TARGOP for the E_{cs} computation: one will be referred to as the "discrete method" and the other the "continuous method." Both methods require the center area, position in latitude and longitude, population, and balanced risk factor.

For the discrete E_{cs} method, the approach has been to divide the population of a given center into four categories:

Category I. That portion of the population residing in structures capable of resisitng impacting fragments with kinetic energy not greater than 516868 ft-lbs. This corresponds to heavy reinforced structures, or people on the lower floors of tall buildings.

Category II. That portion of the population residing in structures capable of resisting impacting fragments with kinetic energy not greater than 28856 ft-lbs. This corresponds to medium reinforced structures.

Category III. That portion of the population residing in structures capable of resisting impacting fragments with kinetic energy not greater than 1045 ft-lbs. This would include people in light-roofed structures made of sheet metal, shingles, etc.

Category IV. That portion of the population in the open to which there is no threat from fragments having an energy less than 35 ft-lbs.

The number of people in each category is then defined on each population library card.

For the continuous E_{cs} method, additional information is required which defines the kinetic energy of resistance of the most protective structure, its plan area, and the number of people expected to occupy it during the reentry of debris. Similar data must be supplied for the least protective structure.

The computation of impact probability (P_I) is discussed here as it applies to the various PDFs. Impact probabilty has two components, P_D (uprange or downrange) and P_C (crossrange), and

$$P_I = P_D \cdot P_C \cdot P_{event} \tag{40}$$

where

$$P_D = P_u + P_d \tag{41}$$

P_{event} = Probability of occurrence of event which produced fragment.

The TARGOP model permits the user to define different forms of PDFs uprange and downrange. Therefore, there are really several integrations to obtain P_D and P_C, depending on the position of the population center:

1. If the population center lies wholly downrange of the fragment impact point, only the downrange PDF needs to be integrated to obtain P_D.

2. If the population center lies wholly downrange of the fragment impact point, only the uprange PDF needs to be integrated to get P_D.

3. If the population center lies partially uprange and partially downrange of the fragment impact point, both uprange and downrange distributions must be integrated to obtain $P_D = P_u + P_d$.

The various possibilities are discussed below.

For the crossrange impact probability P_C, the PDF is given by

$$f_j(v) = \frac{1}{\sqrt{2\pi}\,\sigma_{cj}} \exp - \frac{1}{2} \frac{v}{\sigma_{cj}}^{2} \tag{42}$$

where

σ_{cj} = crossrange standard deviation,

v = crossrange coordinate.

Integrating $f_j(v)$ over the crossrange limits of the ith population center,

$$P_{cij} = \int_{c_{ij}}^{d_{ij}} f_j(v)\, dv \tag{43}$$

where

$$c_{ij} = v_{cij} - 0.5\sqrt{A_{ci}} \tag{44}$$

$$d_{ij} = v_{cij} + 0.5\sqrt{A_{ci}} \tag{45}$$

and

V_{cij} = crossrange coordinate distance to the center of the population center,

A_{ci} = area of population center,

more specifically,

$$v_{cij} = -\cos\psi_j\,(x_{ci}-x_j) + \sin\psi_j\,(Y_{ci}-Y_j) \tag{46}$$

Letting

$$\bar{v} = v/(\sqrt{2}\,\sigma_{cj}), \tag{47}$$

the integral in equation 43 takes the form

$$P_{cij} = \frac{1}{\sqrt{\pi}} \int_{C_{ij}}^{D_{ij}} e^{-\bar{v}^2}\, d\bar{v} \tag{48}$$

where

$$C_{ij} = c_{ij} / (\sqrt{2}\, \sigma_{cj}) \tag{49}$$

$$D_{ij} = d_{ij} / (\sqrt{2}\, \sigma_{cj}) \tag{50}$$

The integral expressed in equation 48 is tabluated for a wide range of limits. The tabular integration approach is much faster than direct functional evaluation, requiring very little additional computer storage to achieve very accurate results.

In developing the downrange impact probability (Pd), there are three possible forms of PDF available in TARGOP. Each must be treated separately as it applies uprange or downrange.

The normal PDF is given by

$$f_j\,(u) = \frac{1}{\sqrt{2\pi}\,\sigma_{dj}} \exp\left[-\frac{1}{2}\frac{u}{\sigma_{dj}}^{2}\right] \tag{51}$$

Integrating over the normalized downrange limits of the ith population center,

$$P_{dij} = \int_{A_{ij}}^{B_{ij}} e^{-u^{-2}}\, d\bar{u} \tag{52}$$

The exponential PDF may be written

$$f_j\,(u) = \frac{1}{\sigma_{dj}}\, e^{u/\sigma_{dj}}, \quad u < o \tag{53}$$

Integrating over the downrange limits of the ith population center,

$$P_{dif} = 0.5 \int_{a_{ij}}^{b_{ij}} \left(\frac{e}{\sigma_{dj}}\; u/\sigma dj\right) du \tag{54}$$

The uniform PDF may be written

$$f_j\ (u) = \frac{1}{\sqrt{12}\ \sigma_{dj}}\ ,\ -\sqrt{12}\ \sigma_{dj} \leq u \leq o \tag{55}$$

$$= 0,\ \text{elsewhere}$$

These same general form equations apply in calculating the uprange impact probability Pu.

The total impact probability computation for one or more fragments is of the standard form

$$(P_I)_n = 1 - (1 - P_A)^n \tag{56}$$

where

n is the number of fragments and

P_A is the impact probability for one fragment impacting the population center.

The total impact probability for M population centers and N fragment groups is given by

$$(P_I)_{TOTAL} = \sum_{i=1}^{M} \sum_{j=1}^{N} (P_I)_{ij} \tag{57}$$

where

$(P_I)_{ij}$ is the probability that the jth fragment impacts the ith population center.

Two limiting computations for casualty expectation have been incorporated into TARGOP. Unsheltered casualty expectation (E_{cu}) is based on all people being in the open with no protection and no limitation on the kinetic energy which might be required to cause a casualty. Sheltered casualty expectation (E_{cs}) considers the benefit of shelters which may protect the people.

E_{cu} is a convenient upper bound, representing the maximum number of possible casualties. It is computed with the equation

$$(E_{cu})_{TOTAL} = \sum_{i=1}^{M} \sum_{j=1}^{N} (P_I)_{ij} \; \rho_{ci} \; \frac{A_{Lj} \; n_j}{(6076.1)^2} \qquad (58)$$

where

$(P_I)_{ij}$ = probability of impacting ith center with ith fragment,

$\rho_{ci} = N_{ci}/A_{ci}$ = population density of ith center,

N_{ci} = total population in ith center,

A_{ci} = total land area in ith center, square nautical miles,

A_{Lj} = lethal area of jth fragment, square feet,

nj = number of fragments with characteristics identical to the jth fragment,

M = total number of population centers,

N = total number of distinct fragment groups.

There are two methods of determining the sheltered casualty expectation (E_{cs}) - the discrete and the continuous method. Under the discrete method of E_{cs} calculation, the kinetic energy $(KE)_j$ of the jth fragment is either read as input data or computed using equation 27 or 28. It is then necessary to find the probabilities of penetrating each of the four classes of protection. The relationships which are assumed to exist between the impacting fragments and the resisting structures are illustrated in Figure 4-4-12. Quantitatively, let $(p_K)_{ij}$ be the probability of penetrating the Kth structure class in the ith center with the jth fragment. The total affected population at the ith center by the jth fragment is then given by

$$(AFP)_{ij} = \sum_{K=1}^{4} N_{cKi} \; (P_K)_{ij} \qquad (59)$$

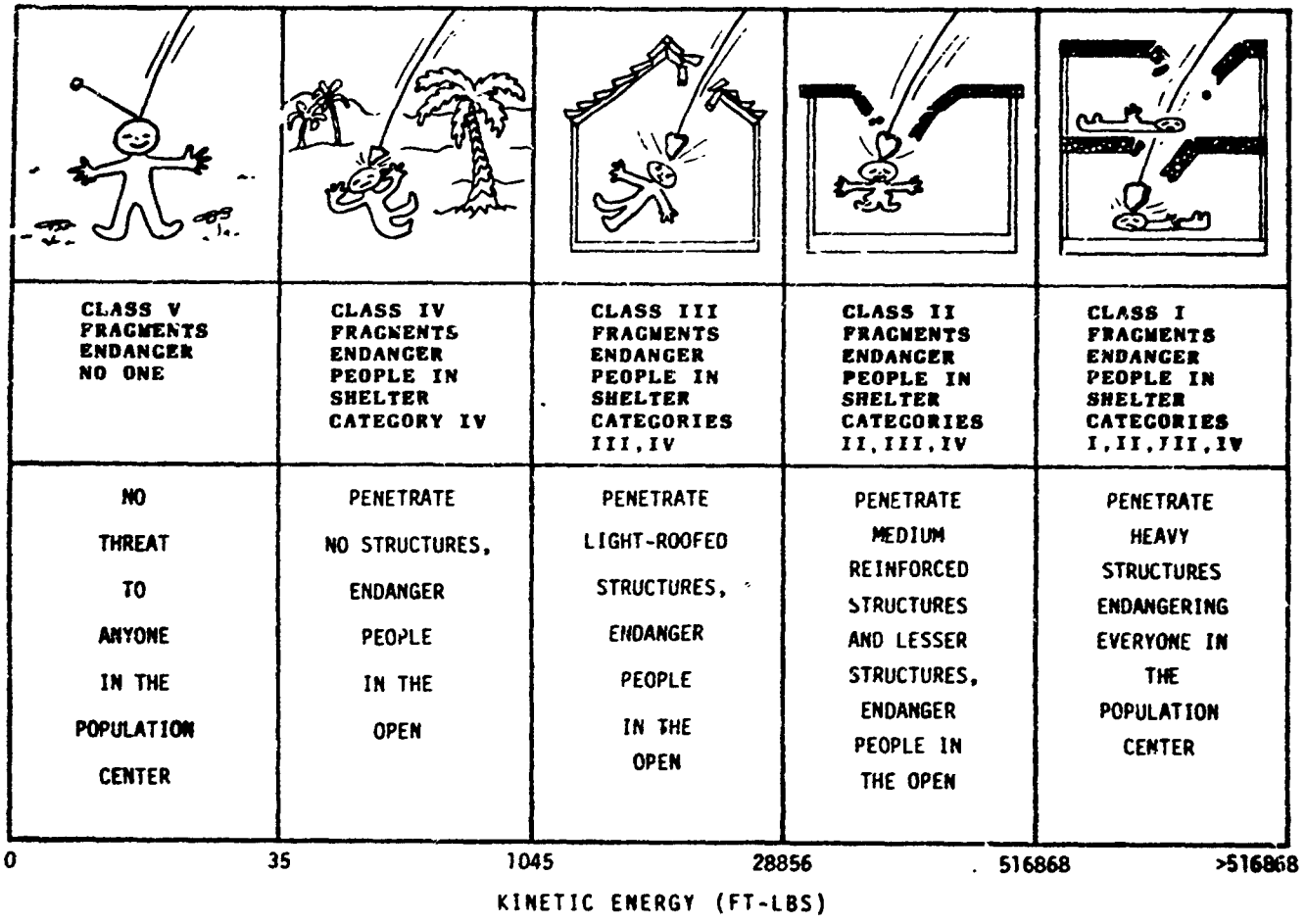

Figure 4-4-12. Energy Relationships between Impacting Fragments and Resisting Structures

where

N_{cKi} = population in class K structure at ith center,

$(p_K)_{ij}$ = probability of penetrating Kth class of protection at ith center with jth fragment.

The total casualty expectation, E_{cs}, is then given by

$$(E_{cs})_{TOTAL} = \sum_{i=1}^{M} \sum_{j=1}^{N} \frac{(P_I)_{ij} (AFP)_{ij} A_{Lj} n_j}{(A_{ci} \quad (6076.1)^2} . \tag{60}$$

The continuous method for computing E_{cs} is based on the fact that population centers often have a multitude of shelters that vary considerably in their capability to protect people. Some provide very little protection, while others are virtually impregnable. With this method, it is assumed that a continuous variation in protection exists over the population center.

The key to the concept is the "casualty density function," shown in Figure 4-4-13. People in shelters with kinetic energy of resistance greater than the impact energy are safe; the others, unsafe.

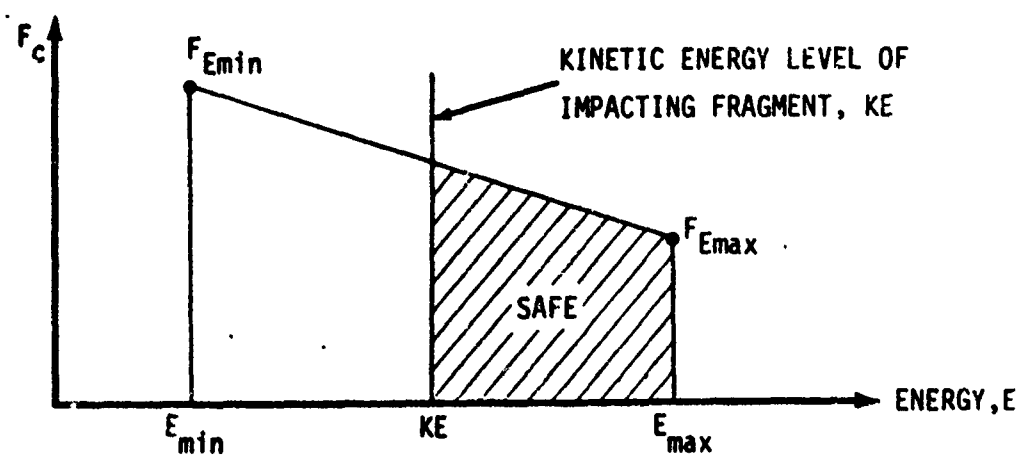

Figure 4-4-13. Casualty Density Function for a Population Center

E_{min} is the kinetic energy of resistance for the least protective shelter and E_{max} is the kinetic energy of resistance for the most protective shelter. As the figure indicates, it is assumed that the casualty density function varies linearly with energy, thus

$$F_c = c_1 E + c_2 \tag{61}$$

where

c_1 and c_2 are constants for the particular population center and are determined as follows:

The integral of F_c is the "sheltered casualty density"

$$\rho_s = \int_{E_{min}}^{KE} n_f F_c \, dE \tag{62}$$

where

KE = kinetic energy of impacting fragment

n_f = normalizing factor.

The normalizing factor is introduced to ensure that the total integral from minimum to maximum energy produces the population density ρ, thus

$$\rho = \frac{N}{A} = \int_{E_{min}}^{E_{max}} n_f F_c \, dE \tag{63}$$

where

N = total population,

A = total area of center.

Substituting equation 61 into 63 and solving for n_f,

$$n_f = N/A\ [0.5c_1\ (E^2_{max} - E^2_{min}) + c_2\ (E_{max} - E_{min})] \tag{64}$$

E_{cs} is then computed using equation 62 for ρ_s instead of using ρ as with unsheltered casualty expectation. Thus, the equation for E_{cs} is

$$(E_{cs})_{TOTAL} = \sum_{i=1}^{M} \sum_{j=1}^{N} \frac{(P_I)_{ij}\ \rho_{sij}\ A_{Lj}\ n_j}{(6076.1)^2} \tag{65}$$

where

ρ_{sij} = casualty density for ith population center due to jth fragment.

The values of the F_c function at E_{min} and E_{max} are determined as follows:

$$F_{E_{min}} = \frac{\text{No. of People in Minimum Protective Shelter}}{\text{(Area of Shelter) (Energy of Resistance of Shelter)}}$$

$$= N_{A_{max}}/(A_{min}\ E_{min})$$

$$F_{E_{max}} = \frac{\text{No. of People in Maximum Protective Shelter}}{\text{(Area of Shelter) (Energy of Resistance of Shelter)}}$$

$$= N_{A_{max}}/(A_{max}\ F_{max})$$

It is often the case that one particular population center is much more politically sensitive to impacting debris than another. This is markedly so when an island with a native population is compared to one inhabited solely by US military personnel. Certainly, it is undesirable to impact the military installation, but it could be much worse for the test program if the native population were endangered. To account for these subjective differences, factors should be introduced to the population library which reflect the relative "reaction sensitivty" for each center.

First, a reference population center is chosen with an R_{ci} factor of 1.0. Each of the remaining centers is then assigned a reaction sensitivity greater than 1.0. These factors are taken as multipliers in computing E_{cu}, and the final result is termed "balanced risk" because the population centers have indeed been balanced with regard to the undesirability of impacting them. Balanced Risk (R_c) is computed as follows and should be compared to equation 58.

$$(R_c)_{TOTAL} = \sum_{i=1}^{M} \sum_{j=1}^{N} \frac{(P_I)_{ij} N_{ci} R_{ci} A_{Lj} n_j}{A_{ci} \; (6076.1)^2} \qquad (66)$$

where

R_{ci} = reaction sensitivity factor for ith center relative to a reference center.

All of the preceding model development has been concerned with a single target point. But the main purpose of TARGOP is the construction of target point contour plots. The underlying assumption which is made to produce the plots is that the impacting fragment characteristics remain constant from grid point to grid point. This is illustraed in Figure 4-4-14.

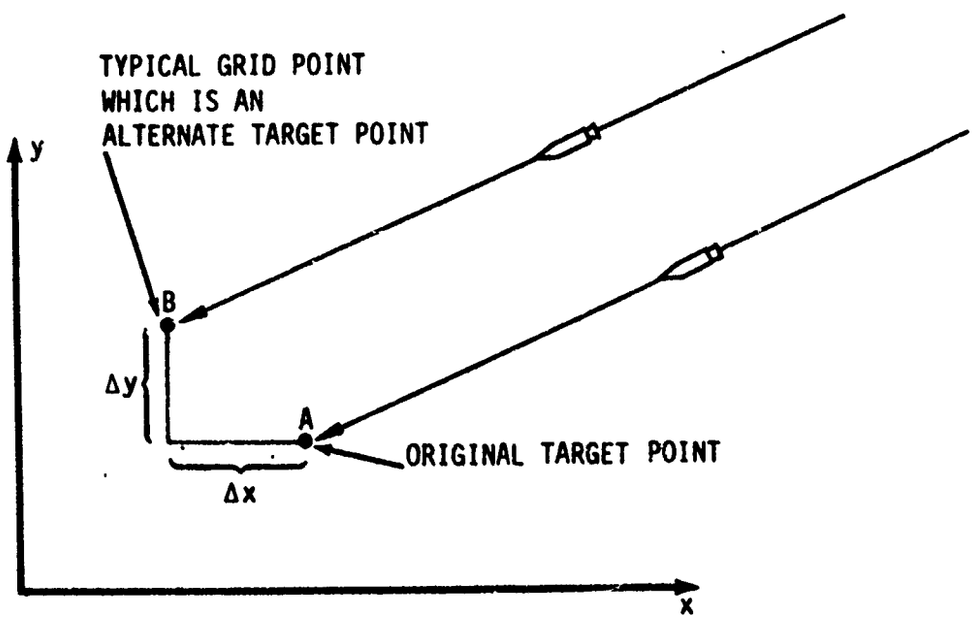

Figure 4-4-14. Relationship between Original Target Point and a Typical Grid Point

All of the fragment data (weights, dispersions, etc.) gathered to run TARGOP are based on one target point, for example point A. This data remains constant for point B except that impact points must be translated by the amounts Δx, Δy. The assumption is valid, provided the distances Δx, Δy are not so large as to cause significant differences in the trajectories for points A and B. The TARGOP model is based on an array of such alternate target grid points in numbers large enough to permit constructing contour plots which graphically represent the continuous variability of the computer risks.

The points are regularly spaced by the amount Δ, and the grid is positioned by specifying its center point (ϕ_0, λ_0). At each grid point, four risk values are computed: P_I, E_{CU}, E_{CS}, and R_c; all of which are totals. Such numbers are characteristically small and in TARGOP are limited to the range of risks greater than 10^{-14} or less than 1.0. By limiting the risks to these values, the contouring analysis is simplified. To further enhance the analysis, the logarithms of the risks are taken to the base 10, then the result is multiplied by -1.0. Resultant contour levels are identified by an integer so that a level 4 curve means the risk is constant at 10^{-4} along the curve, etc. Any point on such a curve is an alternate target point, and a level 4 means that the hazard to the population library is 10^{-4} if the missile were targeted at the point in question. The CONTUR program is based on the assumption that the surface variation between grid points is linear. Figures 4-4-15 through 4-4-20, which follow, are representative of the type of output plots available from the TARGOP/CONTUR programs.

GRID BOUNDARIES
TYPICAL MISSION RUN NO. 2

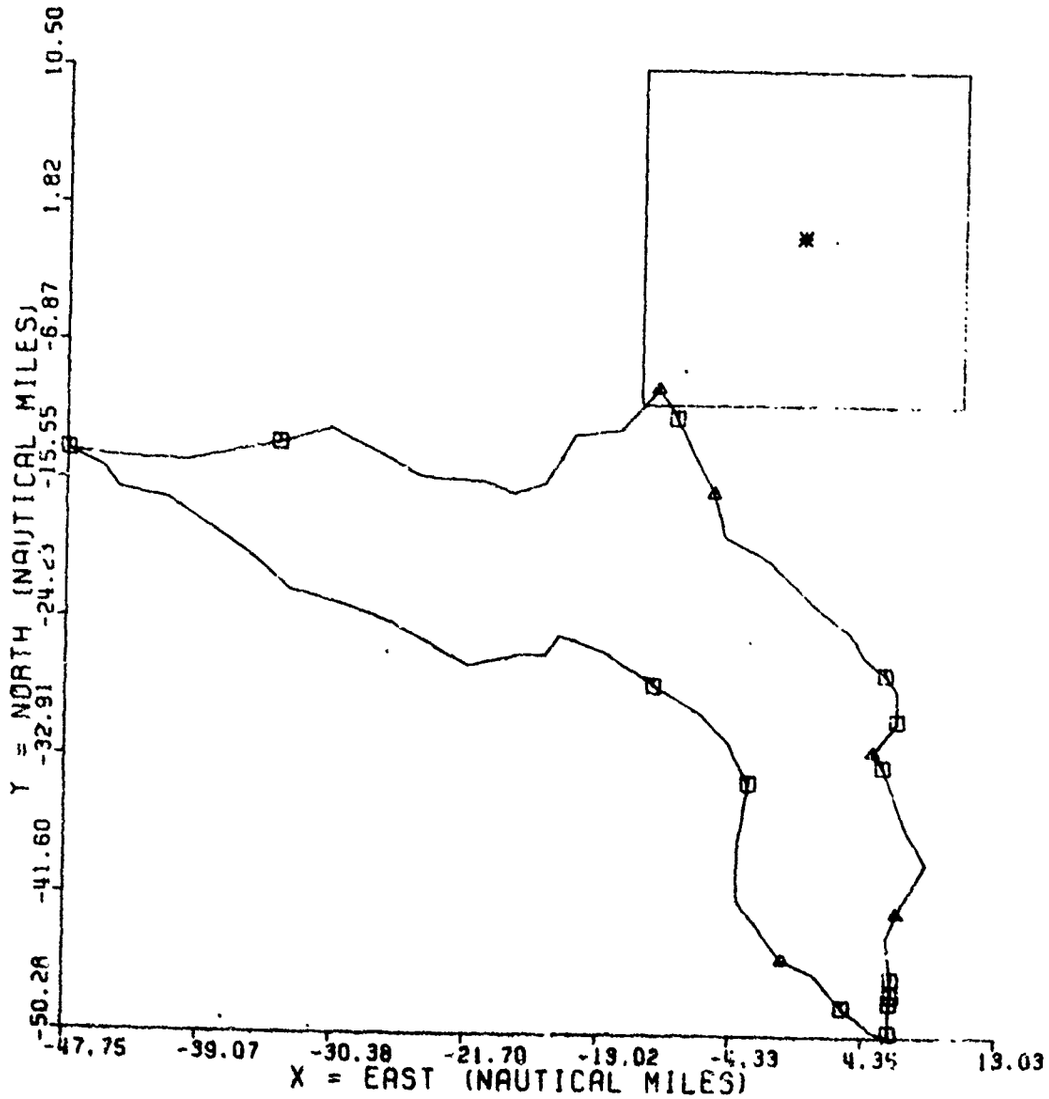

PLOT ORIGIN - LONGITUDE = 166.826 , LATITUDE = 8.718

Figure 4-4-15

3-SIGMA IMPACT ELLIPSES
TYPICAL MISSION RUN NO. 2

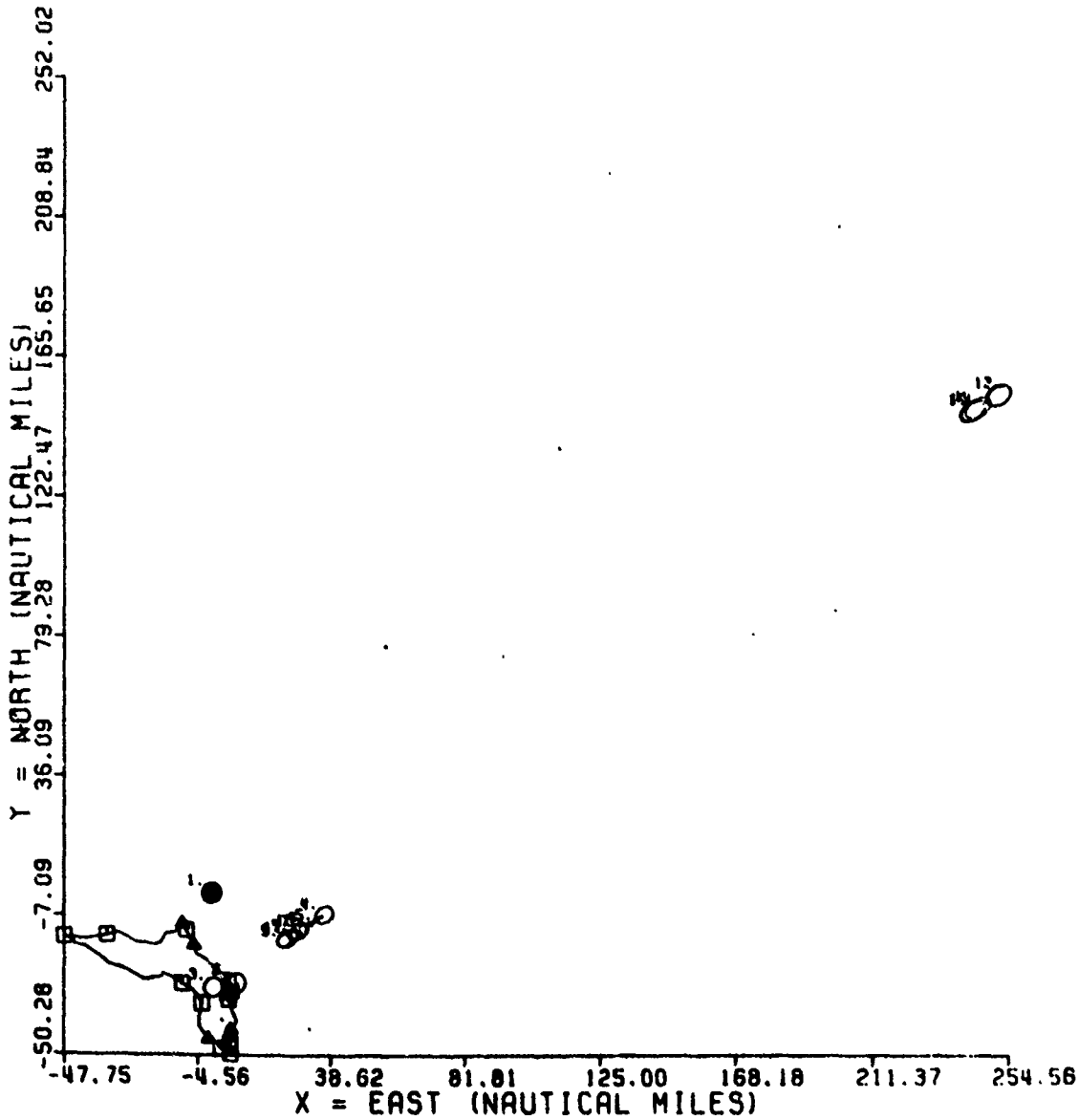

PLOT ORIGIN - LONGITUDE = 166.826 , LATITUDE = 8.718

Figure 4-4-15

PI
TYPICAL MISSION RUN NO. 2

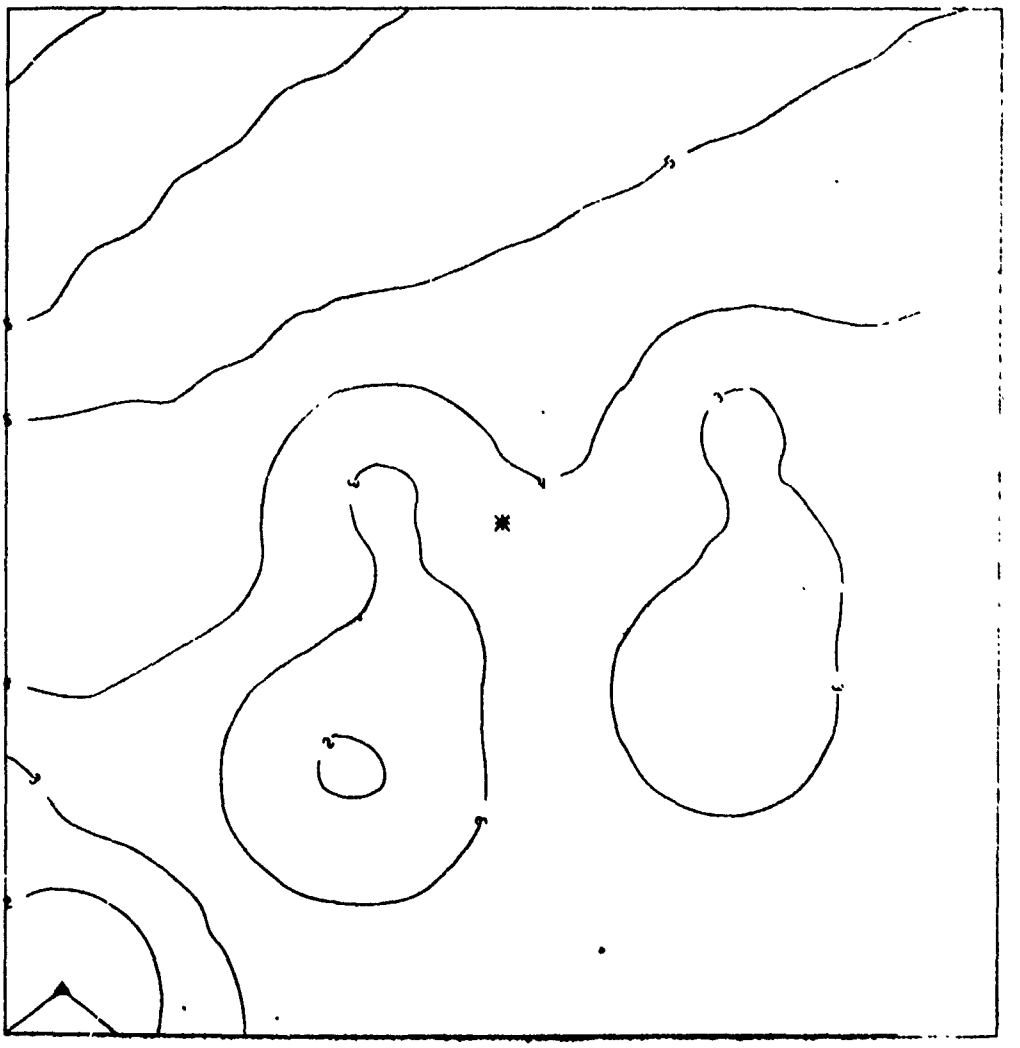

SCALE (NM) 0.00 3.00 6.00
PLOT ORIGIN - LONGITUDE = 167.456 , LATITUDE = 9.381

Figure 4-4-17

ECU
TYPICAL MISSION RUN NO. 2

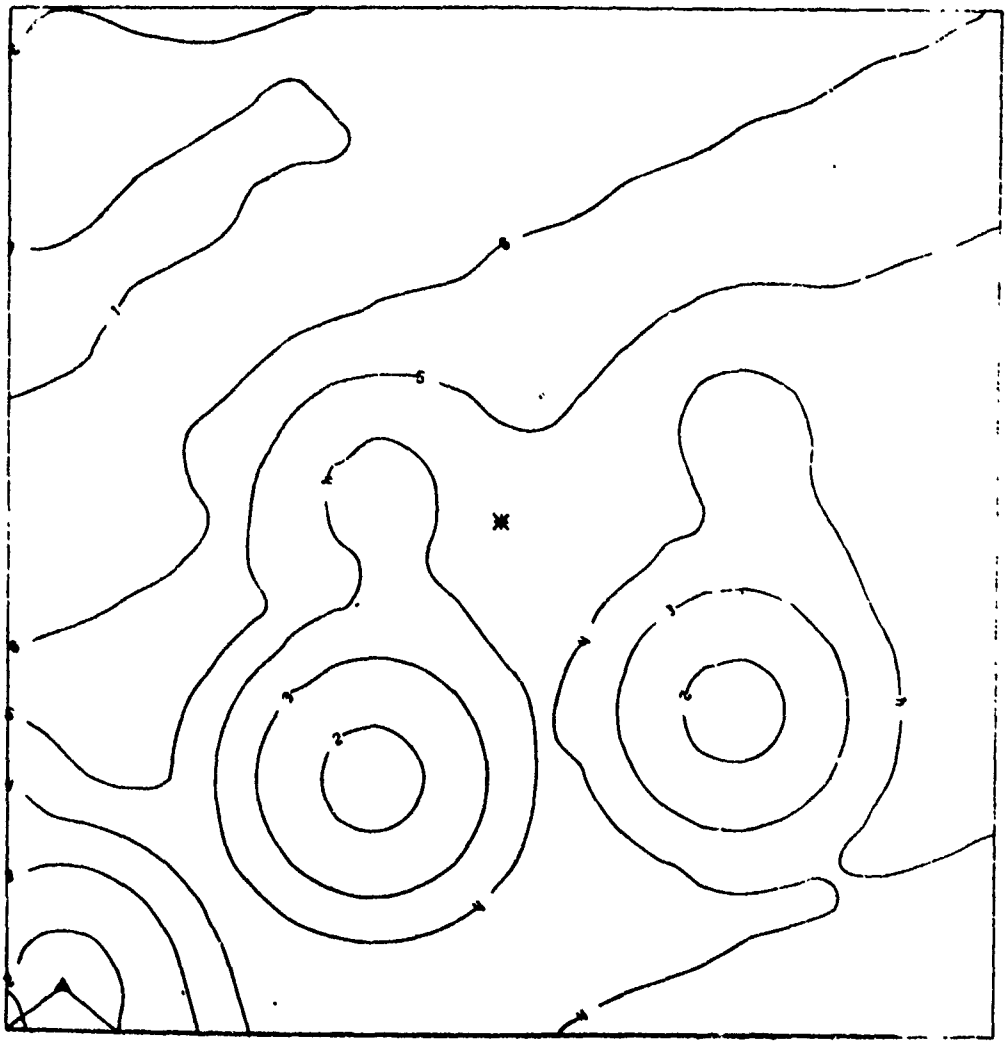

SCALE (NM) 0.00 3.00 6.00
PLOT ORIGIN - LONGITUDE = 167.456 , LATITUDE = 9.381

Figure 4-4-18

ECS
TYPICAL MISSION RUN NO. 2

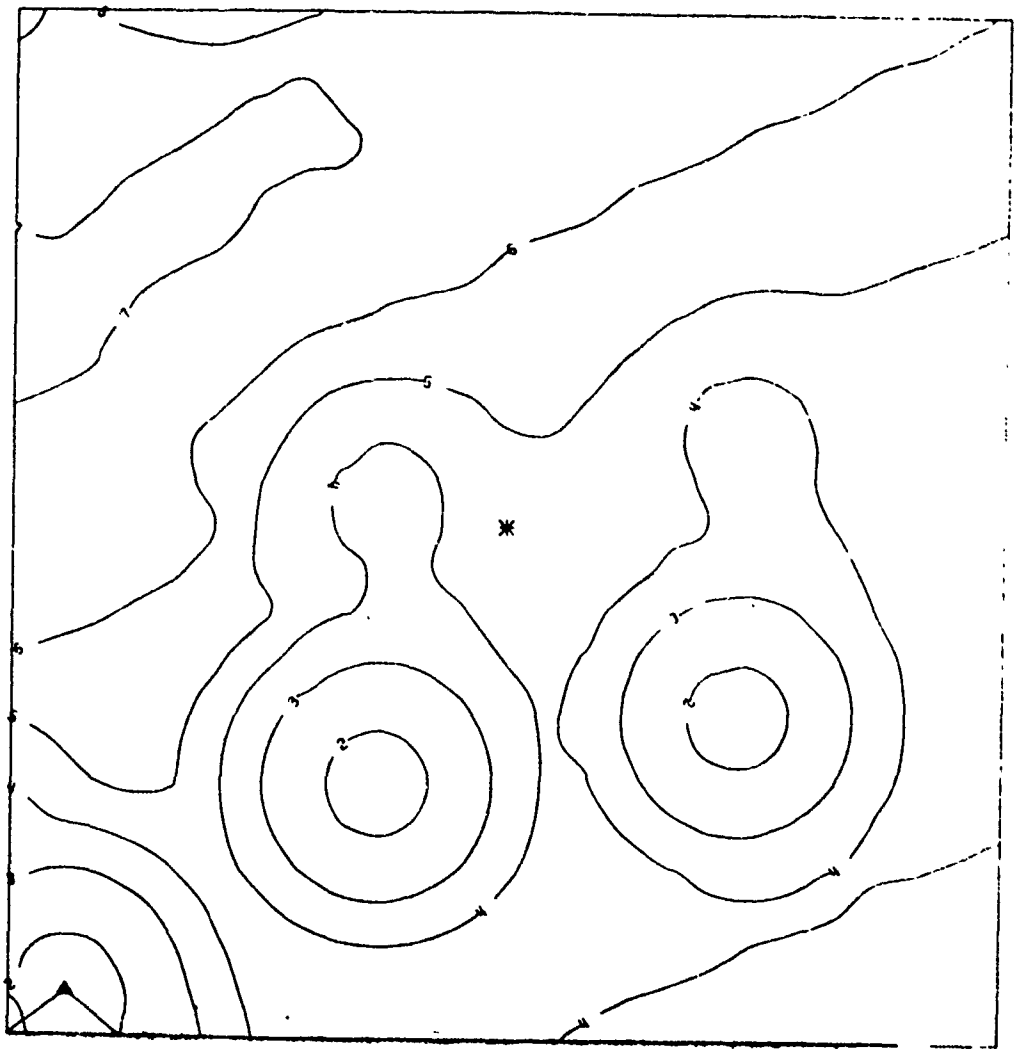

SCALE (NM) 0.00 3.00 6.00
PLOT ORIGIN - LONGITUDE = 167.456 , LATITUDE = 9.381

Figure 4-4-19

RC
TYPICAL MISSION RUN NO. 2

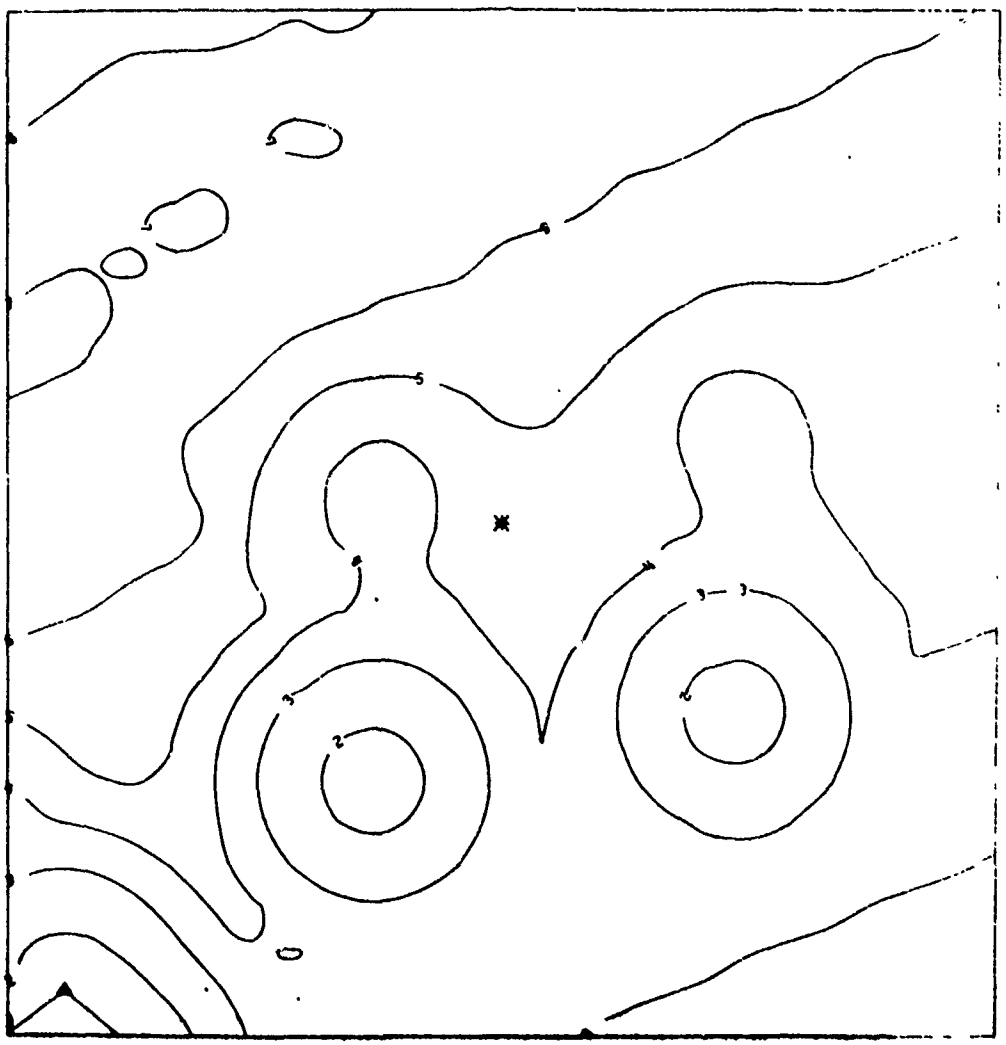

SCALE (NM) 0.00 3.00 6.00
PLOT ORIGIN - LONGITUDE = 167.456 , LATITUDE = 9.381

Figure 4-4-20

References

1. Collins, J. D., M. Jameson, and J. L. Jantz, "Real-Time Debris Patterns for Ballistic Missile Launches," Journal of Spacecraft and Rockets, Vol. 13:5, May 1976.

2. Baker, R. M. L., Jr., T. J. Mucha, D. R. Danby, N. H. Jacoby, Jr., A. W. Johnson, and R. E. Ryan, "Range Safety Debris Pattern Analysis," The Journal of Astronautical Sciences, Vol. XXIII, No. 4, 1975.

3. Kingery, C. N., and B. F. Panhill, "Peak Overpressure vs. Scaled Distance for TNT Surface Charges (Hemispherical Charge)," Memo Rpt. 1518, 1964, Ballistic Research Labs.

4. McMunn, J. C., J. D. Collins and B. Brown, "A Hazards Model for Exploding Solid-Propellant Rockets," Journal of Spacecraft and Rockets, Vol. 6, No. 12, December 1969.

5. Davis, K. S., E. P. DeTurke, and O. A. Refling, "Determination of Casualty Probability in Range Safety Applications," TR-0110 (2301)-2, March 1967, Aerospace Corporation, El Sequndo, CA.

4.5 WHITE SANDS MISSILE RANGE (WSMR) RISK ANALYSIS TECHNIQUES

4.5.1 Range Safety Authority

The commanding General, White Sands Missile Range, New Mexico, is responsible for assuring that there are no unreasonable/unnecessary hazards associated with tests conducted at WSMR. The responsibility for performing this function has been delegated to the Missile Flight Surveillance Division, WSMR.

4.5.2 Minimizing Risk

WSMR operates under the philosophy that all tests are potentially hazardous, and that no risk is acceptable if a test can otherwise be conducted in a prudent and cost effective manner. Risks are minimized by design characteristics of the test article, including redundancy of vital control elements, and by use of a flight termination system (FTS) where required. Operational practices to reduce risks include non-essential personnel evacuations, positive protection of essential personnel in test areas such as blockhouses, barricades, shelters and roadblocks; and test scenarios designed so that the test objectives are met with the lowest risk exposure to essential participating personnel and high value property. Thus, the basic policy of the WSMR flight safety program is to take all prudent and reasonable means to reduce risks in light of national program interests, program objectives, risk levels to life and property, costs and risk to the test itself.

4.5.3 Risk Analysis

Risk analyses are not performed for all tests conducted at WSMR. Studies are normally performed when personnel or high value property cannot be evacuated from the dispersion footprint of a test. Often the results of the analyses are used to position required manned instrumentation sites within the footprint into areas of reduced risks.

WSMR is concerned with both single test risks and cumulative risks associated with test programs. Hazards are evaluated by means of a detailed probability study which includes:

1. the derivation of an impact probability density function,

2. the assessment of lethal areas,

3. the computation of hit and kill probabilities based upon land areas and population densities, and

4. computation of impact effect of missile clean body and destruct debris on those WSMR test site shelters which could be subjected to hazards

by the missile/vehicle test operations. Normally, the debris from an aerodynamic missile must be contained so that existing shelters provide adequate safety.

Since most tests at WSMR are not general in nature, use of generalized risk programs or models is often not feasible. Thus, WSMR conducts a variety of different types of tests:

1. Full scale drones
2. Subscale drones
3. Area Air Defense
4. SHORADS
5. Lasers
6. Medium Range Ballistic Missiles
7. Atmospheric Probes
8. Cruise Missiles
9. Air-to-Air; Air-to-Ground
10. NASA Shuttle Tests
11. Re-entry Vehicle Tests
12. Projectile Tests

4.5.4 General Risk Programs

In general, each test has characteristics that require an entirely new model to be developed. However, WSMR does possess two general risk programs that are used extensively. The first is KILL - used mainly for PERSHING, but can be used and modified for many other applications. The second is RISK - produces drone impact dispersion footprints relative to a given intercept point and can be modified for other applications.

WSMR is currently developing a general purpose program called "Risk to Test." The purpose of the program will be to determine the WSMR real-time system reliability for any specific test or test program. The program will also assist WSMR in identifying trouble support elements inhouse and thus, by correction, increase the probability of successful tests at WSMR.

Risk analyses have been performed for specific tests at WSMR and can be obtained by request. The following is a list of these analyses:

1. Formal reports and other documents:

a. "Population Comparison of Two Corridors," 10 February 1975. (Draft).

b. "PERSHING Kill Probability Study," 6 March 1975.

c. MFR, "One Vehicle Running a Roadblock on Highway 70 During a Hawk vs Drone Mission," 30 April 1975.

d. MFR, "Discussion of Recommendations for Solution to Problem of PERSHING Second Stage Debris Impacting in the Bosque del Apache Wildlife Refuge," 17 June 1975.

e. Technical Report, NR-M 1-75. "Launch Site Study PERSHING II," 1 July 1975.

f. Technical Report, NR-M 2-75, "Power Line Hit Probability," (PII Launch at Page, Arizona), Undated.

g. Technical Report, NR-M 3-75, "Hazard Analysis, Wingate Roadblock Study," 10 September 1975.

h. "Risk to Aircraft Caused by PERSHING II (Page, Arizona)," (Draft).

i. Staff Study, "Off-R[illegible] (WSMR) Targeting of Pershing (PII)."

j. Technical Report, [illegible]R-M 4-75, "Hazard Analysis, PI-A Wingate Firings (Abort Area Si[illegible] [illegible]1 September 1975.

k. DF, "PERSHING II, Delta, Colorado," 12 April 1976.

l. Flight Safety Study, "Risks Pursuant to PQM-102A Overflight of White Sands National Monument Access Road During Landing Approach," 14 June 1976.

m. Draft Report, "XQF-86E Staging from HAFB," June 1976.

n. "Briefing Outline for MG Means on Hazards to Patriot Facility by Stinger Operations," presented by Mr. Bart A. Goode, Chief, Missile Flight Surveillance Division (Draft Papers).

o. MRF, "Study Concerning US Highway 70 Roadblock for LC-32 MQM-34D Launches," 27 June 1977.

2. Studies currently underway:

a. Hazards to HELNOP by Missiles and Drones

b. Hazards to HELSTF by Missiles and Drones

c. General Purpose Hazard Analysis Model for Drones and Missiles (in use but undocumented)

d. "Risk to Test" General Purpose Model (Assigned to Mr. Terry W. Horton)

e. Roland Site Selections Study